

Dissertation
submitted to the
Combined Faculties for the Natural Sciences and Mathematics
of the Ruperto-Carola University of Heidelberg, Germany
for the Degree of
Doctor of Natural Sciences

presented by

Diplom- born in:	M.Sc. Antonino Montalbano Palermo, Italy
Oral-examination:	20/09/2016

Identification and functional
characterization of genetic modifiers for
SHOX deficiency

Referees: Prof. Dr. Gudrun Rappold
Prof. Dr. Thomas Holstein

**Sworn Affidavit according to § 8 of the doctoral degree regulations of
the Combined Faculty of Natural Sciences and Mathematics**

I herewith declare that:

- This thesis is my own and that I have only used the sources indicated and have not made unauthorized use of services of a third party. Where the work of others has been quoted or presented, the source is always given.
- I have not yet presented this thesis or parts thereof to a university as part of an examination or degree.
- I am aware of the importance of a sworn affidavit and the criminal prosecution in case of false or incomplete affidavit.
- I affirm that the above is the truth to the best of my knowledge and that I have not concealed anything.

Place and date:

Signature:

The work carried out during my PhD studies has resulted/will result in the following publications:

- Hoffmann S, Clauss S, Berger IM, Weiss B, **Montalbano A**, Röth R, Bucher M, Klier I, Wakili R, Seitz H, Schulze-Bahr E, Katus HA, Flachsbart F, Nebel A, Guenther SP, Bagaev E, Rottbauer W, Kääh S, Just S, Rappold GA. (2016). Coding and non-coding variants in the *SHOX2* gene in patients with early-onset atrial fibrillation. *Basic Res Cardiol.* 111, doi: 10.1007/s00395-016-0557-2.
- **Montalbano A**, Juergensen L, Roeth R, Weiss B, Fricke-Otto S, Binder G, Ogata T, Fukami M, Decker E, Nuernberg G, Hassel D, Rappold GA. Retinoic acid catabolizing enzyme *CYP26C1* is a genetic modifier in *SHOX* deficiency (in revision).
- **Montalbano A**, Thiel C, Roeth R, Weiss B, Fukami, Ogata T, Binder G, Rappold GA. Spectrum of *CYP26C1* variants in patients with short stature and normal height (in preparation).
- **Montalbano A**, Sumer S, Rappold GA. Cell-cycle dependent regulation of Cas9 expression enhances homology-directed repair in human iPSC (in preparation).

Acknowledgements

This section is to say thanks and greet the many people I met during my PhD.

First of all, I would like to thank Prof. Dr. Gudrun Rappold for giving me the opportunity to work in her lab for four years. I thank her for the support she gave me in these tough years: In the most difficult moment of my PhD she put a lot of efforts to find the best way to finalize my project (like speaking with what she had left of the high-school French to gather data from long time-retired collaborators). More than once she told me that my project was maybe the most difficult she has ever had in her career. Once done we are going to celebrate! :)

I would like also to thank her for she has got enough patience to deal with a Sicilian guy like me. Although Heidelberg is quite far from the *Mittelmeer* and cold compared to North Africa (Sicily could be considered as Northern part of the "Dark continent"), the constant rain could not cool down my hot temper.

I thank also Prof. Dr. Thomas Holstein and Prof. Dr. Christel Herold-Mende for being my TAC members and contributing with suggestions to the development of my PhD project. I thank Prof. Dr. Thomas Holstein, Prof. Dr. Christel Herold-Mende, and Dr. Aurelio Teleman for accepting to be my referees.

I would like to dedicate a special thank you to Prof. Dr. Herbert Steinbeisser. For me he was not only my second supervisor and TAC member, but also a great person to take as example. He was always ready to listen to you and give good scientific (and not only) advices. Despite the circumstances, he stoically kept doing science and being a supportive supervisor. Really impressive! He shall never be forgotten!

Thanks to HBGIS! It has been not only a graduate school providing scientific and career trainings, but also an important hub to connect with other PhD students. HBGIS plays an important role in gathering together students in both scientific and social events. Without HBGIS I would have never met many great people (Alí, Mohammed, Lisa, Peng, Ece, André, Mario, Zeribe, Julia, Giuseppe, Eleni and Akis, et al.).

I would like to thank also the people from the lab.

Birgit 1 took a lot of care of me. She has been always, or almost (*bitte, nicht stören!* when she is busy), an open ear. If I had problems with work, family and love she would sit close, listen and give useful advices. And many thanks for managing the lab; it wasn't for you, we would pipette things with our mouth. Advice for the future generations of PhDs: You have problems, ask Birgit! But do not mess with her, she can slap very hard (personal experience). :)

Thank you Ralph for helping me with my project and being the all-doing/ all-fixing person in the lab. Without you we would probably still use Commodore 64 for data analysis. Advice for the future generations of PhDs: If you have got a problem, ask Ralph!

Thank you Henning, the "young" buck postdoc in the lab. I never laughed so much as when Henning was around in the lab. You pick a topic, he will always find at least an anecdote connected to it and make you laugh out loudly. Advice for the future generations of PhDs: If you want everybody to know something, tell Henning and news will spread faster than light. Thanks to Birgit 2 for the nice time and for having enough patience to survive the "testosterone lab".

Thank you Niko for being such a nice and open person. Our chatting helped me a lot and I will miss talking and making jokes with you. Tsaaaa!

Thank you Ana Cortabitartina for the "crazy" moments we spent together in and out of the lab (we jumped with a parachute from 4000 meters height!). To give advices to the future generations of PhDs about how to deal with Ana would require an entire thesis on its own. Luckily for the future generations, she is almost done with her PhD. :)

Many thanks to Simone + Anna <3 <3 <3, and Sandra, and I'd like to add Anne. The fabulous postdocs. Women rule! I had a lot of fun with you!

Thank you Bianca and sorry for annoying you all the time! You are the newest PhD in the lab at the moment but felt like you have been there since long time (I know that you think that I am a bad person, and you are right. However, this time I mean it in a positive way). For the future generations of PhDs: do anything just to annoy her! (that sorry at the beginning was obviously a fake).

Thank you Ahmed the best! :) Thank you for supporting me in the tough moments. I'll keep my finger crossed for your PhD and girlfriend(s). Advice for the future generations of PhDs: take some time to understand his way of doing things; they may seem strange but in the end are loschical!

Thanks to Simon (Tall boy). Despite the many stuff you already had to do, you found the time to perform the iPSC experiments with me. Advices for the future generations of PhDs: if you have got some food and do not have space in your tummy any more, ask Simon! He's always hungry and can eat a lot without gaining a gram!

Many thanks to Beate for her advices, and thanks to her group of girls: Steffi, Cristina and Tanja (thank you for helping me with German translation). You really are women with "guts"!

I would like to thank also two people who left the AG Rappold's lab long before I started writing my thesis: Slavil and Franzi. You have been very close friends during the period you were in the lab and I miss our time together a lot!

Thanks to the Steinbeisser's lab Kirsten, Susy, Maria, Judith, Annette, Eva, Lily, and Inge. Congratulations for staying always strong together!

Thanks to my Italian friends in Germany: Nino, Lory, Matteo, Lorenzo. Peppe in particular, you gave me a lot of support.

Thanks to the Indian dudes Aseem, Akram, and Hrishikesh! We had some fun together! Dike Bose! Dike Bose!

Many thanks to the Journal club people: Stefan, Sergio, Birgit, Nadine, Edoardo, Ling Shih, Minseong, Kaiqing. It was fun to talk science in front of beers and junk food!

Thanks to the people from the Heidelberg Forum 2015 organization team. In particular Chiara, Patricia and Nina. It was a great experience with all of you.

Finally, I would like to thank three close friends I met here in Heidelberg. I would like to keep such a close friendship also in the future even if far away from each other. Rahul the cocky Indian boy who became a close friend with whom to share good and bad moments of

our PhD. Thank you for teaching me about the Indian culture, including the food and the nasty words... :)

Thank you Marcel! You are not such a bad person for being on the dark side... I really met a great guy with whom I could share many good and bad moments in this tough period of my life. You really are a good friend (and also very bad person at the same moment...). :)

Last but first, thank you Rafi! You really made the difference in the lab for me. We shared together many things (maybe too many ...) :) I even kept Ramadan. I had a great time in the lab thanks to you. I will miss you a lot Sweetheart!

I'm done! For sure I forgot somebody. If you are one of them, sorry for that!

Dear future generations of PhDs I leave you one task you must fulfil: find out who Basti is! Please!

Abstract

Human height is a complex trait with a high heritability. Mutations in the homeobox gene *SHOX* cause *SHOX* deficiency, the most frequent monogenic cause of short stature. *SHOX* deficiency has high penetrance. However, the clinical severity of *SHOX* deficiency varies widely, ranging from short stature without dysmorphic signs to mesomelic (disproportionate) skeletal dysplasia (Léri-Weill dyschondrosteosis, LWD) and different independent studies have reported rare *SHOX* deficiency individuals presenting with normal height and no dysmorphic signs. To shed light on the factors that modify disease severity/penetrance, we studied a three-generation family with five affected individuals presenting with LWD using whole genome linkage and whole exome sequencing analyses. By combining the data obtained with these two independent methods, we found that the variant allele p.Phe508Cys of the retinoic acid catabolizing enzyme *CYP26C1* co-segregated with the *SHOX* variant allele p.Val161Ala in the 5 affected individuals, while the *SHOX* mutant alone was also present in 3 asymptomatic family members.

Screening of a cohort of 68 LWD individuals led to the identification of two unrelated families with *SHOX* deficiency bearing also additional damaging *CYP26C1* variants in the more severely affected family members. These results support a role for *CYP26C1* in influencing the course of disease in *SHOX* deficiency patients.

CYP26C1, similar to *SHOX*, is expressed in human primary chondrocytes and in zebrafish pectoral fins. Luciferase assays performed to functionally characterize the variants identified in *SHOX* and *CYP26C1* demonstrated their damaging effects on their activity: *SHOX* mutants were not able to transactivate the reporter gene expression, whereas damaging variants in *CYP26C1* affect its catabolic activity leading to increased levels of retinoic acid. High levels of retinoic acid significantly decreased *SHOX* expression in human primary chondrocytes and zebrafish embryos. Analysis of *SHOX* promoter unravelled an indirect effect of retinoic acid on *SHOX* expression.

Individual morpholino knockdown of either gene resulted in shortened pectoral fins in zebrafish embryos, which was more pronounced in *SHOX*. Depletion of both genes simultaneously, aggravated the fin phenotype. Together our findings demonstrate that *SHOX* and *CYP26C1* act in a common molecular pathway (retinoic acid signaling) controlling limb growth and describe *CYP26C1* as the first genetic modifier for *SHOX*-associated disease.

Zusammenfassung

Die Körpergröße des Menschen zählt zu den komplexen Merkmalen mit hoher Heritabilität. Die häufigste monogenetische Ursache für Kleinwuchs sind Mutationen im Homöoboxgen *SHOX*, die eine Defizienz des entsprechenden Genproduktes zur Folge haben.

Eine *SHOX* Defizienz zeigt eine hohe Penetranz, wobei die klinischen Symptome stark variieren und von Kleinwuchs ohne Anzeichen von Dysmorphien bis hin zu Kleinwuchs mit mesomelischen (unproportionierten) Skelettfehlbildungen (Léri-Weill Dyschondrosteose, LWD) reichen. In seltenen Fällen treten *SHOX* Defizienzen auch ohne phänotypische Auswirkungen, wie Kleinwuchs oder Skelettdysmorphien auf. Um Faktoren, die die Penetranz bzw. den Schweregrad von Kleinwuchs und auftretenden Dysmorphien beeinflussen, zu identifizieren, wurde in dieser Arbeit eine Familie mit fünf LWD-Individuen, verteilt über drei Generationen, mittels genomweiten Kopplungsanalysen und Exomsequenzierungen untersucht. Auf diese Weise konnte eine heterozygote Variante in dem Retinsäure katabolisierenden Enzym *CYP26C1* identifiziert werden, welche mit der *SHOX* Variante p.Val161Ala in allen fünf LWD-Patienten ko-segregierte. Die entsprechende *SHOX* Variante war hingegen auch in drei nicht betroffenen Familienmitgliedern vorhanden.

Untersuchungen in einer weiteren Kohorte bestehend aus 68 LWC-Patienten führten zur Identifizierung zwei weiterer *CYP26C1* Varianten in *SHOX* defizienten Patienten. Letztgenannte stammen aus zwei nicht verwandten Familien und zeigten jeweils einen schweren *SHOX* Defizienz Phänotyp. Die generierten Daten unterstützen die Hypothese, dass *CYP26C1* die Ausprägung des Phänotyps bei Patienten mit einer *SHOX* Defizienz beeinflusst.

CYP26C1 wird ebenso wie *SHOX* in humanen primären Chondrozyten bzw. in der Brustflosse des Zebrafisches exprimiert. Zur funktionellen Charakterisierung der im *SHOX* und *CYP26C1* Gen gefundenen Varianten, wurden Luziferase Assays durchgeführt. Diese Analysen belegten eine schädigende Wirkung aller Varianten auf die jeweilige Proteinfunktion. Die *SHOX* Mutanten zeigten keine Transaktivierung des Reporterkonstruktes, wohingegen die *CYP26C1* Varianten die katabolische Aktivität des Genproduktes reduzierten und so zu einer erhöhten Retinsäurekonzentration führen. Dieser Anstieg resultiert in einer signifikanten Reduktion der *SHOX* Expression in humanen primären Chondrozyten sowie in Zebrafisch Embryonen.

Morpholino Knockdown Experimente für *SHOX* bzw. *CYP26C1* führten in beiden

Fällen zu einer Verkürzung der Brustflosse in den injizierten Zebrafisch Embryonen, wobei für den *SHOX* spezifischen Genknockdown der zu beobachtende Phänotyp ausgeprägter war. Der gleichzeitige Knockdown beider Gene im Modellsystem verstärkte den Phänotyp.

Zusammengefasst zeigen die Ergebnisse, dass *SHOX* und *CYP26C1* in den Retinsäure Metabolismus involviert sind, die für die Extremitätenentwicklung verantwortlich ist. *CYP26C1* konnte somit als erster Modifier für *SHOX* assoziierte Erkrankungen identifiziert werden.

Table of Contents

List of Figures	xiii
List of Tables	xiv
Abbreviations	xv
1 Introduction	1
1.1 Height Matters	1
1.1.1 Bone development	2
Endochondral ossification	2
Regulators of endochondral ossification	4
Retinoic acid signaling in bone development	5
1.2 Short Stature and the <i>SHOX</i> gene	7
1.2.1 Short stature	7
Idiopathic short stature	7
Léri-Weill dyschondrosteosis	7
Langer mesomelic dysplasia	8
Turner syndrome	9
1.3 <i>SHOX</i> gene, expression regulation and function	10
<i>SHOX</i> gene	10
<i>SHOX</i> expression regulation	10
SHOX function	12
1.4 Aim of the project	13
2 Materials and Methods	14
2.1 Patients and controls	14
2.1.1 Family 1 clinical data	14
2.1.2 Cohort of LWD patients with <i>SHOX</i> deficiency	14
2.1.3 Cohort of ISS and LWD patients with intact <i>SHOX</i>	14
2.1.4 Controls	15
2.2 Whole Genome Linkage Analysis	15
2.3 Whole Exome Sequencing	15
2.4 Reagents	15
2.5 Media and Supplements for Bacteriological Cultures	17
2.6 Media and Supplements for Cell Cultures	19
2.7 Bacterial Strains and Cell Lines	20
Bacterial strains	20

Table of Contents

	Cell lines	20
	Primary cells	20
2.8	Plasmids	20
2.9	Oligos	21
	Primers for whole-exome sequencing Sanger sequencing validation	21
	<i>CYP26C1</i> Sanger sequencing primers	24
	Primers to analyze <i>SHOX</i> p.Val161Ala mutation in the family study	24
	<i>CYP26C1</i> GS Junior Roche sequencing primers	24
	Primers for <i>CYP26C1</i> SLiCE cloning	26
	Mutagenesis primers	27
	RT-PCR primers	28
	qPCR primers	28
	Whole-mount <i>in situ</i> hybridization probes primers	29
	Morpholino sequences	29
	Morpholino efficacy test primers	29
2.10	Antibodies	30
	Primary antibodies	30
	Secondary antibodies	30
2.11	Kits	30
	DNA isolation and purification	30
	PCR	30
	DNA sequencing	31
	Real time PCR	31
	Site-directed mutagenesis	31
	Cloning	31
	Total RNA extraction	31
	cDNA synthesis	31
	<i>in vitro</i> RNA synthesis	31
	Reagents for transfection of eukaryotic cells	32
	Protein assays	32
	Luciferase assay	32
	Detection of <i>in situ</i> hybridization probes	32
2.12	DNA-based Methods	33
	2.12.1 PCR	33
	2.12.2 Real time PCR	33
	2.12.3 DNA purification	33
	2.12.4 Cloning	33
	Restriction digestion	33
	Dephosphorylation	33
	Ligation	33
	psTBlue-1 cloning	34
	Site-directed mutagenesis	34

Table of Contents

SLiCE cloning	34
Transformation	35
Electro-competent cells preparation	36
Chemo-competent cells preparation	36
Transformation efficiency calculation	37
2.12.5 Agarose gel electrophoresis	37
2.12.6 DNA sequencing	38
2.13 RNA-based Methods	39
2.13.1 RNA isolation from human cells	39
2.13.2 Reverse-transcription PCR	39
2.13.3 DIG-RNA probes synthesis	40
2.14 Protein-based Methods	42
2.14.1 Protein isolation	42
2.14.2 Microsome enrichment	43
2.14.3 Determination of protein concentration	43
2.14.4 Western blot	44
2.15 Cell-based Methods	46
2.15.1 Cultivation of eukaryotic cell lines	46
2.15.2 Cryo-conservation	46
2.15.3 Transfection	46
Lipofectamine 2000 transfection of U2OS cells	46
Luciferase assay	48
2.15.4 Treatment of human primary chondrocytes with ATRA	48
2.16 Zebrafish-based Methods	49
2.16.1 Whole-mount <i>in situ</i> hybridization	49
Photography	53
2.16.2 Pectoral fins area measurements	53
2.16.3 Luciferase assays	53
2.16.4 ATRA treatments	53
2.17 Bioinformatics Resources	54
Primer design	54
<i>In silico</i> mutation analysis	54
<i>In silico</i> promoter analysis	54
Databases	54
Illustrations	54
2.18 Statistics	54
3 Results	55
3.1 Genetic Analysis of Family 1	55
3.1.1 Family 1 pedigree	55
3.1.2 <i>SHOX</i> locus analysis	56
3.1.3 Whole-Genome Linkage analysis	57
3.1.4 Whole-exome sequencing analysis	58

Table of Contents

3.1.5	CYP26C1 Phe508Cys variant affects its enzymatic activity . . .	58
3.2	Screening of further LWD and ISS individuals	59
3.3	Functional Studies in Human Cells	63
3.3.1	<i>CYP26C1</i> is expressed in human primary chondrocytes	63
3.3.2	<i>CYP26C1</i> and <i>SHOX</i> are part of the RA pathway	63
3.4	Functional Studies in Zebrafish Embryos	65
3.4.1	Morpholino efficacy analysis	65
3.4.2	<i>shox</i> MO knock-down phenotype	69
3.4.3	<i>cyp26c1</i> MO knock-down phenotype	71
3.4.4	Double <i>shox</i> and <i>cyp26c1</i> MO knock-down phenotype	72
4	Discussion	75
	Identification of <i>CYP26C1</i> as a genetic modifier for <i>SHOX</i> deficiency	75
	<i>CYP26C1</i> exerts its modifier effects by regulating <i>SHOX</i> expression through the control of RA levels	77
	Is there an interaction between RA and estrogen signalling over <i>SHOX</i> expression regulation?	78
	<i>SHOX</i> dosage plays an important role on individual height	79
	<i>CYP26C1</i> , not only a modifier for <i>SHOX</i> deficiency	80
	Conclusions	81
	Bibliography	84
	Appendix	90

List of Figures

1.1	Variability in human height	1
1.2	Endochondral ossification	3
1.3	Chondrocyte differentiation	4
1.4	Retinoic acid pathway	6
1.5	Clinical manifestations of <i>SHOX</i> -deficiency	8
1.6	The <i>SHOX</i> gene and its expression regulation.	11
3.1	Family 1 pedigree	55
3.2	The <i>SHOX</i> variant identified in the family study affects its transcrip- tion activity	57
3.3	The <i>CYP26C1</i> variant identified in the family study affects its enzy- matic activity	59
3.4	Family pedigree charts of the screened LWD patients and functional analysis of the identified variants	61
3.5	Family pedigree of the screened ISS and LWD individuals with no <i>SHOX</i> deficiency and functional analysis of the identified variants	62
3.6	<i>CYP26C1</i> and <i>SHOX</i> are part of the RA signalling pathway	64
3.7	<i>shox</i> MO1 efficacy analysis	66
3.8	<i>shox</i> MO2 efficacy analysis	67
3.9	<i>cyp26c1</i> MO efficacy analysis	68
3.10	Pattern of defects in zebrafish embryos injected with anti- <i>shox</i> mor- pholino	69
3.11	Validation of <i>shox</i> MO1 pattern of defects with <i>shox</i> MO2	70
3.12	Pattern of defects in zebrafish embryos injected with anti- <i>cyp26c1</i> MO	71
3.13	Pattern of defects in zebrafish embryos upon MO reduction of <i>cyp26c1</i> and RA treatment	72
3.14	Pattern of defects in zebrafish embryos co-injected with anti- <i>shox</i> and anti- <i>cyp26c1</i> MOs	73
3.15	Double MO knockdown of <i>shox</i> and <i>cyp26c1</i> leads to reduced pectoral fins.	74
4.1	Schematic representation of <i>CYP26C1</i> modifier effect on <i>SHOX</i> defi- ciency	83
Appendix Figure 1		91
Appendix Figure 2		92
Appendix Figure 3		93

List of Tables

3.1 Family 1 clinical data	56
3.2 Families 2 and 3 clinical data	60
Appendix Table 1	94
Appendix Table 2	97
Appendix Table 3	99
Appendix Table 4	100

Abbreviations

ACAN	Aggrecan
ALDH1a	Aldehyde dehydrogenase 1 a
AP	Alkaline phosphatase
ATRA	All-trans retinoic acid
BMP	Bone morphogenetic protein
BNP	Brain natriuretic peptide
bp	Base pair
°C	Degree Celsius
CNE	Conserved enhancer elements
COL2A1	Collagen type II A1
COL10A1	Collagen type X A1
CTGF	Connective tissue growth factor
CYP26	Cytochrome P450 26
Da	Dalton
ddH ₂ O	Double-distilled water
DEPC	diethyl dicarbonate
DIG	Digoxigenin
DMEM	Dulbecco 's modified eagle medium
DMSO	Dimethyl sulfoxide
DNA	Deoxyribonucleic acid
DNAse	Deoxyribonuclease
dNTP	Deoxyribonucleotide triphosphate
DTT	Dithiothreitol
<i>E. coli</i>	<i>Escherichia coli</i>
eef1 α	Eukaryotic translation elongation factor 1 α
EMSA	Electromobility shift assay
ER	Estrogen receptor
EVS	Exome variant server
ExAC	Exome aggregation consortium
ExoI	Exonuclease I
FBS	Fetal bovine serum
FFDD4	Focal facial dysplasia type IV
FGFR3	Fibroblast growth factor receptor 3
g	Gram
GH	Growth hormone
HPC	Human primary chondrocytes
hpf	Hours post-fertilization

HPRT	Hypoxantin-guanin-phosphoribosyltransferase
HYB	Hybridization buffer
IGF	Insulin-like growth factor
IHH	Indian hedgehog
ISS	Idiopathic short stature
l	Liter
LA SD	Lower arm SD
LB medium	Luria Bertani medium
LMD	Langer mesomelic dyspalsia
LOD score	Logarithm of odds score
LWD	Leri-Weill dyschondrosteosis
M	Molar
MAB	Maleic acid buffer
min	Minute
MLPA	Multiplex ligation-dependent probe amplification
MO	Morpholino
mRNA	Messenger RNA
NKX3/BAPX1	NK3 homeobox 3/bagpipe homeobox homolog 1
NPR2	Natriuretic peptide receptor 2/guanylate cyclase B
OAR	Otp Aristaless Rax
PAR1	Pseudoautosomal region 1
PBS	Phosphate buffer saline
PCR	Polimerase chain reaction
PDVF membrane	Polyvinylidene fluoride membrane
PEI	Polyethylenimine
PFA	Paraformaldehyde
pH	<i>potentia hidrogenii</i>
psi	Pound-force per square inch
RA	Retinoic acid
RALDH	Retinaldehyde dehydrogenases
RAL	Retinaldehyde
RDH	Retinol dehydrogenase
ROL	Retinol
RAR	Retinoic acid receptor
RARE	Retinoic acid responsive element
rhGH	Recombinant human growth hormone
RIPA buffer	Radioimmunoprecipitation assay buffer
RLU	Relative luciferase assay
RNA	Ribonucleic acid
RNAse	Ribonuclease
ROR	RAR-related orphan receptor
rpm	Rotaion per minute
RT-PCR	Reverse-transcription PCR

RUNX2	Runt-related transcription factor 2
RXR	Retinoic X receptor
SD	Standard deviation
SDHA	Succinate dehydrogenase complex subunit A
SDS	Sodio dodecyl sulfate
SHOX	Short stature homeobox
SLiCE	Seamless ligation cloning extract
SOB medium	Super optimal broth medium
SOC	Super optimal broth wth catabolite repression
SOX9	SRY-box 9
SSC	Saline sodium citrate
TBS	Tris-buffered saline
TGF β	Transforming growth factor β
TGP	Thousand genome project
UTR	Untranslated region
WES	whole-exome sequencing
WGS	whole-genome sequencing
YT	Yeast extract tryptone

1 Introduction

1.1 Height Matters

When we walk on the street very tall or very short people catch our attention at once. Extraordinary tall or short people are registered in the Guinness Book of World Records and invited to TV shows all around the world (**Figure 1.1**). Height

may have a strong influence on individuals lives. For example, it has been reported that tall people have better jobs, higher workplace success and they usually emerge as leaders¹.

Height is an easy trait to measure. Stature is defined relative to the age, gender and genetic background of the individual. Tall stature and short stature are defined as a standing height above or below +2 or -2 standard deviations (SDs), respectively.

Height has a high heritability, although many environmental factors may affect it. So far, many genes have been linked to growth disorders, but many more trait-loci may influence height. Identifying the genetic factors that influence height can provide new insights into development. Moreover, finding the causes of growth disorders may improve the management of such conditions.



Figure 1.1: Variability in human height. Chandra Dangi (on the left) and Sultan Kösen (on the right) are the shortest and the tallest people in the world with an height of 54.6 and 251 cm, respectively (picture taken from the web). Human height is variable and is determined both by genotype and environmental factors.

1.1.1 Bone development

Height mostly, but not exclusively, depends on the longitudinal growth of the long bones. Bone tissue formation, called ossification, takes place through two major developmental processes: intramembranous and endochondral ossification. In intramembranous ossification mesenchymal tissue directly converts into bone. Flat bones like the skull typically develop via this process. In endochondral ossification mesenchymal cells first differentiate into cartilage which is later replaced by bone. This process is characteristic of long bones development.

Endochondral ossification

Endochondral ossification involves the aggregation of mesenchymal progenitors which differentiate into cartilage tissue which is finally replaced by bone². Cartilage tissue formation, namely chondrogenesis, is a tightly regulated multi-step process which involves molecular and morphogenetic changes³. Mesenchymal progenitors, once committed to chondrocytic fate, undergo through condensation, differentiation into proliferative chondrocytes, withdraw from cell cycle to initiate hypertrophic differentiation, programmed cell death, and ultimately substitution with bone tissue. During hypertrophy, chondrocytes secrete extracellular matrix components which mediate calcification. Perichondrocytes, cells which surround the cartilage tissue, differentiate into osteoblasts and secrete bone matrix to form the periosteum. Blood vessels start penetrating the periosteum and bring osteoclasts which degrade the cartilage. Eventually, the chondro-osseous junction forms to divide the cartilage template into the two epiphyses (**Figure 1.2**).

The elongation of bones occurs at the epiphysial plates or growth plates³. Each growth plate is characterized by three zones: the resting zone, populated by round resting chondrocytes which represent the pool of cells ready for later phases of proliferation and differentiation; the proliferating zone, consisting of flattened proliferating chondrocytes which organize in columns in the direction of longitudinal growth; hypertrophic zone, composed of chondrocytes which undergo terminal differentiation by withdrawing from the cell cycle and increasing their volumes (**Figure 1.2** and **Figure 1.3**).

Many parameters contribute to the length of the long bones, including proliferation and extracellular matrix deposition. However, the great volume increase of hypertrophic chondrocytes contribute the most to long bone lengthening and to the different growth rates of the skeletal elements within an individual, individuals, and species². Hypertrophic chondrocytes undergo three different phases. In the first phase, there is an initial expansion of the volume characterized by increase in dry mass production and fluid uptake to maintain a normal dry mass density. In the second phase, the enlargement is characterized by cell swelling resulting in a strong

dilution of dry mass density. In the last phase, volume keeps increasing but dry mass and amount of fluid proportionally increment. These processes are modulated to achieve differential growth of individual elements within a species and of homologous elements between species. For example, in the proximal tibia of mice hypertrophic chondrocytes are large. By contrast, in the proximal radius cells are much smaller. It has been shown that, while chondrocytes in the tibia go through the three hypertrophic phases described above, those in the radius reach the second phase and then stop increasing their volume by aborting the second phase and eliminating the third one². Finally, hypertrophic chondrocytes mineralize their extracellular matrix and then undergo programmed cell death. The hypertrophic cartilage is invaded by blood vessels, osteoclasts and osteoblast precursor cells that remodel the cartilage and substitute it with bone tissues³.

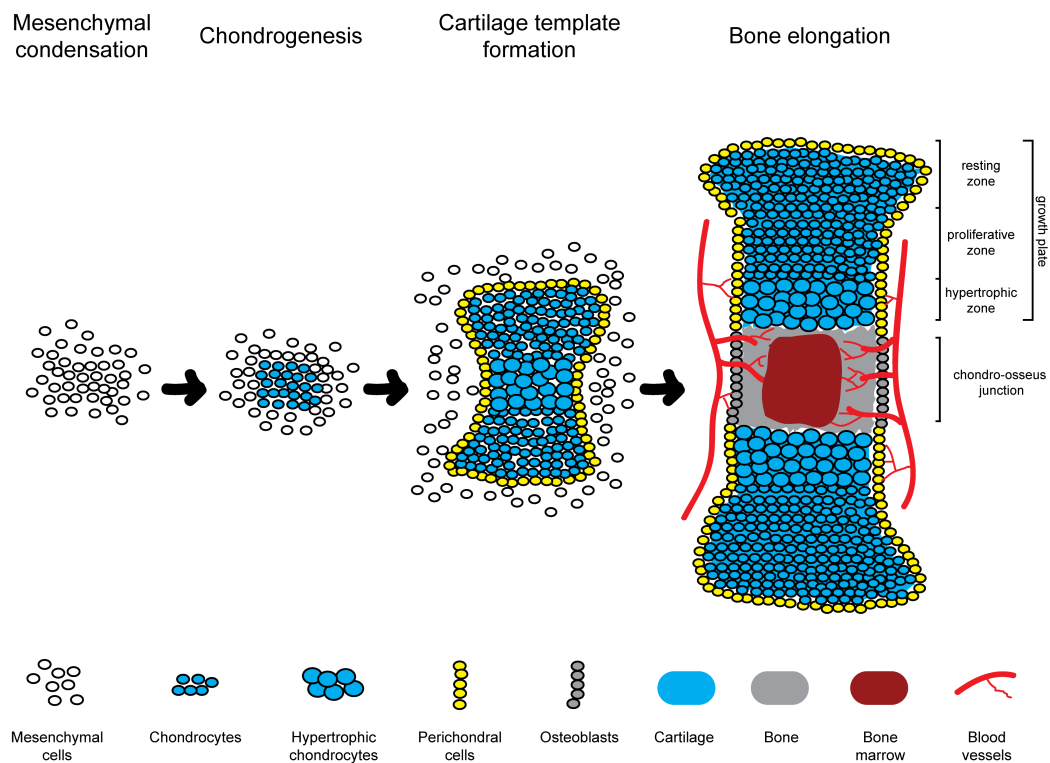


Figure 1.2: Endochondral ossification. At the beginning of endochondral ossification, mesenchymal cells are committed to chondrocyte fate and start to condensate. Cells initiate differentiation and start producing cartilage matrix. The chondrocytes in the cartilage template undergo proliferation, exit the cycle, and become hypertrophic. Cells in the outer layer differentiate into perichondral cells. Finally, during the process of bone formation and elongation, perichondral cells adjacent to hypertrophic and apoptotic chondrocytes differentiate into osteoblasts which, together with blood vessels, invade the cartilage template and substitute it with bone tissue. Figure adapted from ref. 3.

Regulators of endochondral ossification

Endochondral ossification is regulated by a complex network composed of several genes. Different signalling pathways and transcription factors must be tightly regulated during this process and any disturbance may lead to skeletal disorders⁵. Bone morphogenetic proteins (BMPs) and transforming growing factor β (TGF β) are growth factors belonging to the TGF β superfamily that are involved in the initiation of chondrogenesis. Once bound to specific membrane receptors, the signal is transduced inside the cell to induce mesenchymal progenitors to start chondrocyte differentiation (**Figure 1.3**)³.

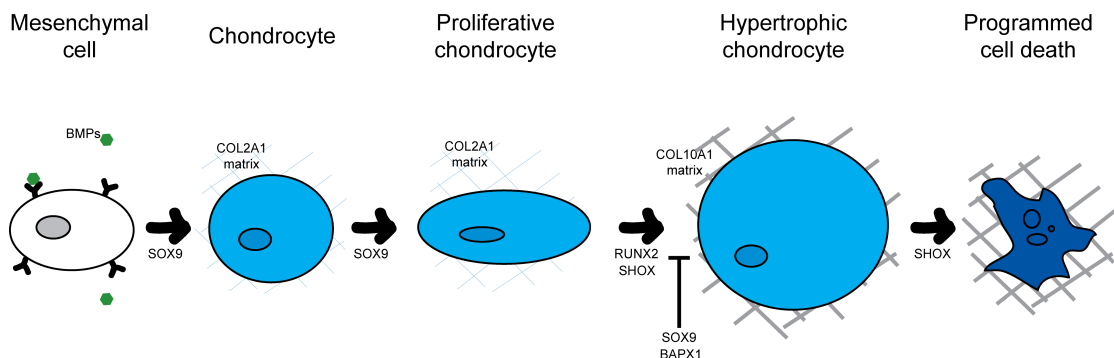


Figure 1.3: Chondrocyte differentiation. Chondrocyte differentiation is regulated by a complex network composed of several genes. Mesenchymal cells upon BMPs signalling become committed to chondrocyte fate. Chondrocyte progenitors start differentiating under the drive of SOX9 and other factors, and start depositing COL2A1 to form the cartilage matrix. Chondrocytes flatten, proliferate, and organize columns in the longitudinal growth direction. Finally, SOX9 expression starts decreasing and RUNX2 increasing to initiate hypertrophy. In this stage, chondrocytes enlarge and start producing COL10A1 matrix. Hypertrophic cells eventually undergo programmed cell death to be substituted by bone tissue. Figure adapted from ref. 3.

SRY-box 9 (SOX9) is a key transcription factor of chondrogenesis and maintenance of chondrocyte identity. Heterozygous mutations in *SOX9* in human have been linked to campomelic dysplasia, a disorder characterized by disproportionate short stature and bowing of the limbs. *SOX9* is expressed in the mesenchymal progenitors and is necessary for their differentiation into chondrocytes. It is expressed by proliferative chondrocytes and during the hypertrophic stages, SOX9 synthesis is downregulated. Indeed, whereas loss of *Sox9* in prehypertrophic cells in mouse results in the conversion to osteoblasts, overexpression of this gene delays ossification. Moreover, SOX9 inhibits terminal differentiation of hypertrophy. Among its target are *SOX5* and *SOX6*, genes involved in the ordered progression through the hypertrophy, and collagen type II (*COL2A1*), a major components of the extracellular matrix of the early stages of endochondral ossification (**Figure 1.3**)^{3;4}.

Another important transcriptional regulator of endochondral ossification is *NK3 homeobox 3 (NKX3)/bagpipe homeobox homolog 1 (BAPX1)*. This gene is expressed in proliferative chondrocytes where it represses *Runt-related transcription factor 2 (RUNX2)* expression to prevent the initiation of chondrocyte hypertrophy⁵.

RUNX2 is an important regulator of hypertrophic differentiation. Its expression starts at the beginning of hypertrophy and is maintained throughout it to promote this differentiation process. *RUNX2* activates the expression of hypertrophic chondrocyte markers such as collagen10A1 (*COL10A1*) and indian hedgehog (*IHH*). Interestingly, *RUNX2* activity is inhibited by *SOX9* through direct protein-protein interaction to prevent cells to undergo hypertrophy^{4,5} (**Figure 1.3**).

The final step of hypertrophic differentiation, which occurs at the boundary between cartilage and newly formed bone, calcium and phosphate trigger chondrocytes to undergo programmed cell death (**Figure 1.3**). It is still not clear whether apoptosis occurs. Despite apoptotic factors like caspase-7 and *BCLX* appear to be involved in the process, structural analysis of hypertrophic chondrocytes show distinguished features from classic apoptosis, and autophagic vacuoles can be observed³.

Retinoic acid signaling in bone development

Many different signaling molecules contribute to the generation of the skeleton. Vitamin A (retinol) and its metabolites are important signaling molecules throughout embryonic development. Vitamin A is a lipid soluble molecule that must be obtained from the diet. Retinoic acid (RA), obtained from retinol in two oxidation steps, is the most active retinoid. RA has been shown to play important roles during skeletogenesis. With regard to endochondral ossification, RA seems necessary during chondroblast differentiation and chondrocyte hypertrophy. Excess of RA in condensed cells prior to chondroblast differentiation induces downregulation of the expression of chondroblast markers, such as *Col2a1*, and increased levels of condensed cells markers that are normally downregulated upon differentiation⁴. RA has also been implicated in later stages of skeletal development. In particular, excess of RA has been shown to induce excess bone, while deficiency of this molecule results in enlarged zones of cartilage with undermineralized matrix. It has also been proposed that RA has an important role in chondrocyte maturation and replacement of hypertrophic cells by bone⁴. Thus, RA has a dual role during endochondral ossification: it controls the early differentiation from condensed cells to chondroblasts and, later on, it regulates hypertrophic differentiation and replacement by bone. Eventually, RA localization, timing and levels control size and shape of bones⁴.

RA exerts its activity mainly through the binding of its nuclear receptor subfamilies retinoic acid receptors (RARs) and retinoic X receptors (RXRs). These receptors bind retinoic acid responsive elements (RAREs) in promoter regions of several genes and

regulate transcription through interactions with coactivators and corepressors. RARs and RXRs subfamilies contain three members each: α , β , γ . Within each subtype, alternative splicing and/or promoter usage generate several isoforms. This diversity may reflect different responses upon RA binding and thus gene regulation. During skeletal development, RARs and RXRs are dynamically expressed and function as important regulators of this process⁴. Interestingly, it has recently been shown that retinoids can stimulate rapid, non-genomic signaling through extra-nuclear RARs. Activation of these latter pathways triggers phosphorylation relays which regulate downstream transcription events. Eventually, the retinoids pathway is even more complicated by the potential to regulate RAR-related orphan receptors (ROR α , β , γ). RORs have also been implicated in ossification⁶.

It has been shown that both excess and deficiency of RA can have dramatic effects on development. Therefore, it is of paramount importance to fine tune its levels over time and space. RA levels depend on the activity of two groups of oxidizing enzymes: the retinaldehyde dehydrogenases (RALDHs or ALDH1a) and the cytochrome P450 retinoic acid enzymes (CYP26s). First, retinol is oxidized by retinol dehydrogenases (RDHs) to retinal. RALDHs (RALDH1, 2, and 3) then catalyze the oxidation of retinaldehyde to RA, through an irreversible reaction. The cytochrome P450 26s subfamily of enzymes (CYP26A1, B1, and C1) catalyze the oxidation of RA to 4-oxo- and 4-hydroxy-RA, retinoids which are readily excreted and seem not to play a role in development⁸ (**Figure 1.4**). During development, RALDHs and CYP26s are differentially expressed in different tissues suggesting the importance of the spatio-temporal fine tuning of RA levels.

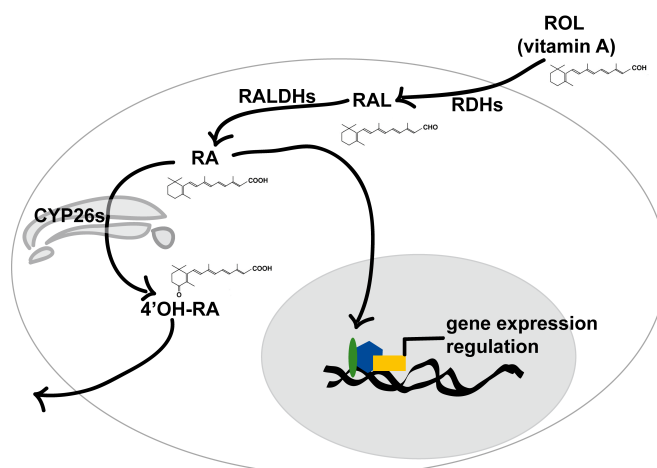


Figure 1.4: Retinoic acid pathway. Retinol (ROL), vitamin A, is assumed through diet and distributed to cells through the blood flow. Once in the cell, it may be stored or oxidized to retinal (RAL) by RDHs in the cytosol. Retinal can be oxidized to RA by RALDHs. RA can go to the nucleus to regulate gene expression or go to the microsomes, where it is catabolized by CYP26s to 4'-hydroxy-retinoic acid (4'-OH-RA), which is readily excreted by cells.

1.2 Short Stature and the *SHOX* gene

1.2.1 Short stature

Short stature affects approximately 3% of children worldwide and is diagnosed when height is significantly below the average of the general population for that person's age and gender. More precisely, short stature is statistically defined as two standard deviations (SD) below the mean population height for age, sex and ethnic group (less than the third percentile) or, when evaluating shortness in relation to family background, more than two standard deviations below the mid-parental height⁷.

As discussed above, bone development is a highly complex process which involves several factors. To date, several etiologies of short stature are known^{9;10} and many genes underlying growth control have been identified e.g. *COL2A1*¹¹ and *fibroblast growth factor receptor 3 (FGFR3)*¹². The *short stature homeobox-containing (SHOX)* gene has been associated with a broad phenotypic spectrum ranging from short stature without dysmorphic signs to profound dysplasia^{13–15}. Its varied clinical manifestations include idiopathic/isolated short stature, Léri-Weill dyschondrosteosis and Langer mesomelic dysplasia¹⁶ (**Figure 1.5**).

Idiopathic short stature

Idiopathic short stature (ISS)(OMIM 300582) is defined as a height below 2 SD in regard to age, gender and ethnic group in the absence of specific causative disorders. This term refers to individuals who do not present disorder of the growth hormone (GH)/insulin like growth factor (IGF) axis. *SHOX* was associated to ISS in 1997¹³. Nowadays it has been estimated that *SHOX* deficiency accounts for 2 to 16 % of ISS cases¹⁷. Children with ISS and *SHOX* deficiency are treated with recombinant human growth hormone (rhGH).

Léri-Weill dyschondrosteosis

Léri-Weill dyschondrosteosis (LWD) (OMIM 127300) is a skeletal dysplasia characterized by mesomelic short stature and Madelung deformity. LWD has a dominant pattern of inheritance. Mesomelic short stature refers to a disproportionate shortening of the forearms and lower legs. Madelung deformity is a skeletal abnormality of the distal radius resulting from premature closure of the distal radial growth plate leading to an increased inclination of the radius, triangulation of the carpus and dorsal displacement of the distal ulna. Madelung deformity is often associated with decreased range of movement of the wrist and pain. Affected individuals may also have other minor skeletal abnormalities e.g. micrognathia. The clinical manifestations of LWD become more pronounced with age and are often more severe in females than males. LWD was first associated to *SHOX* deficiency in 1998 by two different groups

where they showed that mutations and deletions in the *SHOX* locus co-segregated with the phenotype in several families^{14;15}.

Mutations in *SHOX* regulatory regions have also been associated to LWD¹⁸. It has been estimated that *SHOX* deficiency is responsible for 80-90% of LWD cases. Hence, *SHOX* deficiency accounts for most LWD patients and it is thought that those unresolved cases contain mutations in uncharacterized *SHOX* regulatory regions.

Treatment of LWD recommends administration of recombinant human growth hormone (hrGH). This therapy has been shown to improve the final adult height, although data suggest that it seems insufficient to prevent the development of disproportionate growth and Madelung deformity²⁰. Madelung deformity is treated with approaches like cumbersome splint or brace to keep straight the wrist to alleviate discomfort and, in severe cases, an invasive surgical intervention is necessary.

Langer mesomelic dysplasia

Langer mesomelic dysplasia (OMIM 249700) is characterized by severe limb aplasia or severe hypoplasia of the ulna, and a thickened and curved radius and tibia. Individuals present also Madelung deformity and other minor skeletal abnormalities like micrognathia. Langer mesomelic dysplasia (LMD) is more severe than LWD, supporting the hypothesis that it is an homozygous state of dyschondrosteosis. Indeed, LMD is a more severe form of LWD caused by homozygous loss of function of *SHOX*^{14;15}. Complete *SHOX* deficiency accounts for 100% cases of LMD. To date, there is no therapy for this condition.

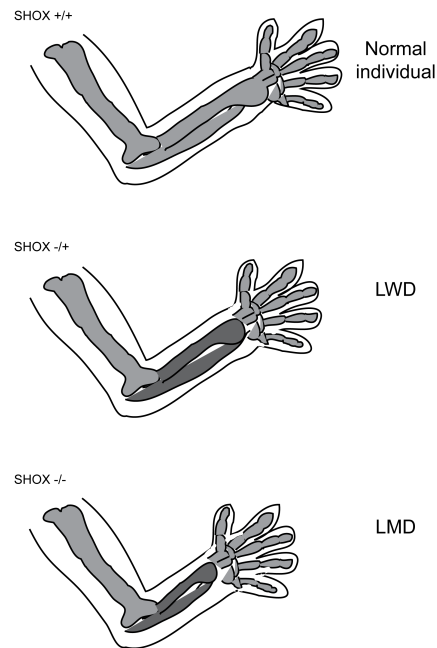


Figure 1.5: Clinical manifestations of *SHOX*-deficiency. Heterozygous mutations or deletions in *SHOX* allele lead to LWD a skeletal dysplasia characterized by mesomelic shortening of the limbs. Complete loss of functional *SHOX* causes LMD, a more severe phenotype characterized by extreme mesomelic short stature.

Turner syndrome

Turner syndrome clinical features include short stature, gonadal dysgenesis and skeletal abnormalities. Among the skeletal defects, patients can present cubitus valgus, micrognathia, high-arched palate, webbed neck, Madelung deformity. The genetic bases of Turner syndrome is partial or complete loss of one copy of the X chromosome in females. Individuals with Turner syndrome may also have cognitive deficits, diabetes, heart and kidney abnormalities and autoimmune diseases²². This condition affects about 1:2000 to 1:5000 of girls and women²¹. *SHOX* deficiency has been proposed as the cause for the skeletal abnormalities observed in Turner syndrome patients²³. Interestingly, Turner syndrome cases with trisomy of chromosome Xp, as well as for other numerical sex chromosomes abnormalities (e.g. 47,XXX) have been reported to be tall^{24;25}. Tall stature in these individuals has been linked to *SHOX* overdosage. *SHOX* overdosage leads to a delayed growth plate fusion and consequently to longer limbs²⁵. Turner syndrome associated short stature is treated with hrGH to accelerate growth.

1.3 *SHOX* gene, expression regulation and function

SHOX gene

The *SHOX* gene spans approximately 42 kb and localizes in the pseudoautosomal region (PAR1) shared between the X and Y chromosomes (chrX: 585079-607558; hg19). It consists of 6 exons encoding for two different isoforms, *SHOXa* and *SHOXb*, which differ in the 3'-end encoded exon 6¹⁶. However, RT-PCR analysis performed in fetal and adult human tissues revealed 4 novel exons which have been proposed to contribute to the fine-tuning of *SHOX* expression during development²⁶.

SHOX is expressed in the human developing limbs already at five weeks post fertilization as a band along the middle part of the limb. Analyses of human fetal and pubertal growth plates revealed *SHOX* expression in resting, proliferative, and terminally differentiated hypertrophic chondrocytes^{27;28}. Interestingly, analysis of the growth plates of LWD patients revealed a disordered distribution of the chondrocytes instead of the typical columnar organization, clearly showing abnormal endochondral ossification in *SHOX* deficiency individuals²⁷. *SHOX* is also expressed in the first and second pharyngeal arches, structures that develop into maxilla, mandible and ear²³. Noteworthy, patients with *SHOX* deficiency and Turner syndrome may present a combination of skeletal defects in the anatomical structures where *SHOX* is expressed: mesomelia, Madelung deformity, micrognathia, high-arched palate, low-set ears.

SHOX expression regulation

SHOX expression is restricted during development. Several studies have identified different mechanisms regulating *SHOX* expression¹⁶. One of the first investigations identified two alternative promoters, P1 and P2, upstream of exon 1 and exon 2, respectively. Activation of P1 or P2 generates two mRNA differing in the 5'-UTR (**Figure 1.5**). The authors demonstrated that P1 usage leads to the synthesis of transcripts containing seven AUG codons in the 5'-UTR which compete with *SHOX* starting codon, resulting in reduced translation efficiency²⁹.

Highly conserved enhancer regions have been found upstream and downstream of the *SHOX* gene. Gene reporter experiments showed enhancer activity of these regions in U2OS human cell line, chicken buds and zebrafish embryos^{31-33;40}. Furthermore, mutations and deletions of these enhancer sequences have been identified as cause of many cases of short stature. However, the molecular mechanisms controlling these regulatory sequences are not known yet. Studies in chick limb buds revealed the first evidences of proximal and distal signals regulating *Shox* expression. In particular, it has been shown that *Fgf4* and *Fgf8*, *Bmp4*, and RA reduced *Shox* mRNA levels (**Figure 1.6**)³⁴.

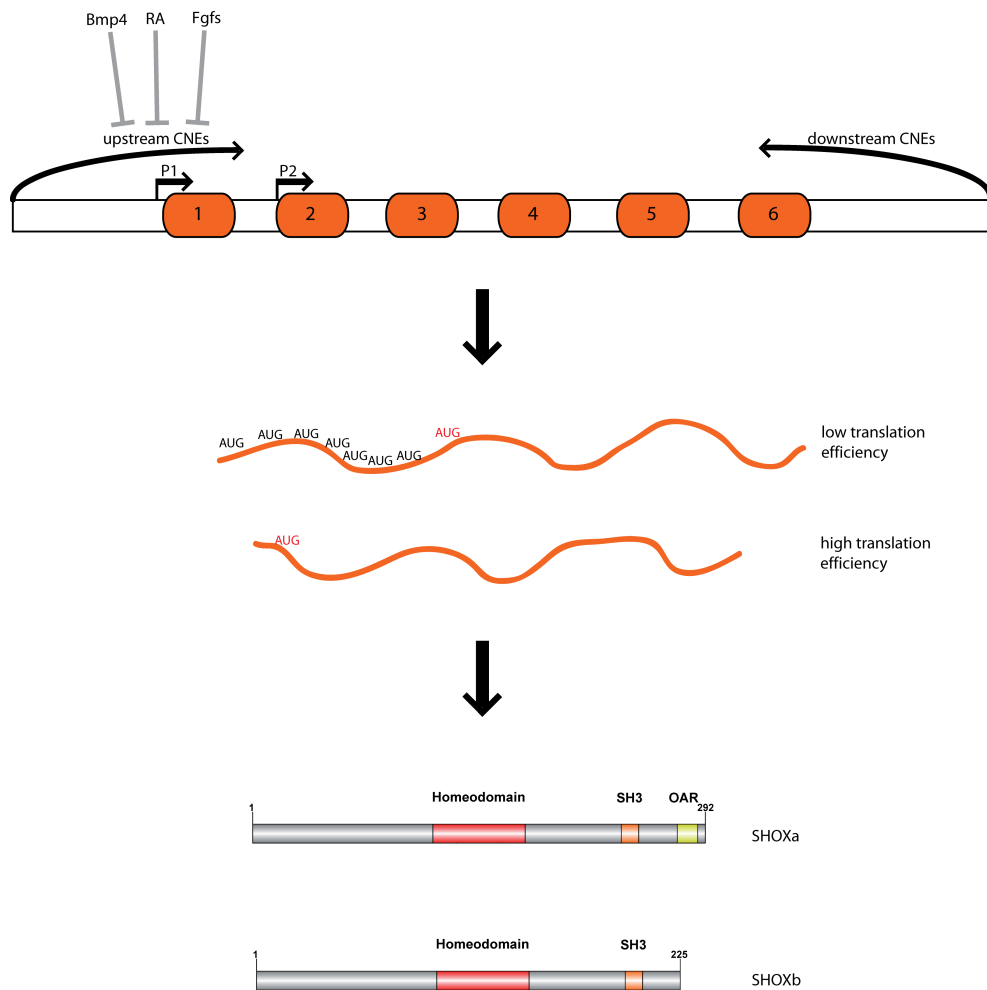


Figure 1.6: The *SHOX* gene and its expression regulation. *SHOX* localizes in PAR1 and is composed of 6 exons. Two promoters control *SHOX* expression, P1 and P2. P1 controls the synthesis of longer 5'UTR transcripts carrying seven untranslated AUG codons which may compete with the *SHOX* starting codon leading to low translation efficiency. The P2 product lacks these elements resulting in high efficient translation of *SHOX*. *SHOX* expression is also regulated by upstream and downstream conserved enhancers elements (CNEs). Moreover, experiments in chicken identified Fgf4, Fgf8, Bmp4 and RA as signal molecules capable of inhibiting *SHOX* expression in the limb buds. Finally, *SHOX* encodes for two isoforms differing in the C-terminal sequence, SHOXa and SHOXb. SHOXb lacks the OAR domain and it may be unable to transactivate its targets, but it may form heterodimers with SHOXa to regulate its transcriptional activity.

SHOX function

SHOX gene encodes for a transcription factor belonging to the homeobox-containing genes¹⁶. *SHOXa* and *SHOXb* isoforms are translated in proteins of 292 and 225 amino acids, respectively. Both isoforms contain the homeodomain, which consists of 60 amino acids. This structure is composed of three α -helices which form a helix-turn-helix motif and constitute the DNA-binding domain. Electromobility shift assay (EMSA) analysis showed that SHOX binds to palindrome motifs 5'-TAAT(N)₂₋₃ATTA-3', where N is the number of nucleotides separating the palindrome sequence. Missense mutations within the homeodomain have been reported in individuals with ISS, LWD, and LMD.

SHOX exerts its DNA binding and transcriptional activity through the formation of homo- and hetero-dimers through the homeodomain³⁵. Studies identified *brain natriuretic peptide (BNP)*, *aggrecan (ACAN)*, *FGFR3*, and *connective tissue growth factor (CTGF)* as direct targets of SHOX³⁶⁻³⁹. These genes are expressed in limbs and play a role in endochondral ossification, further supporting a role of *SHOX* in bone formation and short stature.

The two SHOX protein isoforms differ in the C-terminal sequence. In this sequence the transactivation domain Otp Aristaless Rax (OAR) is present. SHOXb lacks the OAR domain; therefore it has been suggested that it cannot perform transcriptional activity alone. However, SHOXb may regulate SHOXa transcriptional activity through the formation of heterodimers³⁵.

Missense mutations found in *SHOX* deficiency individuals helped revealing other important features of SHOX protein. Studies on LWD patients reported that substitution of A170 and R173, for example, affects the localization of SHOX protein. These studies led to the identification of the non-canonical nuclear localization signal in the peptide sequence AKCRK, which resides within the homeodomain⁴⁰⁻⁴².

High expression of SHOX can be noted in the hypertrophic region, thus cells which will soon undergo cell death to be substituted by bone tissue. It has been shown that SHOX overexpression in U2OS cells and human primary chondrocytes induces arrest in G2/M phases of the cell cycle, altered expression of cell cycle genes such as p21Cip1, oxidative stress, and cell death^{28;44}. Overexpression of SHOX bearing mutations in the homeodomain does not lead to these events, indicating that they are dependent on SHOX transcriptional activity^{28;43;44}. However, direct evidence of SHOX as regulator of genes involved in these pathways have not been reported yet.

1.4 Aim of the project

A phenotype results from the interactions between genotype and environment. It has always been of interest to understand how these relationships lead to the phenotypic variability among individuals. Although many genes have been associated to disease phenotypes, many clinical reports have shown that a phenotype might not occur as often as the related genotype.

SHOX deficiency has a high penetrance. However, the clinical severity of *SHOX* deficiency varies among individuals, even in family members with the same *SHOX* gene mutation^{45;46}. In rare cases, family members with the identical mutation present with normal stature^{19;47;48}. The aim of this study was to identify potential modifier gene(s) as basis for the observed clinical variability in LWD individuals presenting with mesomelia and Madelung deformity. This project started when we screened for mutations in the *SHOX* gene in a large German family with LWD. Finding affected and normal height individuals carrying the same *SHOX* damaging variant offered us a rare opportunity to investigate the genetic origin of the observed clinical variability. The primary goal of this project was therefore to perform genetic analyses for candidate genetic modifier(s) identification. These analyses led to the retinoic acid-metabolizing enzyme *CYP26C1* as potential modifier gene. In the second part of this thesis, functional analysis in human cells and zebrafish embryos were performed to further corroborate the hypothesis of *CYP26C1* as modifier gene for *SHOX* deficiency.

2 Materials and Methods

2.1 Patients and controls

2.1.1 Family 1 clinical data

Family 1 comprised 17 German individuals with five affected members diagnosed with Léri-Weill dyschondrosteosis. DNA was available from 14 individuals (I:1, I:2, I:3, II:3, II:4, II:6, II:7, II:8, III:1, III:2, III:3, III:4, III:5, III:6). Four females (I:2, I:3, II:7, III:2) presented a Madelung deformity (MD). In one affected male (II:3), the MD was borderline. Three female individuals (II:4, II:8, and III:1) presented with short stature, but no dysmorphic phenotype and no *SHOX* deficiency. The index patient (III:2) was treated with growth hormone from the age of 8.9 years onwards. Age of menarche was of 12 years. Further details on the clinical data are given in the Results part and on **Table 3.1**.

2.1.2 Cohort of LWD patients with *SHOX* deficiency

The sample comprised 68 unrelated cases with LWD and proven *SHOX* deficiency; it comprised 60 Europeans (28 Germans) and 9 Japanese. Two out of the 68 cases carried damaging mutations in *CYP26C1* and all the available family information was retrieved (see below).

Family 2 comprised 4 French people with two affected children; parents were unaffected. Patient II:2 presented LWD with mesomelia and Madelung deformity (available clinical data are given in **Table 3.2**). Patient II:1 presented with short stature but did not show dysmorphic signs.

Patient 3 is a Japanese girl with mesomelia and Madelung deformity (available clinical data are given in **Table 3.2**). The parents and the brother were reported having normal stature and no dysmorphic signs.

2.1.3 Cohort of ISS and LWD patients with intact *SHOX*

The cohort of ISS individuals without *SHOX* deficiency ($n = 234$) comprised 96 Germans, 13 Belgians, 10 Americans, and 115 Japanese.

The cohort of patients with LWD without *SHOX* deficiency ($n = 22$) is composed of 17 Germans, 2 French, 1 Italian, 1 Dutch, 1 Swedish.

Family 4 comprised a German family with a son affected by ISS. Clinical data from this individual nor of the parents could not be retrieved.

Family 5 comprised a Japanese family with the three ISS affected siblings (SD are given in **Figure 3.5**). Both parents were reported with stature within the normal range.

2.1.4 Controls

As controls we screened 140 Germans individuals with normal stature.

2.2 Whole Genome Linkage Analysis

Whole genome linkage analysis was performed by Dr. Gudrun Nuenrnberg (Center for Molecular Medicine Cologne and Cologne Center for Genomics, Cologne, Germany).

2.3 Whole Exome Sequencing

Whole exome sequencing was performed by Dr. Tim Strom (Institute of Human Genetics, Helmholtz Zentrum München, Neuherberg, Germany).

2.4 Reagents

Acetic Anhydride	Sigma
All Trans Retinoic Acid (ATRA)	Sigma-Aldrich
Adenosyn triphosphate (ATP)	Sigma-Aldrich
Bacto™ Tryptone	BD
Biozym LE Agarose	Biozym
Bromophenol Blue	Sigma-Aldrich
CellLytic™ B Cell Lysis Reagent	Sigma Aldrich
Citric acid	Sigma-Aldrich
Diethylpirocarbonate (DEPC)	Sigma-Aldrich
Dimethylformamide	Sigma-Aldrich
DL-Dithiothreitol (DTT)	Sigma-Aldrich
Ethylenediamine-tetracetic acid (EDTA)	AppliChem
Ethanol	Sigma-Aldrich

Materials and Methods

Formamide	Roth
Glucose	Merck
Glycerol	Sigma-Aldrich
Glycin	Sigma-Aldrich
Heparin	Sigma-Aldrich
Isopropyl- β -D-thiogalactopyranosid (IPTG)	Serva
Isopropanol	Sigma-Aldrich
KCl	Merck
KH_2PO_4	Merck
Maleic Acid	Roth
MgCl_2	AppliChem
MgSO_4	Merck
Na_2HPO_4	Merck
Na Citrate	AppliChem
NaCl	Sigma-Aldrich
Na Deoxycholate	Sigma-Aldrich
NaOH	Sigma-Aldrich
Igepal (NP-40)	Chem-Cruz
Paraformaldehyde	Roth
Polyacrilamide (37,5:1)	Roth
Proteinase K	Sigma-Aldrich
Sodium dodecyl sulfate (SDS)	Fluka
Torula yeast RNA	Sigma-Aldrich
Triethanolamine	Merck
Tris-HCl	Roth
Triton X-100	Merck
Tween-20	Roth
X-Gal	Serva
Yeast Extract	BD

2.5 Media and Supplements for Bacteriological Cultures

LB Medium	10 g Bacto-Tryptone 5 g Yeast Extract 10 g NaCl Add ddH ₂ O to 1 l and sterilize by autoclaving for 20 min at 15 psi
LB Agar Plates	Add 15 g Bact-Agar (BD) to 1 l LB Medium before autoclaving (1.5% agar)
SOB Medium	20 g Bacto-Tryptone 5 g Yeast Extract 2 ml 5M NaCl 10 ml 1M MgCl ₂ 0.5 ml 1M KCl 10 ml 1M MgSO ₄ Add dd H ₂ O to 1 l and sterilize by autoclaving for 20 min at 15 psi
SOC Medium	Add 20 ml of filter-sterilized 20% (w/v) glucose stock solution to 1 l SOB medium
2x YT Medium	16 g Bacto-Tryptone 10 g Yeast Extract 2 g NaCl Add dd H ₂ O to 800 ml, adjust pH to 7.2, fill up to 1 l, and sterilize by autoclaving for 20 min at 15 psi
Ampicillin (Roth)	100 mg/ml stock solution in 70% ethanol; used at 1:1000 dilution
Kanamycin (Roth)	30 mg/ml stock solution in ddH ₂ O; filter-sterilized; used at 1:1000 dilution
Chloramphenicol (Roth)	37.5 mg/ml stock ddH ₂ O; filter-sterilized; used at 1:1000 or 1:3000 dilutions
Streptomycin (Biochrom)	20 mg/ml stock ddH ₂ O; filter-sterilized; used at 1:2000
X-Gal (Serva)	20 mg/ml stock solution in Dimethylformamide; used at 1:1000 dilution

L-Arabinose (Sigma) 20% (w/v) arabinose stock solution in ddH₂O; filter-sterilized; used at 1:100 dilution

2.6 Media and Supplements for Cell Cultures

Dulbecco's Modified Eagle Medium (DMEM) (1x) High Glucose	(Gibco)
Opti-MEM [®] Reduced Serum Medium (1x) with GlutaMAX [™]	(Gibco)
Dulbecco's Phosphate Buffer Saline (DPBS)	(Gibco)
Fetal Bovine Serum "Gold" (FBS)	(PAA)
0.05% Trypsin-EDTA (1x) with Phenol Red	(Gibco)
Non-Essential Amino Acid supplement (NEAA) (100x)	(Gibco)
Penicillin-Streptomycin (Pen-Strep) (100x)	(Gibco)
L-Glutamine (200 mM) (100x)	(PAA)

2.7 Bacterial Strains and Cell Lines

Bacterial strains

DH5 α	<i>fhuA2</i> Δ (<i>argF-lacZ</i>)U169 <i>phoA glnV44</i> Φ 80 Δ (<i>lacZ</i>)M15 <i>gyrA96 recA1 relA1 endA1 thi-1 hsdR17</i>
NovaBlue GigaSingles™ Competent Cells	<i>endA1 hsdR17</i> (<i>r_{K12}</i> ⁻ <i>m_{K12}</i> ⁺) <i>supE44 thi-1 recA1 gyrA96 relA1</i> <i>lacF</i> [<i>proA</i> ⁺ <i>B</i> ⁺ <i>lacI^q</i> Z Δ M15:: <i>Tn10</i> (<i>Tc^R</i>)](Novagen/Merck)
XL10-Gold Ultracompetent Cells	<i>Tet^r</i> Δ (<i>mcrA</i>)183 Δ (<i>mcrCB-hsdSMR-mrr</i>)173 <i>endA1 supE44</i> <i>thi-1 recA1 gyrA96 relA1 lac Hte</i> [<i>F'</i> <i>proAB lacI^q</i> Z Δ M15 <i>Tn10</i> (<i>Tet^r</i>) <i>Amy Cam^r</i>](Agilent)
PPY	<i>F endA1 recA1 galE15 galK16 nupG rpsL</i> Δ <i>lacX74</i> Φ 80 <i>lacZ</i> Δ M15 <i>araD139</i> Δ (<i>ara,leu</i>)7697 <i>mcrA</i> Δ (<i>mrr-hsdRMS-mrcBC</i>) <i>cynX</i> ::[<i>araC pBAD-redα EM7-redβ</i> <i>Tn5-gam</i>] λ -

Cell lines

HEK293	Human Embryonic Kidney cell line; ATCC
U-2 OS	Human Osteosarcoma cell line; ATCC

Primary cells

Human Primary Chondrocytes

2.8 Plasmids

pUC19	Invitrogen
pcDNA4/TO	Invitrogen
pIRES2-EGFP	Clontech
pGL3promoter	Promega
pRL-TK	Promega

pSTBlue-1

Novagen/Merck

2.9 Oligos

Primers for whole-exome sequencing Sanger sequencing validation

Primers were designed using Primer3⁴⁹.

Gene symbol	Sequence (5'-3')
<i>EXO1</i>	for TGTTCCTGTTCTTTAGTTGCAGA rev AGGATACTGCCAGCGTAGC
<i>SYNDIG1</i>	for TGACTTCCTTTTTCTTCTCCAACCTC rev ACAAATAAATCCATGGGTAGGAAA
<i>CYP26C1</i>	for CCTCCAGCCGCTTCCATTAC rev CGTTTGCGAACATTTGTTGA
<i>OPN4</i>	for CGAGTGCCCTGCAAGGATAG rev TCCCAACCCTTTAGCCACT
<i>LAMA1</i>	for GACACACACGGCGAGATAGAGATT rev CCCCTCTCTCCTGAGATGTTCAAT
<i>TXNDC11</i>	for CAGCCATTAGCTGCCAGAGT rev GGGCCTTAGAAAACCAGGAG
<i>BIRC7</i>	for ACCTAAAGACAGTGCCAAGTGC rev GAAACACTCAGCCAGCAGAGAC
<i>USP19</i>	for CCCGCTCCTTAGCCAACTCT rev CCTGGTGTTCAGGCCCTCTC
<i>MACF1</i>	for ACTTCTCCACCAAGCTGAGGTC rev CAACTGTTTGTTTCAGGGCTTC
<i>NRAP</i>	for AGCCTTGGTTGTATCCGCTAACA rev TCCAACCTTCTTGTGATGGGTGA
<i>USP28</i>	for TGAGCAGTACAGATTTTCCCAAT rev GACTTACAGGTGCCTTATCGCTTG

<i>CLTC</i>	for GGTCTGCTTCGCCTGTGTAGA rev TTCTGCCCAAAGATGAGCTTG
<i>FLYWCH1</i>	for GGGACAAGGTGTATTGGACCTG rev ACCTCTGGAGGCAAGAGTCAAG
<i>PLB1</i>	for CTGAAAAGCCCCAGAACTCCT rev TGTCCAAGGGTGTGAGGATCT
<i>FAT2</i>	for CACCATGTCAGAGCCCTCAT rev AGTCGTGATGCCAGAGCCTA
<i>GPD1</i>	for CCGTTGCCTTGGAGAAGTAG rev GAGATGGCTAAGTGGGGTTG
<i>ZNF267</i>	for AGTGA CTCTCAGGTCTTACTGTGC rev TTCTCTGCTATTGTGTAAGGCTTGA
<i>PIP5K1B</i>	for GGAGCCAATTTGGGACATTA rev AAACCTTCCTTACCCGGCAGT
<i>ACAN</i>	for GGTCACTGGTAAGAGAGGGACTCA rev TTATGGACAAGGCTGTTTTTGTCA
<i>OR1S2</i>	for TTCCGTAGAACAGTAATGCAAT rev CAACCAGGCTGAACATCAAA
<i>LARP7</i>	for TTCTGGCATAACCATTGGAA rev AGGATCTCGAGTTTCCAGCA
<i>SLC10A2</i>	for ATCGGCCTCCATTACTTTTTCAC rev AATGAACCCTCTTGGCCACTTA
<i>PCDH8</i>	for GCCACTTCTAGGGAGCCATTG rev CTCTATGGGCACGAGCACTTC
<i>ZNF33B</i>	for TCACTTCCTAACAAAAGCCATCC rev GCCAGAAGTCACA ACTCACTCA
<i>SUPV3L1</i>	for AATTTGGAGGGCTTTCCATC rev ACCAAAAATCCCCCAGTACC

<i>PIK3R6</i>	for CAGCCTAATTACCCGCCTCT rev CCCTGGAGCACTATTTCCAC
<i>AOC2</i>	for CATCCCTGAGGTCTCGGAAC rev GATATAACCCGTGGCATGGAC
<i>DOCK1</i>	for TGGTCTCGATTCCACACAGC rev TTGGGCACTACGGTCAGAAA
<i>RIMBP2</i>	for TGACGTGGCTGTAGTTGCTG rev ATCGACGACATCGGAGAAGA
<i>IGSF3</i>	for TGACGTGGCTGTAGTTGCTG rev ATCGACGACATCGGAGAAGA
<i>TNKS1BP1</i>	for CTATATGGGGCCATGCACTT rev CTGGCTGAGTTGCCTTCCTG
<i>KIF4A</i>	for AAGCCCGTGCACTCTCTTTA rev ATGAAAGGCAAGACCACACC
<i>LIG4</i>	for TGATGTTCTCAGACCCTGCAAT rev CTCCACCAAGCAGCATTTTATG
<i>PCLO</i>	for GTGGTTGGCTTTACCATCTTGG rev AGACTTCCCCAAAGAAGGATGC

***CYP26C1* Sanger sequencing primers**

Primers were designed using Primer3⁴⁹.

Name	Sequence (5'-3')
<i>CYP26C1</i> -Exon1	for CTTATAAATCTCGGGCTTTGC rev GGGAAGAAGGGACCGTATTA
<i>CYP26C1</i> -Exon2	for CCAGGGACAGGAAGTTGTG rev CCGACGTATCTACGGTCCA
<i>CYP26C1</i> -Exon3	for GAGAAAGGACCGGAACTGG rev GAGCCTCGGAGGAAGGTC
<i>CYP26C1</i> -Exon4	for TGAGAAGGTTTCTGGGTAAGTG rev GTCATTACTGGAACCCAGGTCT
<i>CYP26C1</i> -Exon5	for CGACTTCAAAAACCGTACACA rev TCTGAGGGCAAAAGAGGTG
<i>CYP26C1</i> -Exon6	for GTGGTCAGGCTGATCTCCTC rev TGGCGAACATTTGTTGAAAG

Primers to analyze *SHOX* p.Val161Ala mutation in the family study

Primers were designed using Primer3⁴⁹.

<i>SHOX</i> -Exon3	for GCCACGTTGCGCAAAACCTC rev CCCGAGGACCAGGCGATG
--------------------	--

***CYP26C1* GS Junior Roche sequencing primers**

Primers were designed using Primer3⁴⁹.

Barcodes were attached to each primer:

5'-ACACTGACGACATGGTTCTACA-specific forward primer-3'

5'-TACGGTAGCAGAGACTTGGTCT-specific reverse primer-3'

Name	Sequence (5'-3')
<i>CYP26C1</i> -Exon1a	for CTTATAAATCTCGGGCTTTGC

	rev AACTAACCAGTGCAGCGTTT
CYP26C1-Exon1b	for GAGCTGCCTGTCAGTGCT rev GGGAAGAAGGGACCGTATTA
CYP26C1-Exon2a	for CCAGGGACAGGAAGTTGTG rev ACCGCACCTAGCAGTGTG
CYP26C1-Exon2b	for ACAGTGTTCAAGACGCACCT rev CCGACGTATCTACGGTCCA
CYP26C1-Exon3a	for GAGAAAGGACCGGAACTGG rev TGAGAAGAGGTTCTCCACGAG
CYP26C1-Exon3b	for AGTCTACGACGCCTCCAAAG rev GAGCCTCGGAGGAAGGTC
CYP26C1-Exon4a	for TGAGAAGGTTTTCTGGGTAAGTG rev CTTGCACTGTGAATGATTAGGTC
CYP26C1-Exon4b	for ATCTTTCTTCTCTCCCTGAACATC rev GTCATTACTGGAACCCAGGTCT
CYP26C1-Exon5a	for CGACTTCAAACCGTACACA rev AGCTCCTCCCGAATCTTG
CYP26C1-Exon5b	for GCTCGTCCTGCTGCTACTG rev CAGCACCTCCTTGACCAC
CYP26C1-Exon5c	for AAGATTCTGGGAGGAGCTG rev TCTGAGGGCAAAGAGGTG
CYP26C1-Exon6a	for GTGGTCAGGCTGATCTCCTC rev GAACGGGATGTAATGGAAGC
CYP26C1-Exon6b	for GATGTATAGCATCCGGGACAC rev GTCAGAGGCATAGCCCATTG
CYP26C1-Exon6c	for CTGCGGCTCTTTTTCCAC rev TGGCGAACATTTGTTGAAAG

Primers for CYP26C1 SLiCE cloning

Name	Sequence (5'-3')
pcDNA4-HisMaxC/CYP26C1exon1 (3')	TGGTACCGAGCTCGGATCC/ ATGTTCCCTTGGGGGCTGAG
CYP26C1exon1/CYP26C1exon2 (5')	AGCGCGAGCC/ CTGAACTAACCAGTGCAGCG
CYP26C1exon1/CYP26C1exon2 (3')	CACTGGTTAGTTCAG/ GGCTCGCGCTTCCACAGTTCTC
CYP26C1exon2/CYP26C1exon3 (5')	GCGCCAGGAC/ CTTGCGCCGCCGCCGG
CYP26C1exon2/CYP26C1exon3 (3')	GCGGCGCAAG/ GTCCTGGCGCGCGTGTTC
CYP26C1exon3/CYP26C1exon4 (5')	CCCGGATGCC/ CTTGCGTAGGCCACTGAAGGG
CYP26C1exon3/CYP26C1exon4 (3')	GGCCTACGCAAG/ GGCATCCGGGCAAGGGAC
CYP26C1exon4/CYP26C1exon5 (5')	CACAGCCGACTC/ CTTCAGCTCCTGCATGGAGGG
CYP26C1exon4/CYP26C1exon5 (3')	GCAGGAGCTGAAG/ GAGTCGGCTGTGGAGCTCC
CYP26C1exon5/CYP26C1exon6 (5')	GGATCTGGTAGCC/ GTCGAGCTCGAAGGTGCGC
CYP26C1exon5/CYP26C1exon6 (3')	CTTCGAGCTCGAC/ GGCTACCAGATCCCCAAGG
CYP26C1exon6/pcDNA4-HisMaxC (5')	TGGATATCTGCAGAATTC/ TCAGAGGCATAGCCCATTCC

Mutagenesis primers

Primers were designed according to the recommendations in the manual QuickChange Lightning Site-directed mutagenesis Kit (Stratagene).

Name	Sequence (5'-3')
SHOX Val161Ala	for CTCCGAGGCGCGCG[T>C]GCAGGTAGGAAC rev GTTCCTACCTGC[A>G]CGCGCGCCTCGGAG
SHOX Leu132Val	for AGCAGCTGAACGAG[C>G]TCGAGCGACTCTTC rev GAAGAGTCGCTCGA[G>C]CTCGTTCAGCTGCT
SHOX Arg153Leu	already present in our lab (Schneider K. U. et al., 2005)
CYP26C1 Phe508Cys	for CGGCTCTTT[T>G]CCACCCCCTCACGCCTTCGG rev GAGGGGTGG[A>C]AAAAGAGCCGCAGCCCGTC
CYP26C1 Cys459Ala	for GTGCGCGCAGC[TG>GC]CCTCGGCCAGGAGC/ TGGCGC rev CTGGCCGAGG[CA>GC]GCTGCGCGCACCGCCG/ CCG
CYP26C1 Arg378His	for CAAGGAGGTGCTGC[G>A]CCTCCTGCCGCC rev GGCGGCAGGAGG[C>T]GCAGCACCTCCTTG
CYP26C1 Gln119Pro	for CAGTGGCCGC[A>C]GAGTGCGCACATCC rev GGATGTGCGCACTC[T>G]GCGGCCACTG

RT-PCR primers

Primers were designed using Primer3⁴⁹.

Name	Sequence (5'-3')
<i>SOX9</i>	for GAAGGACCACCCGGATTACA rev CGTTGACATCGAAGGTCTCG
<i>SHOX</i>	for AAGTTTTGGAGAGCGGACTG rev GCCTCTGTTTCAGCTTGGTC
<i>CYP26C1</i>	for GTTCCCTTCAGTGGCCTACG rev ACAGCCGACTCCTTCAGCTC

qPCR primers

Primers were designed using Universal Probe Library Assay Design Center (Roche).

Species	Name	Sequence (5'-3')
	<i>HPRT</i>	for TGATAGATCCATTCCTATGACTGAGA rev AAGACATTCTTTCCAGTTAAAGTTGAG
Human	<i>SDHA</i>	for TGGGAACAAGAGGGCATCTG rev CCACCACTGCATCAAATTCATG
	<i>SHOX</i>	for TGTTCAAGGACCACGTAGACA rev GCGCTTCTCTTTGCATTCAT
	<i>β-actin</i>	for GCAATGAGCGTTTCCGTTGC rev TGGATACCGCAAGATTCCATACCC
Zebrafish	<i>eef1α</i>	for TCTCTACCTACCCTCCTCTTGGTC rev TTGGTCTTGGCAGCCTTCTGTG
	<i>shox</i>	for GGTCGCTCCTTACGTGAATATGGG rev TGCAACTGAGCCTGAACCTGTTG

Whole-mount *in situ* hybridization probes primers

Primers were designed using Primer3⁴⁹.

Name	Sequence (5'-3')
<i>sox9</i>	for AAAGCGGATCTGAAACGAGA rev CCATCATGCACTGAACGAAC
<i>col2a1</i>	for CATCAACGGGCAGATTGAGG rev CAGCACGACTTTATTTTGCGT
<i>sox</i>	for CGAATCCACGTTGAGCAGA rev TGAGTGTACGGCCTTTTC

Morpholino sequences

Morpholino where purchased from Gene Tools

Name	Target	Sequence (5'-3')
<i>cyp26c1</i> MO	exon3-intron3 junction	AACTACGGTTATCCTCACCTTGCGC
<i>sox</i> MO1	exon2-intron2 junction	CGCATGGAAGAATGGGAGCTTACCT
<i>sox</i> MO2	exon1-intron1 junction	CGTGCAGAAGAACTCACCGTCAGA

Morpholino efficacy test primers

Primers were designed using Primer3⁴⁹.

Name	Sequence (5'-3')
<i>cyp26c1</i> MO test	for TATAGGATCCTTTTGGGCAAACCTCTCATC rev TATAGGATCCAGTAATCGCTGGCTTGCTGT
<i>sox</i> MO1 test	for TATAGGATCCGAGTTTAGCGTGACAAGGGC rev TATAGGATCCGGTGAGGATGGGAGTGTGTT
<i>sox</i> MO2 test	for TATAGGATCCTGAGCAGATAAAAGATTCGCGTTA rev TATAGGATCCGAAACTGCAACTGAGCCTGAACCT

2.10 Antibodies

Primary antibodies

Target	Organism	Number	Company
human CYP26C1 IgG	rabbit	SAB1300952	Sigma-Aldrich

Secondary antibodies

Target	Organism	Label	Number	Company
rabbit IgG	donkey	IRDye [®] 800CW	926-32213	LI-COR

2.11 Kits

DNA isolation and purification

MinElute [™] PCR Purification Kit	Qiagen
MinElute [™] Reaction Cleanup Kit	Qiagen
MinElute [™] Gel Extraction Kit	Qiagen
QIAquick [®] Nucleotide Removal Kit	Qiagen
GeneJET Plasmid Miniprep Kit	Thermo Scientific
PureLink [™] HiPure Plasmid Midiprep Kit	Invitrogen

PCR

Taq DNA Polymerase with ThermoPol [®] Buffer	New England Biolabs
Paq5000 DNA Polymerase	Agilent Technologies
HotStarTaq DNA Polymerase	Qiagen
Phusion Hot Start II High Fidelity DNA Polymerase	Thermo Scientific
Q5 [®] High-Fidelity DNA Polymerase	New England Biolabs

DNA sequencing

ExoI	Thermo Scientific
DYenamic™ ET Dye Terminator Premix	GE-HealthCare
Sephadex™ G-50 Fine DNA Grade	GE-HealthCare
MultiScreen 96-well plates	Millipore

Real time PCR

SensiFAST™ SYBR® Lo-ROX Kit	Bioline
-----------------------------	---------

Site-directed mutagenesis

QuickChange® Lightning Site-Directed Mutagenesis Kit	Stratagene
--	------------

Cloning

FastDigest™ Restriction Enzymes	Thermo Scientific
FastAP Thermosensitive Alkaline Phosphatase	Thermo Scientific
T4 DNA Ligase	Thermo Scientific
pSTBlue-1 AccepTor™ Vector	Novagen
Mix & Go <i>E.coli</i> Transformation Kit and Buffer Set	Zymo Research

Total RNA extraction

TRIzol®	Ambion
---------	--------

cDNA synthesis

SuperScript® II First-Strand Synthesis System for RT-PCR	Invitrogen
--	------------

in vitro RNA synthesis

MEGAscript® T7 Kit	Ambion
MEGAscript® SP6 Kit	Ambion

DIG RNA Labeling Mix

Roche

Reagents for transfection of eukaryotic cells

Lipofectamine[®] 2000

Invitrogen

PEI

Sigma

Protein assays

Bicinchoninic Acid Kit for Protein Determination

Sigma

1x Protease-Inhibitor Mix G

SERVA

Luciferase assay

Dual-Luciferase[®] Reporter Assay System

Promega

Signal RARE Reporter Assay Kit (LUC)

Qiagen

Detection of *in situ* hybridization probes

Blocking Reagent

Roche

Anti-Digoxigenin-AP Fab fragments

Roche

BM Purple AP Substrate precipitating

Roche

2.12 DNA-based Methods

2.12.1 PCR

PCR were performed to amplify DNA fragments for subsequent sequencing, cloning, mutagenesis and expression analysis. Amplification conditions were set according to the manufacturer's manuals.

2.12.2 Real time PCR

Real time PCRs were performed using the SensiFAST™ SYBR® Lo-ROX Kit and run in the 7500 Fast Real Time PCR System (Applied Biosystems).

Reaction mix were assembled as follows:

10 μ l	SensiFAST SYBR Lo-ROX Mix (2x)
0.8 μ l	Forward primer (10 μ M)
0.8 μ l	Reverse primer (10 μ M)
2 μ l	Template DNA
X μ l (final volume 20 μ l)	DNase-free water

2.12.3 DNA purification

PCR fragments or linearised vectors were purified using MinElute™ PCR Purification, Reaction Cleanup, and Gel Extraction Kits following the manufacturer's manuals. Plasmid DNAs were purified using GeneJET Plasmid Miniprep Kit or PureLink™ HiPure Plasmid Midiprep Kit from 5 ml or 100 ml overnight culture, respectively.

2.12.4 Cloning

Restriction digestion

Plasmids and PCR fragments were digested with FastDigest restriction enzymes according to the recommendations.

Dephosphorylation

Digested vectors were dephosphorylated with FastAP Thermosensitive Alkaline Phosphatase to prevent self ligation.

Ligation

Vectors and inserts were purified, mixed in a molar ratio 1:3, and ligated using T4 DNA Ligase according to the manufacturer's recommendations.

psTBlue-1 cloning

RNA *in situ* probes were prepared from DNA template and cloned in pSTBlue-1 vector. PCRs were performed with HotStarTaq DNA polymerase from cDNA prepared from 36 hours post-fertilization zebrafish embryos. PCR fragments were gel-purified and then cloned in the vector using the pSTBlue-1 AccepTor™ Vector according to manufacturer's protocol.

Site-directed mutagenesis

Mutations were introduced in SHOX and CYP26C1 with the QuikChange Lightning Site-Directed Mutagenesis Kit. Primer design and reactions were carried out following the manufacturer's manual.

SLiCE cloning

SLiCE (Seamless Ligation Cloning Extract) is a bacterial cell extract used to assemble multiple DNA fragments DNA molecules via single in vitro recombination reaction⁵⁰. This strategy requires short end homologies (≥ 15 bp) between fragments.

To prepare SLiCE extract:

- Streak PPY glycerol stock (kind gift obtained from Dr. Yongwei Zhang) on a LB agar plate (10 $\mu\text{g/ml}$ streptomycin and 12.5 $\mu\text{g/ml}$ chloramphenicol);
- Incubate at 37°C overnight;
- Pick up a single colony and grow into a 50 ml tube containing 25 ml 2x YT medium with 10 $\mu\text{g/ml}$ streptomycin;
- Incubate at 37°C shaking 250 rpm overnight;
- Dilute cells to 0.03 OD₆₀₀ in a 500 ml flask of 2x YT medium with 10 $\mu\text{g/ml}$ streptomycin;
- Incubate at 37°C 250 rpm until the culture reaches 0.6 OD₆₀₀;
- Induce expression by adding L-arabinose to a final concentration of 0.2%;
- Incubate for 4-6 hours at 37°C 250 rpm;
- Transfer cells into two 50 ml centrifuge tubes and pellet at 5,000 x g for 20 minutes at 4°C;
- Wash pellets with 50 ml ddH₂O and repeat centrifugation step;
- Resuspend pellets in 300 μl CelLytic™ B Cell Lysis Reagent;
- Transfer cells into a low-binding 1.5 ml tube and incubate at room temperature for 10 minutes to allow lysis;
- Centrifuge lysates at 20,000 x g for 2 minutes at room temperature;
- Collect supernatant into a new 1.5 ml tube, mix with equal volume of 100% autoclaved glycerol and dispense in low-binding PCR tubes;
- Store SLiCE extract at -80°C

SLiCE cloning were performed as follows:

- Linearise vector by restriction digestion or PCR;
- Amplify inserts by PCR reaction with primers containing homologies (18-20 nt) to the vector or the flanking fragments;
- Gel purify vector and inserts;
- Assemble SLiCE reaction as described below;
- Incubate at 37°C for 1 hour and then place on ice;
- Transform into electro/chemo competent DH5 α cell strain.

SLiCE reactions were assembled as follows:

X μ l	linearised vector (50-100 ng)
X μ l	assembly fragments (1:1 or 1:3 molar ratio vector:fragment)
1 μ l	10x SLiCE buffer
1 μ l	10x PPY SLiCE extract
X μ l (final volume 10 μ l)	Nuclease-free water

SLiCE buffer (stored at -20°C):

500 μ l	1 M Tris-HCl pH 7.5
50 μ l	2 M MgCl ₂
100 μ l	100 mM ATP
10 μ l	1 M DTT
440 μ l	Nuclease-free water

Transformation

Transformations in DH5 α cells were performed as follows:

Electro-competent cells:

- Purify ligation reaction (or SLiCE reaction);
- Add DNA to 100 μ l of thawed cells;
- Electroporate at 1,800 V and followed by adding 500 μ l of pre-warmed SOC medium;
- Incubate cells for 60 minutes at 37°C in a bench shaker at 300 rpm;
- Distribute 50-100 μ l of bacteria on pre-warmed LB-agar plates with appropriate antibiotic and grown overnight at 37°C.

Chemo-competent cells:

- Purify ligation reaction (or SLiCE reaction);
- Add 1-2 μ l of DNA to 100 μ l of thawed cells;
- Incubate 5-10 minutes on ice and add 500 μ l of pre-warmed SOC medium;
- Incubate cells for 60 minutes at 37°C in a bench shaker at 300 rpm;
- Distribute 50-100 μ l of bacteria on pre-warmed LB-agar plates with appropriate antibiotic and grown overnight at 37°C.

Electro-competent cells preparation

- Streak cells on a LB-agar plate without antibiotics;
- Pick up one colony and let it grow in 50 ml LB-media without antibiotics shaking at 250 rpm at 37°C overnight;
- Prepare 4x 2 ml flasks with 500 ml LB-media without antibiotics and 1x 2ml flask with 400 ml LB-media without antibiotics and add 5 and 4 ml of overnight culture, respectively;
- Let the cells grow shaking at 250 rpm until they reach 0.4 OD₆₀₀ ;
- Transfer cells in pre-chilled (on ice) centrifuge tubes;
- Incubate on ice for 30 minutes;
- Centrifuge at 8,000 g at 4°C for 15 minutes;
- Wash pellet with 200 ml of autoclaved ice-cold ddH₂O;
- Repeat centrifugation step;
- Wash pellet with 100 ml of autoclaved ice-cold ddH₂O;
- Repeat centrifugation step;
- Wash pellet with 40 ml autoclaved ice-cold ddH₂O with 10% v/v autoclaved glycerol;
- Transfer cells to ice-cold 50 ml tubes;
- Repeat centrifugation step;
- Resuspend pellet with a 1:1 volume of autoclaved ice-cold ddH₂O with 10% v/v autoclaved glycerol;
- Aliquot 100 µl of cells into pre-chilled 1.5 ml tubes (-20°C);
- Put tubes immediately in liquid nitrogen;
- Store at -80°C.

Chemo-competent cells preparation

Chemocompetent cells were prepared with the Mix & Go *E.coli* Transformation Kit and Buffer Set:

- Streak cells on a LB-agar plate without antibiotics;
- Pick up one colony and let it grow in 50 ml LB-media without antibiotics at 250 rpm at 37°C overnight;
- Grow 0.5 ml of overnight culture in 50 ml of ZymoBroth™ (Zymo Research) medium until they reach 0.4 OD₆₀₀;
- Prepare fresh Wash and Competent Buffer by diluting each of them 1:1 with Dilution Buffer, keep on ice;
- Transfer cells in 50 ml ice-cold tubes;

- Incubate on ice for 10 minutes;
- Centrifuge at 2,500 g at 4°C for 10 minutes;
- Wash pellet on ice in 5 ml ice-cold Wash Buffer;
- Repeat centrifugation step;
- Remove as much as possible of Wash Buffer and gently resuspend the cells in 5ml ice-cold Competent Buffer;
- Aliquot on dry-ice 0.05-0.1 ml of cells into pre-chilled (-20°C) 1.5 ml tubes;
- Store at -80°C.

Transformation efficiency calculation

Transformation efficiency of prepared electro- or chemocompetent cells was calculated as follows.

- Transform 1 μ l (10 pg) of control pUC19 DNA into 50 μ l cells;
- Grow by adding 500 μ l of SOC medium;
- Dilute 50 μ l in 1 ml;
- Plate 50 μ l of cells;
- Count colonies;
- Calculate efficiency with the formula:

$$\text{Transformation Efficiency} = \text{n}^\circ \text{ colonies} \times \mu\text{g DNA} \times \text{dilution factor}$$

2.12.5 Agarose gel electrophoresis

Agarose gels 1-2 % in 1x TAE buffer were run at 80-150 V to verify or gel purify DNA fragments. Depending on the size of the bands to analyse, the markers GeneRuler 100 bp Plus DNA Ladder (Thermo Scientific) or GeneRuler 1 kb DNA Ladder (Thermo Scientific) were used.

TAE buffer 50x (stored at room temperature):

242 g	Tris-HCl
100 ml	0.5 mM EDTA
57.1 ml	glacial acetic acid
Adjust to pH 8.3	
X 1 (final volume 1 l)	ddH ₂ O

2.12.6 DNA sequencing

After PCR amplicons were treated with ExoI and FastAP to degrade single strand DNA molecules and dephosphorylate free dNTPs:

0.25 μ l	ExoI (20 U/ μ l)
0.50 μ l	FastAP (1 U/ μ l)
0.75 μ l	PCR product
2.5 μ l	Nuclease-free water

After treatment PCR products were prepared for Sanger sequencing as follows:

2 μ l	PCR product
0.25 μ l	Primer Forward or Reverse (20 μ M)
1 μ l	DYenamic TM ET Dye Terminator Premix
1.75 μ l	Nuclease-free water

Cycling conditions:

30x	95°C	20 seconds
	60°C	2 minutes

Finally, 15 μ l nuclease-free water were added to each sample. Reactions were then purified with pre-hydrated SephadexTM G-50 Fine DNA Grade in MultiScreen 96-well plates. Briefly, the plates were filled with sephadex and hydrated with 300 μ l of ddH₂O overnight (3-4 hours are sufficient). Plates were then spun down at 3500 x g for 5 minutes and washed with 100 μ l of ddH₂O. Sequencing reactions were finally loaded on the plate, centrifuged at 3500 x g for 5 minutes and run on the MegaBACETM System (GE Healthcare). Data were analysed using the MegaBACE Sequence Analyzer (v3.0).

2.13 RNA-based Methods

2.13.1 RNA isolation from human cells

Total RNA was isolated from cells as follows.

- Remove growth media from cells;
- Wash cells once or twice with PBS;
- Add a volume of TRIzol® adequate to cover the surface of the well;
- Pipette up-down several times to resuspend the cells;
- Transfer the volume into RNase-free tubes and incubate 5 minutes at room temperature to allow cell lysis;
- Add chlorophorm 0.2 ml per ml of TRIzol used and shake vigorously the tubes for 15 seconds;
- Incubate the tubes for 2-3 minutes at room temperature;
- Centrifuge at 12,000 x g for 15 minutes at 4°C;
- Transfer the aqueous phase to a new RNase-free tube;
- Add 100% isopropanol 0.5 ml per 1 ml of TRIzol;
- Incubate at room temperature for 10 minutes;
- Centrifuge at 12,000 x g for 10 minutes at 4°C;
- Remove the supernatant from the tube, leaving the RNA pellet;
- Wash the pellet with 1 ml of 75% ethanol per 1 ml of TRIzol and briefly vortex;
- Centrifuge at 7,500 x g for 5 minutes at 4°C;
- Remove supernatant and air-dry pellet;
- Add 15-50 µl of RNase-free water and up-down pipette the solution to resuspend the pellet;
- Incubate in a heat block at 55-60°C for 10-15 minutes;
- Proceed to downstream applications or store at -80°C.

2.13.2 Reverse-transcription PCR

RT-PCR was performed using the SuperScript™ II Kit according to the manual.

1 µg total RNA was reverse transcribed as follows:

- Prepare:

X µl	total RNA (1 µg)
1 µl	dNTPs (10 µM)
1 µl	Random examers (50 ng/µl)
X µl (final volume 10 µl)	Nuclease-free water

- Incubate reactions for 5 minutes at 65°C and cool down on ice for more than 1 minute;
- Add:

2 μ l	RT-buffer (10x)
4 μ l	MgCl ₂ (25 mM)
2 μ l	DTT (0.1 M)
1 μ l	RNaseOUT™ inhibitor (40 U/ μ l)
- Mix gently and brief centrifuge;
- Incubate at 25°C for 2 minutes;
- Add 1 μ l of SuperScript™ II RT (200 U/ μ l) enzyme and mix by pipetting gently up and down;
- Incubate at 25°C for 10 minutes;
- Incubate at 42°C for 90 minutes;
- Incubate at 70°C for 15 minutes;
- Add 1 μ l RNase H (2 U/ μ l) and incubate at 37°C for 20 minutes;
- Add 40 μ l of Nuclease-free water.

2.13.3 DIG-RNA probes synthesis

DIG-RNA synthesis of probes for whole-mount *in situ* hybridization were prepared using the DIG RNA Labeling mix with the MEGAscript® SP6/T7 Transcription Kit as follows:

- Linearise the pSTBlue-1 vector containing the probe sequence with the appropriate restriction enzyme;
- Gel-purify the linearised vector;
- Prepare:

X μ l	corresponding to 1 μ g of linearised vector
2 μ l	Transcription Buffer with DTT (10x)
2 μ l	DIG RNA Labeling Mix (10x)
1 μ l	RNaseOUT™ inhibitor (40 U/ μ l)
1 μ l	SP6 (20 U/ μ l) or T7 (15 U/ μ l) RNA polymerase
X μ l (final volume 20 μ l)	Nuclease-free water
- Incubate at 37°C for 2 hours;
- Add 1 μ l of TURBO DNase (2 U/ μ l);
- Incubate at 37°C for 15 minutes;
- Add 1 μ l of EDTA (0.5 M);
- Add 1.3 μ l LiCl (8 M);

Materials and Methods

- Add 70 μ l cold absolute Ethanol (-20°C) and incubate at room temperature for 1 hour;
- Centrifuge at maximum speed with bench microcentrifuge at 4°C for 30 minutes;
- Discard the supernatant and wash with 1 ml of cold 75% Ethanol-DEPC water (-20°C);
- Centrifuge at maximum speed with bench microcentrifuge at 4°C for 10 minutes;
- Let the pellet air-dry at room temperature for 10-15 minutes;
- Resuspend the pellet with 20 μ l of 2x SSCT-50% Formamide;
- Check the probe on an agarose gel and store at -20°C.

SSC 20x:

87.65 g	NaCl
44.1 g	NaCitrate

Bring volume to 350 ml with DEPC water
Adjust pH to 4.5/5.0 with Citric acid (1 M)
Bring volume to 500 ml
Autoclave

2x SSCT-50% Formamide:

5 ml	2x SSCT
5 ml	50% Formamide

2.14 Protein-based Methods

2.14.1 Protein isolation

Proteins were isolated from cells grown in 6-well plates as follows:

- Place cell plates on ice and wash twice with PBS;
- Add 300 μ l of RIPA or Tris-Triton buffer supplemented with 1x Protease-Inhibitor Mix G and use the cell scraper to harvest them;
- Transfer the cells in a 1.5 ml tube and incubate on ice for 10 minutes to allow lysis;
- Centrifuge at maximum speed with a bench microcentrifuge at 4°C for 30 minutes;
- Transfer the supernatant containing the protein lysate in a new 1.5 ml tube and store at -80°C.

RIPA buffer:

25 mM	Tris-HCl pH 7.6
150 mM	NaCl
1%	NP-40
1%	sodium deoxycholate
0.1 %	SDS

Tris-Triton buffer:

10 mM	Tris-HCl pH 7.4
100 mM	NaCl
1%	Triton X-100
10%	Glycerol
1%	sodium deoxycholate
0.1 %	SDS

2.14.2 Microsome enrichment

Microsomal preparations were obtained following the instruction of a protocol which can be found at www.biomol.de/infos-general.html?id=246. The protocol works as follows:

- Place cell plates on ice and wash 3 times with 2 ml of resuspension solution;
- Resuspend the cells with a cell scraper in 1.5 ml of resuspension solution supplemented with 1x Protease-Inhibitor Mix G;
- Centrifuge at 360 g with a bench microcentrifuge at 4°C for 2 minutes;
- Resuspend pellet with 1 ml of 100 mM potassium phosphate buffer pH 7.4 containing 10 mM EDTA;
- Sonicate the cell suspension for 20 x 1 second to lyse the cells;
- Centrifuge cell lysate at 10,700 g at 4°C for 1 hour;
- Homogenize the pellet in 100-150 μ l 50 mM potassium phosphate buffer pH 7.4 containing 0.1 mM EDTA and 10% glycerol;
- Store at -80°C.

Resuspension buffer:

8 mM	Na ₂ HPO ₄
1.5 mM	KH ₂ PO ₄
2.7 mM	KCl

2.14.3 Determination of protein concentration

Protein concentration in cell lysates or microsome-enriched lysates was measured with the BCA assay according to manufacturer's protocol.

2.14.4 Western blot

Protein expression was analysed by blotting the cell lysates as follows:

SDS-PAGE:

- Mix 20-30 μ g of protein lysate with SDS sample buffer;
- Heat up for 3-5 minutes at 95°C in water bath;
- Load samples in 10% polyacrilamide gels;
- Run samples at 130 V, 35 mA for 2 hours in NuPAGE[®] Electrophoresis System.

Sample buffer (6x):

0.225 mM	Tris-HCl
50%	Glycerol
5%	SDS
0.05%	Bromophenol Blue
0.25 mM	DTT

Running buffer (5x):

0.25 M	Tris-HCl
2.5 M	Glycin
1%	SDS

Blotting:

- Activate the PDVF membrane (Immobilon-FL Membrane, Millipore) in methanol;
- Assemble the "blotting sandwich";
- Run at 25 V, 125 mA for 90 minutes at room temperature in NuPAGE[®] XCell Blotting devices;
- Wash the PDVF membrane in TBS for 5 minutes;
- Incubate in TBS + Odyssey Blocking Solution (LI-COR) 1:1 for 1 hour at room temperature;
- Wash in TBS-T for 5 minutes;
- Incubate in TBS-T + Odyssey Blocking Solution 1:1 with the primary antibody (anti-CYP26C1 was diluted 1:100) overnight at 4°C on an orbital rotator;
- Wash 3 times with TBS-T for 5 minutes;
- Incubate in TBS-T + Odyssey Blocking Solution 1:1 with the secondary antibody (diluted 1:8000) for 1 hour at room temperature light protected on an orbital rotator;
- Wash 3 times with TBS-T for 5 minutes light protected;
- Proceed with Odyssey Infrared Imaging System (LI-COR).

Materials and Methods

Transfer buffer (10x):

0.25 M	Tris-HCl pH 8.3
1.92 M	Glycin

TBS (10x):

0.5 M	Tris-HCl pH 7.5
1.75 M	NaCl

TBS-T:

TBS 1x with 0.1% Tween20

2.15 Cell-based Methods

2.15.1 Cultivation of eukaryotic cell lines

Human primary chondrocytes (obtained as previously described in Marchini et al., 2004²⁸) U2OS (ATCC) and HEK293 (ATCC) were maintained in DMEM medium supplemented with 10% FBS, 100 U/ml Pen-Strep and 2 mM L-Glutamine in a humidified atmosphere with 5% CO₂ at 37°C. For HEK293 and U2OS cells every two-three days growth medium was removed, cells were washed with PBS and trypsinized with 0.05% Trypsin-EDTA for 2-5 minutes at 37°C. Trypsinization was stopped by adding fresh growth medium and cells diluted 1:10.

2.15.2 Cryo-conservation

Cells were cryo-conserved in liquid nitrogen tanks. Briefly, trypsinized cells were spun down and resuspended in FBS containing 5-10% DMSO. Aliquots of 1.5 ml were distributed in cryo vials and gradually frozen at -80°C in styrofoam boxes. After 24 hours, aliquots were transferred into liquid nitrogen tanks.

2.15.3 Transfection

Lipofectamine 2000 transfection of U2OS cells

U2OS cells were transfected with Lipofectamine[®] 2000 according to manufacturer's manuals.

- Add DNA and Lipofectamine into two separate tubes containing Opti-MEM[®] Reduced Serum Medium (1x) with GlutaMAX[™];
- Incubate Lipofectamine for 5 minutes;
- Mix the DNA tube with the Lipofectamine tube;
- Incubate at room temperature for 20 minutes;
- Add dropwise the mix directly to the cells;
- Change the media after 3-4 hours of transfection;
- Allow transfection for 24 hours.

Lipofectamine 2000 transfection for SHOX luciferase assays

To test SHOX mutants, luciferase experiments were performed with the *FGFR3* promoter, a known SHOX target. SHOX wild type or mutants were cloned in the expression vector pcDNA4/TO. *FGFR3* promoter -3430/+464 was cloned in pGL3basic³⁸. As control reporter vector for transfection normalization pRL-TK was used. Transfections were performed in U2OS cells with Lipofectamine 2000 as described above. Experiments were performed in 24-well plates (1 x 10⁵ cells per well), each condition in triplicate.

Reaction mix per well:

300 ng	pcDNA4/TO empty vector, SHOX wild type or SHOX mutants
300 ng	pGL3-FGFR3(-3430/+464)
150 ng	TK-Renilla
2 μ l	Lipofectamine 2000
2 x 50 μ l	Opti-MEM

Transfection was allowed for 24 hours prior to Luciferase reporter assay was performed.

Lipofectamine 2000 transfection for CYP26C1 luciferase assays

To test CYP26C1 mutants the Cignal RARE Reporter Assay Kit (SABiosciences) was used. The kit provides Firefly luciferase as gene reporter under the control of retinoic acid responsive elements (RARE). Renilla luciferase was provided by the kit and was used for transfection normalization. CYP26C1 wild type or mutants were cloned in the expression vector pIRES2-EGFP (gently provided by Prof. Dr. Thomas Boettger). Transfections were performed in U2OS cells with Lipofectamine 2000 as described above. Experiments were performed in 96-well plates (1 x 10⁴ cells per well), each condition in triplicate.

Reaction mix per well:

100 ng	pIRES2-EGFP empty vector, CYP26C1 wild type or CYP26C1 mutants
100 ng	Cignal RARE System Kit
0.5 μ l	Lipofectamine 2000
2 x 25 μ l	Opti-MEM

Transfection was allowed for 24 hours. Cells were then treated with mock control or 250 nM ATRA. After 24 hours treatment cells were prepared for Luciferase reporter assay.

Lipofectamine 2000 transfection for *SHOX* promoter luciferase assays

To test whether RA directly regulates SHOX P2 promoter and CNE3 where cloned in pGL3basic firefly luciferase reporter gene as previously described³³. rTK-RL was used for transfection normalization. Experiments were performed in 24-well plates (1 x 10⁵ cells per well), each condition in triplicate.

Reaction mix per well:

500 ng	pGL3-empty vector, or CNE3-SHOX P2 wild type promoter or mutant promoter
50 ng	TK-Renilla
1.5 μ l	Lipofectamine 2000
2 x 50 μ l	Opti-MEM

Transfection was allowed for 24 hours. Cells were then treated with mock control or 250 nM ATRA. After 24 hours treatment cells were prepared for Luciferase reporter assay.

Luciferase assay

Luciferase reporter assays were performed with the Dual-Luciferase[®] Reporter Assay System (Promega) according to the manufacturer's protocol. Briefly, cells were washed twice with PBS and lysed with 60 μ l (24-well plate format) or 20 μ l (96-well plate format) of Passive Lysis Buffer per well. Cells were incubated in lysis buffer for 15 minutes at room temperature. Lysis was further supported by freezing at -80°C and thawing before analysis. Cell lysates were scraped with pipette tip and aliquoted in 96-well polypropylene flat bottom white plates (Greiner Bio-one). Analysis were performed in the Berthold Centro LB 960 luminometer.

2.15.4 Treatment of human primary chondrocytes with ATRA

Human primary chondrocytes were treated with ATRA to test its effect on SHOX expression. Briefly, cells were cultivated in 6-well plates. Once achieved full confluency cells were treated with 10-100 nM ATRA for 6 hours. Finally, total RNA was extracted with TRIzol.

2.16 Zebrafish-based Methods

Morpholino injection in zebrafish embryos were performed by Lonny Jürgensen and Prof. Dr. David Hassel (Department of Internal Medicine III - Cardiology, University Hospital Heidelberg, Heidelberg, Germany). ATRA treatment, RNA isolation, cDNA synthesis and luciferase assays were performed by me and Lonny Jürgensen.

The *shox* and *cyp26c1* morpholinos were obtained from Gene Tools. The standard control morpholino (Gene Tools) was used as control.

MO efficiency test was performed by PCR on the provided cDNA. Amplicons were gel-extracted and cloned in pUC19. Finally, single clones were Sanger sequenced.

2.16.1 Whole-mount *in situ* hybridization

Whole-mount *in situ* hybridization experiments were performed as described previously⁵¹.

Fixation:

- Fix embryos with 4% PFA in PBS for 1-4 hours at room temperature or 4°C overnight;
- Wash embryos with PBST DEPC water for 5 minutes at room temperature;
- Repeat washing step;
- Take embryos through a methanol row of 10%-30%-50%-70%-100%-100%, rocking for 5 minutes at room temperature each step of the row;
- Embryos can be stored at -20°C for at least 6 months.

4% PFA in PBS:

100 ml	DEPC water
8 g	paraformaldehyde
200 μ l	NaOH (10 N)

PBST DEPC:

100 ml	PBS-DEPC (10x)
900 ml	DEPC H ₂ O
1 ml	Tween-20

Proteinase K digestion:

- Take embryos through a reverse methanol row 100%-70%-50%-30%-10%-PBST DEPC-PBST DEPC, rocking for 5 minutes at room temperature each step of the row;
- Place a metal heat block in the oven at 65°C;
- Digest with 10 μ g/ml of proteinase K in PBST DEPC at room temperature according to the following guidelines for embryos hours post-fertilization (hpf):

<24 hpf	3-5 minutes
24 hpf	8-10 minutes
48 hpf	18-20 minutes
75 hpf	26-30 minutes

- Rinse quickly in PBST DEPC;
- Wash in PBST DEPC for 5 minutes at room temperature;
- Fix in 4% PFA in PBS DEPC water for 20 minutes at room temperature;
- Rinse quickly in PBST DEPC water;
- Wash in PBST DEPC water for 5 minutes at room temperature.

Acetic anhydride treatment:

- Replace PBST DEPC water with DEPC water;
- Replace quickly DEPC water with a fresh mixture of acetic anhydride (2.5 μ l/ml in 0.1 M triethanolamine pH 7.0 DEPC);
- Incubate for 1 hour rocking at room temperature;
- Place an aliquot of HYB⁻ in the 65°C oven;
- Wash in PBST DEPC for 10 minutes at room temperature;
- Repeat washing step.

Acetic anhydride mixture:

2.5 μ l	Acetic Anhydride
1 ml	0.1 M Triethanolamine in DEPC water

SSC 20x:

87.65 g	NaCl
44.1 g	NaCitrate

Bring volume to 350 ml with DEPC water
Adjust pH to 4.5/5.0 with Citric acid (1 M)
Bring volume to 500 ml
Autoclave

HYB⁻ (store at -20°C):

50%	ultrapure deionized Formamide
5x	SSC (20x)
0.1%	Tween-20

Pre-hybridization:

- Place embryos in 0.5 ml screw-top tubes with 500 μ l of prewarmed HYB⁻;
- Incubate at 65°C for 5 minutes;
- Place HYB⁺ in the 65°C oven;
- Replace HYB⁻ with HYB⁺;
- Incubate 1-48 hours, usually 3-4 hours are sufficient.

HYB⁺ (store at -20°C):

HYB ⁻	
5 mg/ml	torula yeast RNA
50 μ g/ml	heparin

Hybridization:

- Warm up more HYB⁺ at 65°C;
- Add the probe (30-50 ng per sample) to 500 μ l of pre-warmed HYB⁺;
- Incubate the mixture for 10 minutes before adding it to the embryos;
- Add pre-warmed mixture to the embryos (be aware of keeping the embryos on the metal heat block to keep them warm);
- Incubate overnight at 65°C.

Washing:

- Wash embryos with prewarmed 50%/2x SSCT at 65°C for 30 minutes (perform the washing steps on the metal heat block);
- Repeat washing step;
- Wash with pre-warmed 2x SSCT at 65°C for 15 minutes;
- Incubate with RNase A (10 μ g/ml) in pre-warmed 2x SSC at 37°C for 15-30 minutes;
- Wash with pre-warmed 2x SSCT at 37°C;
- Wash with pre-warmed 0.2x SSCT at 65°C for 30 minutes;
- Repeat washing step;
- Rinse with 0.2x SSCT at room temperature;
- Wash with 0.2x SSCT at room temperature for 5 minutes.

2x SSCT:

5 ml	20x SSC
50 μ l	Tween-20
45 ml	DEPC water

50% Formamide/2x SSCT:

5 ml	2x SSCT
5 ml	50% Formamide

Detection:

- Transfer embryos to a 24-well plate;
- Replace 0.2x SSCT with 2% Blocking Reagent (in MAB solution);
- Incubate at room temperature for 1-5 hours and rotate on an orbital shaker;
- Dilute 1:3000 the Anti-Digoxigenin-AP Fab fragments in 2% Blocking Reagent (in MAB solution);
- Replace Blocking Reagent with the antibody solution;
- Incubate at 4°C overnight on an orbital shaker;
- Wash embryos in 2% Blocking Reagent (in MAB solution) at room temperature for 25 minutes;
- Wash embryos with MAB solution at room temperature for 25 minutes;
- Repeat washing step twice;
- Bring the BM Purple AP Substrate to room temperature;
- Wash with Staining Buffer at room temperature for 5 minutes;
- Repeat washing step twice;
- Remove as much as possible the Staining Buffer;
- Add 500 μ l of BM Purple AP Substrate;
- Stain at room temperature light protected checking every 30 minutes. If the desired expression is not seen, one can leave the embryos at 4°C overnight;
- Wash with PBST at room temperature for 10 minutes;
- Repeat washing step;
- Fix in 4% PFA-PBS at room temperature for 1 hour;
- Wash with PBST at room temperature for 5 minutes;
- Replace PBST with 100% glycerol;
- Store at 4°C until ready to take photographs;

MAB solution pH 7.5 (sterilize by filtering):

100 mM	Maleic Acid
150 mM	NaCl
X volume	DEPC water

Staining buffer (prepare fresh):

50 mM	MgCl ₂
100 mM	NaCl
0.1 %	Tween-20
1 mM	Levamisol
100 mM	Tris-HCl pH 9.5 (add last)
X ml	autoclaved ddH ₂ O

Photography

Embryos were placed on microscope slides. Images were taken with the microscope SZX16, cellD Imaging Software (Olympus).

2.16.2 Pectoral fins area measurements

Pectoral fins area was measured with Fiji ImageJ⁵².

2.16.3 Luciferase assays

Luciferase experiments in zebrafish were performed injecting one-cell stage embryos with 1-2 nl of a 25 nM stock of Cignal RARE Reporter System plasmids and 1-2ng of control MO or *cyp26c1* MO. After 24 hr injection embryos were separated in groups of 20-30, lysed in 50 μ l of Passive Lysis Buffer and assayed with the Dual Luciferase[®] Assay System as described above. Each experiment was performed in triplicate and repeated three times.

2.16.4 ATRA treatments

Treatments of zebrafish embryos with RA were performed as follows: wild type embryos were left developing for 24 hours. At 24 hpf, embryos were separated in groups of 10-15 and treated with mock control, 50 or 100 nM ATRA for 6 hours. Finally, RNA was extracted and used for *shox* expression analysis as described above.

2.17 Bioinformatics Resources

Primer design

Primers for cloning *in situ* hybridization probes, for sequencing, and for testing MO efficacy were designed using Primer3⁴⁹. Primers for quantitative PCR were designed using Universal ProbeLibrary Assay Design Center (Roche).

In silico mutation analysis

Mutation Taster	http://www.mutationtaster.org ⁵⁷
PolyPhen2	http://genetics.bwh.harvard.edu/pph2/index.shtml ⁵⁸
SIFT	http://sift.jcvi.org ⁵⁹
Provean	http://provean.jcvi.org ⁶⁰

In silico promoter analysis

Analysis of *SHOX* P2 promoter for the identification of putative RARs and RXRs binding sites was performed using PROMO^{53;54}.

Databases

NCBI	http://www.ncbi.nlm.nih.gov/
Ensembl Genome Browser	http://ensembl.org/index.html
UCSC	http://genome.ucsc.edu/
1000 genomes	http://www.1000genomes.org
Exome Variant Server	http://evs.gs.washington.edu/EVS/
ExAC Browser	http://exac.broadinstitute.org
UniProtKB	http://www.uniprot.org/help/uniprotkb
ExPASy	http://www.expasy.org
ZFIN	http://zfin.org

Illustrations

Figures were prepared using Adobe Illustrator CS2. Protein and DNA schemes were drawn using Illustrator of Biological Sequences (IBS)⁵⁵.

2.18 Statistics

Statistics were performed using GraphPad Prism version 5 for Windows (GraphPad Software, La Jolla, California, USA).

Statement: Some of the description have been taken and adapted from the theses of former PhD students in the lab (Dr. Carolin Wohlfarth and Dr. Slavil Peykov).

3 Results

3.1 Genetic Analysis of Family 1

3.1.1 Family 1 pedigree

We recruited a three generation German family with five affected individuals displaying LWD with dysmorphic signs and Madelung deformity. According to the pattern of transmission of the trait, an autosomal dominant inheritance was hypothesized (**Figure 3.1**).

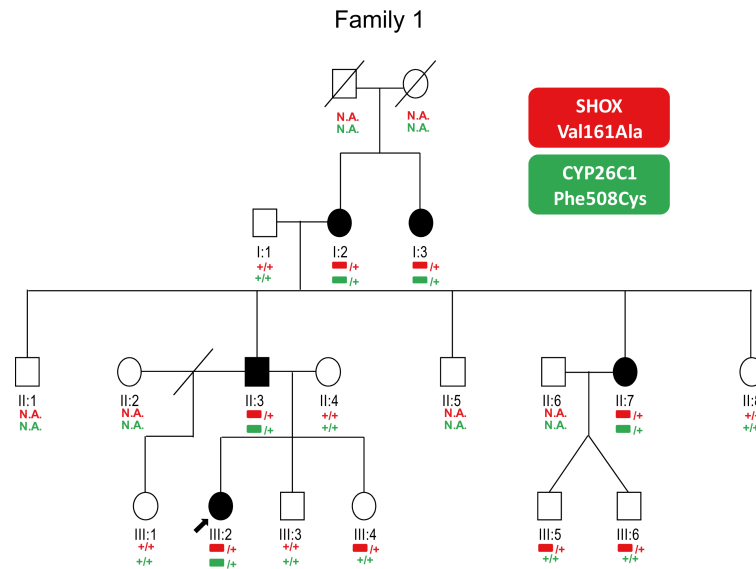


Figure 3.1: Family 1 pedigree. Filled symbol, LWD affected individual; slash, divorced; symbol with a slash, deceased individual; red bar, individual with *SHOX* mutation; green bar, individual with *CYP26C1* mutation; +, wild type allele; N.A., DNA not available; arrow, index patient.

The index patient (**Figure 3.1** individual III:2) showed mesomelic short stature with a SD of -3.7 when first diagnosed. She started developing Madelung deformity at the age of 7 years old. At 8 years and 9 months, the proband started receiving growth hormone therapy. After 4 years of GH therapy the height improved to -1.83 SD. Three female affected family members, I:2, I:3, and II:7, presented with mesomelic short stature with an SD of -4.51, -3.73 and -3.14, respectively. Moreover, these patients presented with Madelung deformity. The father (II:3) of the proband showed also mesomelic short stature (SD = -2.63), and a borderline Madelung deformity. The mother (II:4), an aunt (II:8), and the stepsister (III:1) presented with short stature too, but did not show other skeletal abnormalities (**Table 3.1**).

Patients ID	Age	Gender	Height SD	LA SD	Madelung deformity
I:1	72	M	-1.85	+0.57	No
I:2	72	F	-4.51	-2.21	Yes
I:3	81	F	-3.73	-	Yes
II:1	51	M	-1.23	-	No
II:2	-	F	-	-	No
II:3	46	M	-2.63	-2.00	(Yes)
II:4	42	F	-3.33	-1.15	No
II:5	40	M	-0.92	-	No
II:6	-	M	-	-	No
II:7	37	F	-3.14	-	Yes
II:8	32	F	-2.75	-1.50	No
III:1	21	F	-3.73	-1.20	No
III:2 (proband)	8.9	F	-3.6	-2.72**	Yes
III:3	12.9	M	-0.62	+0.10	No
III:4	8.5	F	-1.96	-1.67	No
III:5	16	M	-0.43	-	No
III:6	16	M	-0.72	-	No

Table 3.1: Family 1 clinical data. M, male; F, female; -, data not available; Height SD, height standard deviation; LA SD, lower arm standard deviation; Madelung deformity: Yes, present; No, not present; (Yes), borderline; **, these data were taken at the age of 14 years.

3.1.2 *SHOX* locus analysis

Variants in the *SHOX* gene have been estimated to account for 70-90% of LWD. Therefore, *SHOX* locus was analysed in this family first. A *SHOX* heterozygous missense variant, c.482T>C (p.Val161Ala), was found by Sanger sequencing in the proband and her father. Val161 is highly conserved among Shox vertebrate homologues and resides within the DNA binding domain (**Figure 3.2b, c**). Functional analysis of this mutation in U2OS cells by luciferase assay on the *FGFR3* promoter, a known *SHOX* target, demonstrated that it strongly affects *SHOX* transcriptional activity (**Figure 3.2d**). When Sanger sequencing on the other affected and non-affected family members was carried out, the *SHOX* mutation Val161Ala was found in individuals with mild phenotype or normal stature too: the sister and two cousins (**Figure 3.1**, individuals III:4, III:5 and III:6). Multiplex ligation-dependent probe analysis (MLPA) was performed to exclude major genetic lesions in and around *SHOX* locus (data not shown). Therefore, we asked whether there may be other genetic reason(s) which may explain this variability.

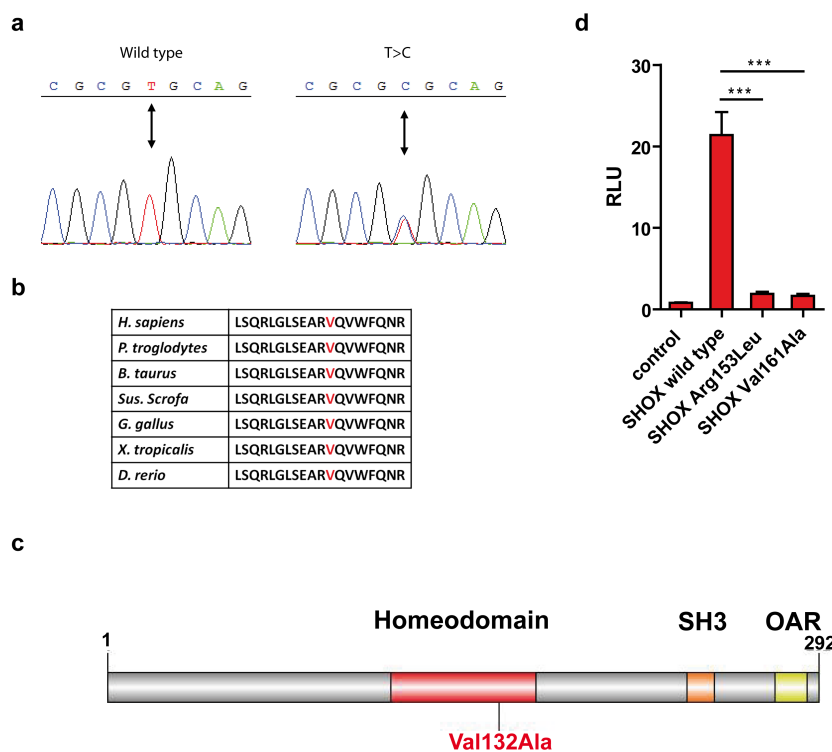


Figure 3.2: The *SHOX* variant identified in the family study affects its transcription activity. (a) Sanger sequencing was used to validate the *SHOX* variant identified. (b) Alignment of the amino acid sequences of vertebrate Shox proteins, showing the conservation of Val161. (c) Schematic representation of SHOX protein. Val161 resides in the homeodomain. SH3, Src Homology 3 domain. OAR, Otp Aristaless Rax domain. (d) Luciferase assay testing SHOX Val161Ala mutation on *FGFR3* promoter in U2OS cells (n=4). pcDNA4-TO empty vector was used as negative control. Arg153Leu was published as mutation affecting SHOX protein activity⁴² and was therefore used as positive control. Data are shown as means \pm SD; RLU, Relative Light Units; * p-value = 0.0286, two-tailed Mann-Whitney non-parametric t test.

3.1.3 Whole-Genome Linkage analysis

Whole-genome linkage analysis was performed in collaboration with Dr. Gudrun Nuernberg (Center for Molecular Medicine Cologne, Cologne, Germany) on the family members: I:1, I:2, I:3, II:3, II:4, II:7, II:8, III:1, III:2, III:3, III:4, and III:6. This analysis identified linkage *disequilibrium* with a max LOD score of 2.4 in a 19.2 Mb region of chromosome 10 (chr10: 85477515-104681710; hg19) (**Appendix Figure 1** and **Appendix Figure 2**). The LOD score obtained was the maximum expected for this family. This region encompasses 263 genes, but could not be further refined. Moreover, we identified a 2.02 Mb sequence in the PAR1 region of chromosome X (chrX:706800-2735491; hg19) with a LOD score of 1.7 (**Appendix Figure 1** and **Appendix Figure 3**). This region localizes close to *SHOX* locus as expected. The reason for the reduced LOD score in PAR1 are individuals III:4 and III:6 who carry the disease haplotype although they are unaffected.

3.1.4 Whole-exome sequencing analysis

The development of next-generation sequencing methodologies like whole-genome sequencing (WGS) and whole-exome sequencing (WES) revolutionized the way of approaching candidate genes identification. We decided therefore to adopt these technologies for this study. In 2012 whole exome sequencing analysis was performed in collaboration with Dr. Tim Strom (Institute of Human Genetics, Helmholtz Zentrum München, Neuherberg, Germany) on the index patient and her father. Established methods were applied for variant filtering according to the hypothesized autosomal dominant transmission of the phenotype⁵⁶. A list of 98 variants in 97 genes was obtained (**Appendix Table 1**). All variants were tested using the mutation prediction tools PolyPhen2, Mutation Taster, SIFT and PROVEAN, leading to 36 variants predicted as disease causing/damaging by at least one of these programs. Sanger sequencing of the 36 variants was performed in affected and non-affected family members. I found that only the mutations in *OPN4* (chr10: 88419701-88419701; hg19) and *CYP26C1* (chr10: 94828408-94828408; hg19) segregated with the phenotype. Both genes reside within the chromosome 10 region as defined by linkage analysis. *OPN4* is a member of the G protein-coupled receptor superfamily involved in photoreception in the retina⁶¹. *CYP26C1* encodes for a member of the cytochrome P450 superfamily of enzymes involved in the catabolism of RA⁶². RA was previously shown to play a key role in limb development⁶³ and *CYP26B1*, another member of the *CYP26* family, is known to be involved in skeleton development⁶⁴. Moreover, RA has been previously shown to inhibit *Shox* expression in chicken limbs³⁴. Therefore we decided to further investigate *CYP26C1* as a candidate modifier in *SHOX* deficient short stature patients.

3.1.5 CYP26C1 Phe508Cys variant affects its enzymatic activity

In *CYP26C1* a heterozygous missense variant was found, c.1523T>G (p.Phe508Cys), which is highly conserved among vertebrates and was predicted as damaging by all four prediction tools applied (**Figure 3.3a-c**). To assess whether this variant affects *CYP26C1* enzymatic activity, I performed the CignalTM RARE-System, a RA-responsive luciferase reporter assay, in U2OS cells as described⁶⁴. Over-expression of *CYP26C1* wild type reduced the luciferase activity, confirming that it degrades RA. The residue Cys459 is predicted by homology as being the iron-binding amino acid. This residue was mutated to Ala to inhibit *CYP26C1* catalytic activity; it was therefore used as positive control. This mutant showed significantly reduced RA catabolic activity as expected (**Figure 3.3d**). The *CYP26C1* Phe508Cys mutant was not able to reduce luciferase activity when compared to the wild type form, suggesting that this variant impairs *CYP26C1* enzymatic activity (**Figure 3.3d**).

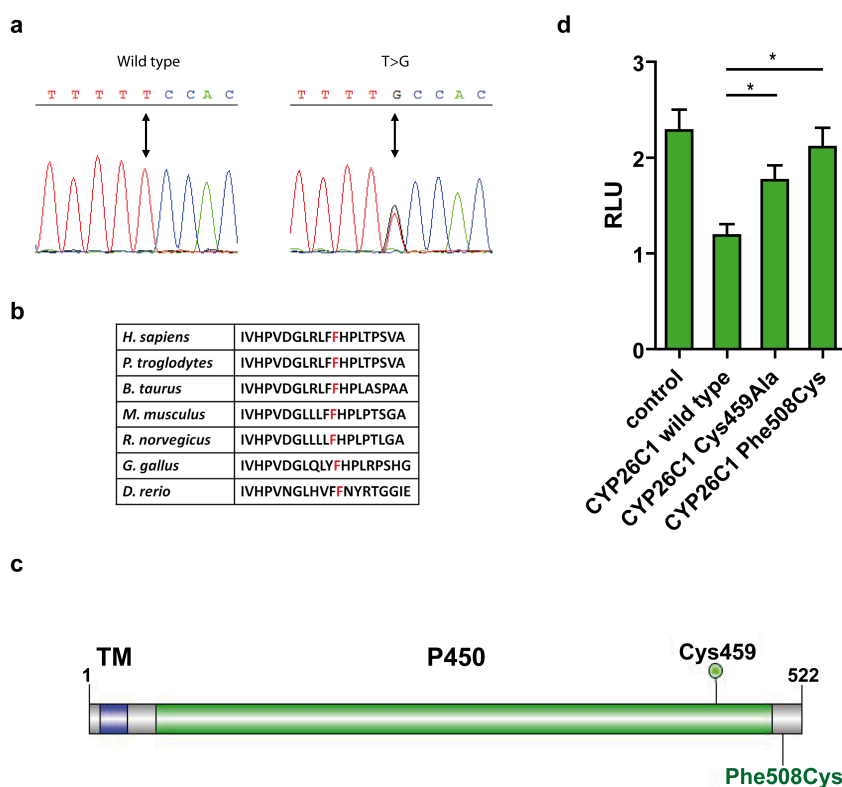


Figure 3.3: The *CYP26C1* variant identified in the family study affects its enzymatic activity. (a) Sanger sequencing was used to validate the *CYP26C1* variant identified. (b) Alignment of the amino acid sequences of vertebrate *CYP26C1* proteins, showing the conservation of Phe508. (c) Scheme of *CYP26C1* protein. TM, Transmembrane helix; Cys459 represents the Iron binding residue. (d) Signal-RARE system luciferase assay testing *CYP26C1* Phe508Cys mutation in U2OS cells treated with 250 nM RA for 24h (n=4). pIRES2-EGFP empty vector was used as control. The iron binding residue Cys459 was mutated to Ala as positive control. Data are shown as means \pm SD; RLU, Relative Light Units; * p-value = 0.0286, two-tailed Mann-Whitney non-parametric t test.

3.2 Screening of further LWD and ISS individuals

To find out whether the co-occurrence of *SHOX* and *CYP26C1* variants in severe phenotypes is a unique finding specific only to family 1, we screened *CYP26C1* in a cohort of 68 individuals with LWD and in a cohort of 140 controls with normal height where *SHOX* deficiency was excluded. The complete list of the variants identified can be found in **Appendix Table 2**. Synonymous, intronic and common variants were excluded from further analysis.

We identified two further cases with co-occurrence of *SHOX* and *CYP26C1* variants (**Figure 3.4**). Available clinical data are listed in **Table 3.2**.

Family 2 had one affected daughter (II:2) presenting with short stature, mesomelia and Madelung deformity. The sister (II:1) presented with short stature but skeletal dysmorphism

were not diagnosed. Both parents presented with normal stature and no dysmorphisms. A heterozygous *SHOX* missense mutation c.394C>G (p.Leu132Val) was found in the unaffected father and the two siblings. This variant was previously shown to alter homodimerization and reduce DNA binding abilities⁴². Screening of *CYP26C1* identified a heterozygous missense mutation c.1133G>A (p.Arg378His) only in the affected daughter (**Figure 3.4a, Family 3**). The third case was a girl with short stature, mesomelia and Madelung deformity carrying a *de novo* heterozygous deletion of *SHOX* and a missense variant in *CYP26C1*, c.356A>C (p.Gln119Pro). Both parents and the brother were reported having normal stature. The *CYP26C1* variant was inherited by the father. Since the *SHOX* deletion is *de novo*, this family cannot demonstrate specific co-segregation although it adds to overall evidence that damaging variants in *SHOX* and *CYP26C1* co-occur in individuals with severe LWD phenotypes (**Figure 3.4a, Family 2**).

Functional analysis of the *SHOX* and *CYP26C1* variants found in these two cases demonstrated their negative impact on the protein activity (**Figure 3.4b and c**). We conclude that, in addition to family 1, two out of 68 LWD patients with *SHOX* deficiency presented with damaging variants in *CYP26C1* while no damaging mutations were identified in 140 control individuals with normal height. In all families where clinical information was available, all individuals with damaging mutations in both *SHOX* and *CYP26C1* had the more severe skeletal phenotype.

Screening of the controls lead to the identification of common synonymous and intron variants. The variants found are listed in **Appendix Table 3**.

Family	Patients ID	Age	Gender	SD	LA SD	Madelung deformity
Family 2	I:1	-	M	-	-	No
	I:2	-	F	-	-	No
	II:1	-	F	-	-	No
	II:2	6	F	-3.38	-4.71	Yes
Family 3	I:1	51	M	+0.1	-	No
	I:2	47	F	+0.8	-0.1	No
	II:1	26	M	+0.5	-0.9	No
	II:2	16	F	-2.6	-3.6	Yes

Table 3.2: Families 2 and 3 clinical data. M, male; F, female; -, data not available; Height SD, height standard deviation; LA SD, lower arm standard deviation.

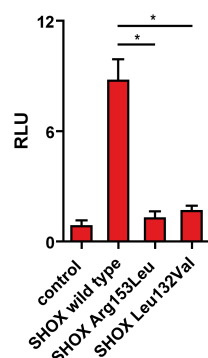
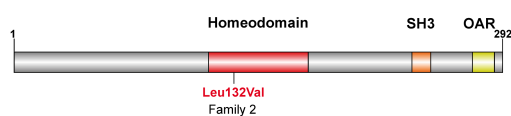
Finally, in order to test whether *CYP26C1* mutations alone could lead to short stature or dysmorphic signs, a group of 256 affected individuals (234 ISS and 22 LWD), where *SHOX* deficiency was excluded, was screened with the GS Junior System (Roche). The variants found are available in **Appendix Table 4**. We identified two rare missense variants in two independent ISS individuals, c.148C>T (p.Pro50Ser) and c.356A>C (p.Gln119Pro) predicted as damaging (**Figure 3.5a and b**). Phenotypic information of the family carrying the variant c.148C>T (p.Pro50Ser) were not available. Functional analysis of this variant did not show any significant effect on protein activity (**Figure 3.5c**). Variant c.356A>C (p.Gln119Pro) was found in a family with three affected siblings. Based on the inheritance of the trait, we obtained no convincing evidence that this variant alone is causative for short stature, although the mutation segregated with the most affected individuals and showed a significant impact

on CYP26C1 catabolic activity (**Figure 3.5a and c**). Altogether, these genetic data do not support the hypothesis that *CYP26C1* alone is causative for short stature or skeletal abnormalities.

a



b



c

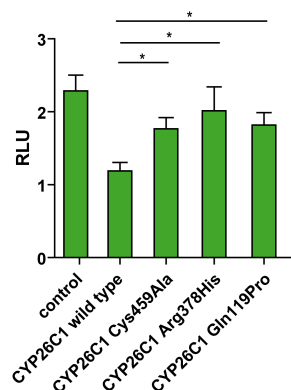


Figure 3.4: Family pedigree charts of the screened LWD patients and functional analysis of the identified variants. (a) Pedigree of the LWD families carrying variants in both *SHOX* and *CYP26C1*. Filled symbol, short stature affected individual; red text, *SHOX* locus; green text, *CYP26C1* locus; +, wild type allele; N.A., DNA not available; *, individual with mesomelia and Madelung deformity. (b) Scheme of SHOX protein (upper panel). Leu132 resides in the homeodomain. Luciferase assay testing SHOX Leu132Val mutation on *FGFR3* promoter in U2OS cells (n=4). pcDNA4-TO was used as control. Arg153Leu was published as mutation affecting SHOX protein activity and was therefore used as positive control. Data are shown as means \pm SD; RLU, Relative Light Units; *** p-value < 0.001, one-way ANOVA Bonferroni's multiple comparison test. SH3, Src Homology 3 domain. OAR, Otp Aristaless Rax domain. (c) Scheme of CYP26C1 protein. Gln119 and Arg378 reside within the P450 domain. Signal-RARE system luciferase assay testing CYP26C1 Gln119Pro and Arg378His mutations in U2OS cells treated with 250 nM RA for 24 hours (n=4). pIRES2-EGFP was used as control. The iron binding residue Cys459 was mutated to Ala as positive control. Data are shown as means \pm SD; RLU, Relative Light Units; * p-value = 0.0286, two-tailed Mann-Whitney non-parametric t test. TM, Transmembrane helix.

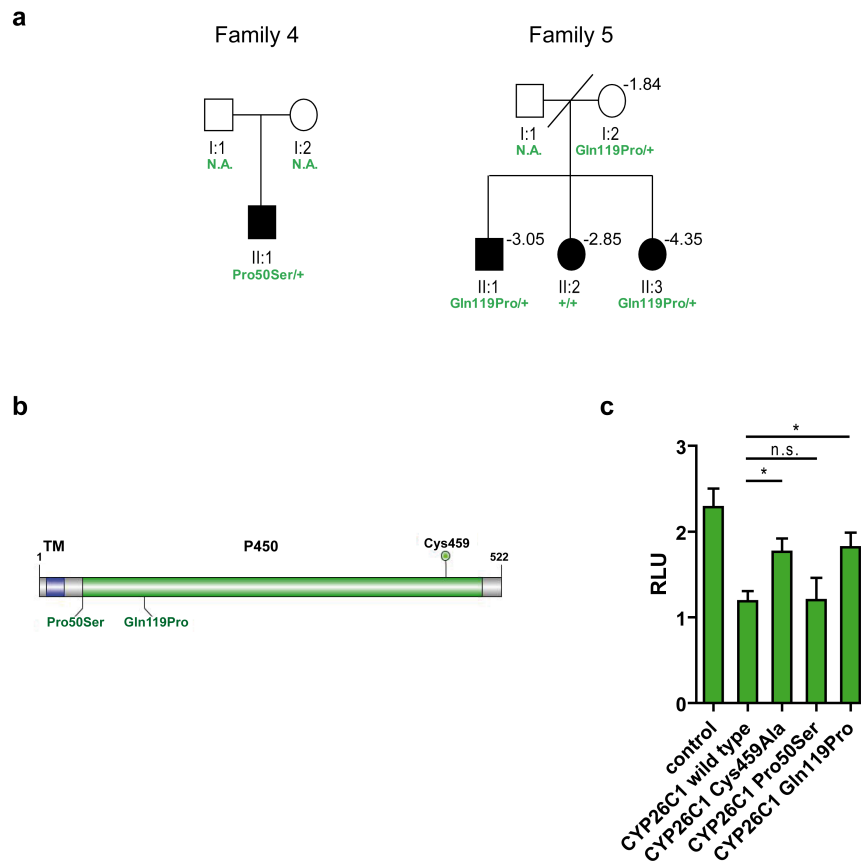


Figure 3.5: Family pedigree charts of the screened ISS and LWD individuals and functional analysis of the identified mutations. (a) Pedigree of the families studied. Filled symbol, short stature affected individual; slash, divorced; green text, CYP26C1 locus; +, wild type allele; N.A. DNA not available; arrow, index patient. (b) Scheme of CYP26C1 protein. Pro50 and Gln119 reside within the P450 domain. TM, Transmembrane helix. Cys459 represents the Iron binding residue. (c) Signal-RARE system luciferase assay testing CYP26C1 Pro50Ser and Gln119Pro mutations in U2OS cells treated with 250 nM RA for 24 hours (n=4). pIRES2-EGFP was used as control. The iron binding residue Cys459 was mutated to Ala as positive control. Data are shown as means \pm SD; RLU, Relative Light Units; * p-value = 0.0286, two-tailed Mann-Whitney non-parametric t test.

3.3 Functional Studies in Human Cells

3.3.1 *CYP26C1* is expressed in human primary chondrocytes

To investigate whether *CYP26C1* is expressed in human primary chondrocytes similar to *SHOX* PCR was performed on cDNA and products corresponding to the predicted size were obtained (**Figure 3.6a**). Sanger sequencing of these bands confirmed that they correspond to the *CYP26C1* transcript. Western blotting analysis were performed to assess *CYP26C1* expression at the protein level. As control to verify band sizes, recombinant *CYP26C1* was overexpressed in U2OS cells. *CYP26C1* protein is reported to be expressed in the microsomes. Therefore, cytosolic and microsomal protein fractions from human primary chondrocytes were obtained. Immuno blotting of human primary chondrocytes confirmed *CYP26C1* expression (**Figure 3.6a**).

3.3.2 *CYP26C1* and *SHOX* are part of the RA pathway

It has been previously shown that RA can down-regulate *SHOX* expression in the developing limbs in chicken embryos³⁴. Therefore we asked whether RA could affect *SHOX* expression in human primary chondrocytes. Treatment of primary chondrocytes with 10-50 nM of all-trans retinoic acid (ATRA) did not lead to a significant effect on *SHOX* mRNA expression (**Figure 3.6b**). Treatment with 100 nM ATRA resulted in a significant reduction of *SHOX* levels (**Figure 3.6b**). Hence, high levels of ATRA decrease *SHOX* expression in human chondrocytes.

To test whether RA regulates *SHOX* expression by a direct binding of RARs or RXRs to the promoter region, I cloned the P2 promoter together with the CNE3 enhancer as previously described³³. *SHOX* promoter P1 was also tested, but even under the CNE3 enhancer did not show any activation of the firefly luciferase when compared to the empty vector (data not shown). CNE3 was chosen as enhancer because it was reported with the strongest activity over luciferase expression (Verdin et al., 2015). Treatment of the CNE3-P2 construct with ATRA led to a significant reduction of luciferase expression (**Figure 3.6c**), corroborating the hypothesis that RA regulates *SHOX* expression. In order to elucidate whether RA regulation occurs via direct or indirect mechanisms, *in silico* analysis of putative transcription factors binding sites was performed. This analysis identified three putative RXR α binding sites. Site-specific mutation of these sequences did not change ATRA effect on luciferase expression suggesting that an indirect regulation takes place (**Figure 3.6c**). These results provide evidence that *CYP26C1* and *SHOX* are members of the same pathway: *CYP26C1* regulates *SHOX* expression by regulating retinoic acid intracellular levels (**Figure 3.6d**). Further analyses need to be carried out to elucidate the molecular mechanisms underlying such regulation.

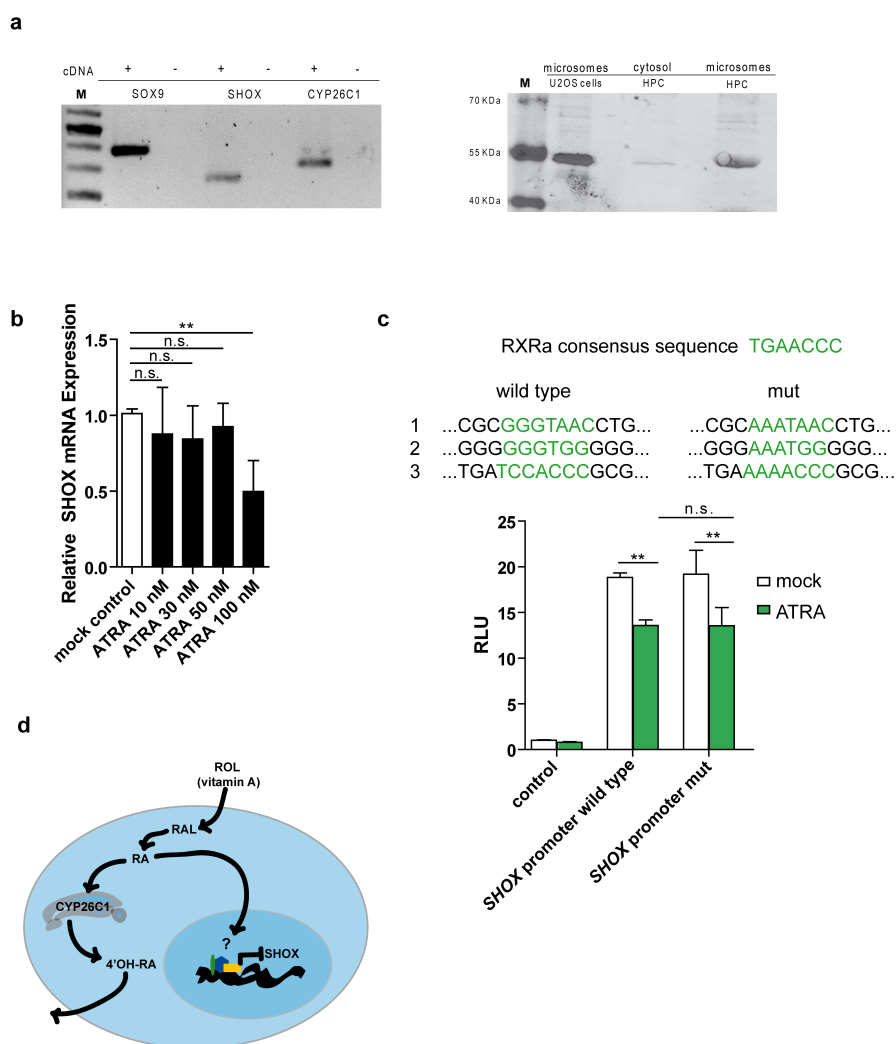


Figure 3.6: *CYP26C1* and *SHOX* are part of the RA signalling pathway. (a, left panel) RT-PCR showing the expression of *CYP26C1* mRNA in human primary chondrocytes. *SOX9* was used as chondrocyte marker. (a, right panel) Western blot showing the expression of *CYP26C1* in human primary chondrocytes on protein level. Overexpression of *CYP26C1* in U2OS cells was carried out to compare band sizes. *CYP26C1* protein is expressed in human primary chondrocytes microsomes. +, cDNA; -, water; M, marker; HPC, human primary chondrocytes. (b) Relative expression of *SHOX* mRNA normalized to the housekeeping genes *SDHA* and *HPRT* in human primary chondrocytes treated with all-trans retinoic acid (ATRA) 10 nM or 100 nM for 6h (n=5). Data are shown as means \pm SD; n.s., not significant, ** p-value = 0.0079, two-tailed Mann-Whitney non-parametric t test. (c) *In silico* analysis of *SHOX* P2 promoter identified three putative RXR α binding sites which were mutated to test their direct effect on *SHOX* expression regulation upon treatment with ATRA 250 nM (n=4). Data are shown as means \pm SD; RLU, relative luciferase unit; * p-value = 0.0286, n.s., not significant, two-tailed Mann-Whitney non-parametric t test. (d) *CYP26C1* and *SHOX* are members of the RA pathway. Vitamin A, retinol (ROL), enters the cell and is oxidized to retinaldehyde (RAL). RAL is then oxidized to retinoic acid (RA). RA can enter the nucleus and regulate the expression of its targets. *CYP26C1* controls RA intracellular levels by oxidizing this molecule in more hydrosoluble retinoids molecules like 4'-hydroxy-retinoic acid (4'-OH-RA), which can be readily excreted out of the cell. High levels of RA downregulate *SHOX* expression.

3.4 Functional Studies in Zebrafish Embryos

3.4.1 Morpholino efficacy analysis

Human pathologies have mostly been modelled using mammal systems such as mice. However, mice do not have any *Shox* orthologue. Therefore, we decided to use zebrafish (*Danio rerio*) as model in collaboration with Dr. David Hassel (Department of Internal Medicine III - Cardiology, Heidelberg University Hospital, Heidelberg, Germany). Zebrafish has been extensively used as model organism well suited to developmental and genetic analysis. The advantages of zebrafish as model are: high genetic and organ system homology to humans, high fecundity, external fertilization, ease of genetic manipulation, and transparency through early adulthood that enables imaging analysis of most tissues. Morpholino oligonucleotides (MOs) are the most used anti-sense knockdown tools in zebrafish. MOs have demonstrated to be useful in probing candidate gene function, and testing mutant phenotypes. Hence, to gain insight into the role of *Shox* and *Cyp26c1* interaction on limb development, we performed antisense MO knockdown experiments in zebrafish embryos.

Human and zebrafish *Shox* and *Cyp26c1* proteins share a 65% and 54% identity, respectively. Both genes have been shown to be expressed in pectoral fins^{65;66}. The *shox* and *cyp26c1* morpholinos were obtained from Gene Tools; sequences are available in the Materials and Methods chapter. Knockdown of *shox* was obtained using the splicing MO, MO1; phenotype specificity was confirmed using a second splicing MO, MO2. MO1 only was used for *in situ* hybridization analysis and double knockdown experiments. Knockdown efficacies are shown in **Figure 3.7** and **Figure 3.8**. Knockdown of *cyp26c1* was obtained using an already published MO⁶⁷. Efficacy is shown in **Figure 3.9**.

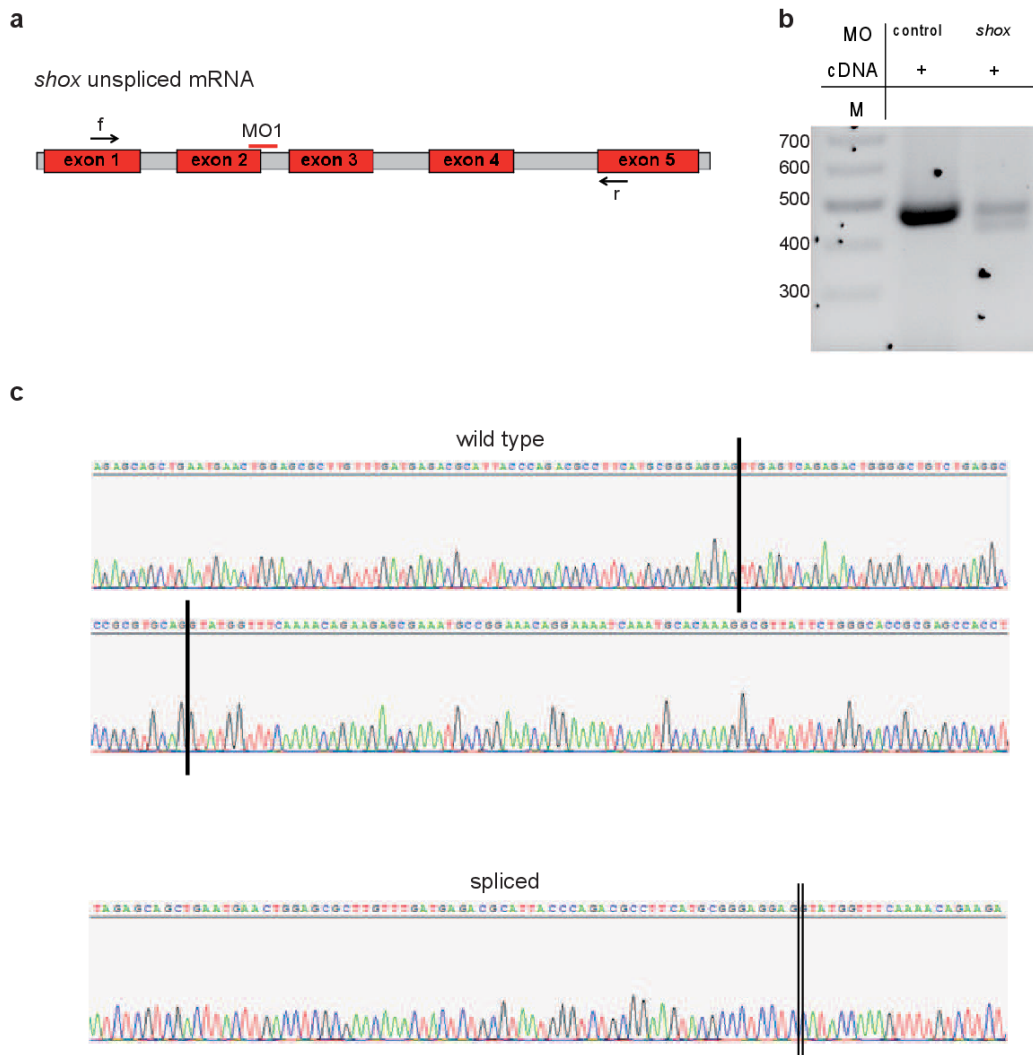


Figure 3.7: *shox* MO1 efficacy analysis. (a) Scheme of *shox* unspliced mRNA. Red bar, region targeted by *shox* MO1; arrows, position of the primers to analyse MO efficacy; f, forward primer; r, reverse primer. (b) RT-PCR analysis of *shox* MO1 efficacy. The 430 bp band represents the expected wild type product. Water was used as negative control (-) for the PCR. Samples were obtained from 48hpf embryos. (c) RT-PCR products were cloned in pUC19 and sequenced. *shox* MO1 leads to a spliced product leading to frameshift, p.L142Rfs37*. Black vertical segments enclose the out-spliced sequence.

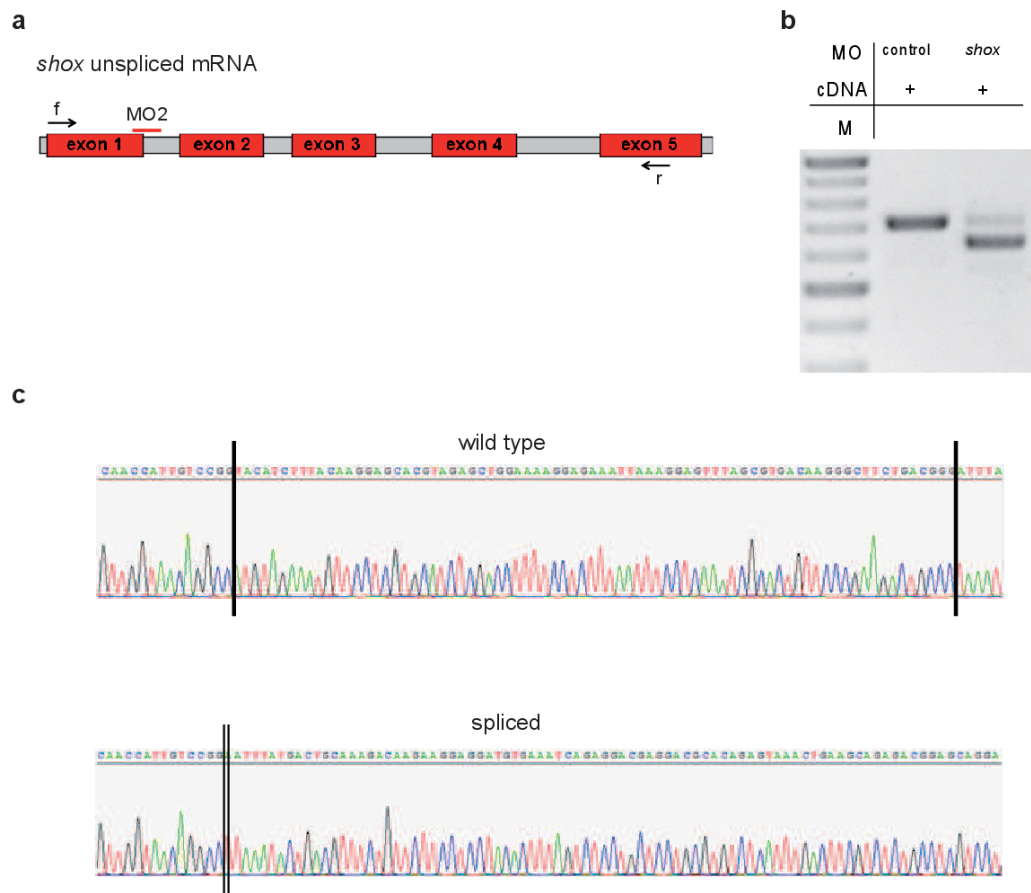


Figure 3.8: *shox* MO2 efficacy analysis. (a) Scheme of *shox* unspliced mRNA. Red bar, region targeted by *shox* MO2; arrows, position of the primers to analyse MO efficacy; f, forward primer; r, reverse primer. (b) RT-PCR analysis of *shox* MO2 efficacy. The 680 bp band represents the expected wild type product. Water was used as negative control (-) for the PCR. Samples were obtained from 48hpf embryos. (c) RT-PCR products were cloned in pUC19 and sequenced. *shox* MO2 leads to a spliced product leading to frameshift, p.V59Pfs11*. Black vertical segments enclose the out-spliced sequence.

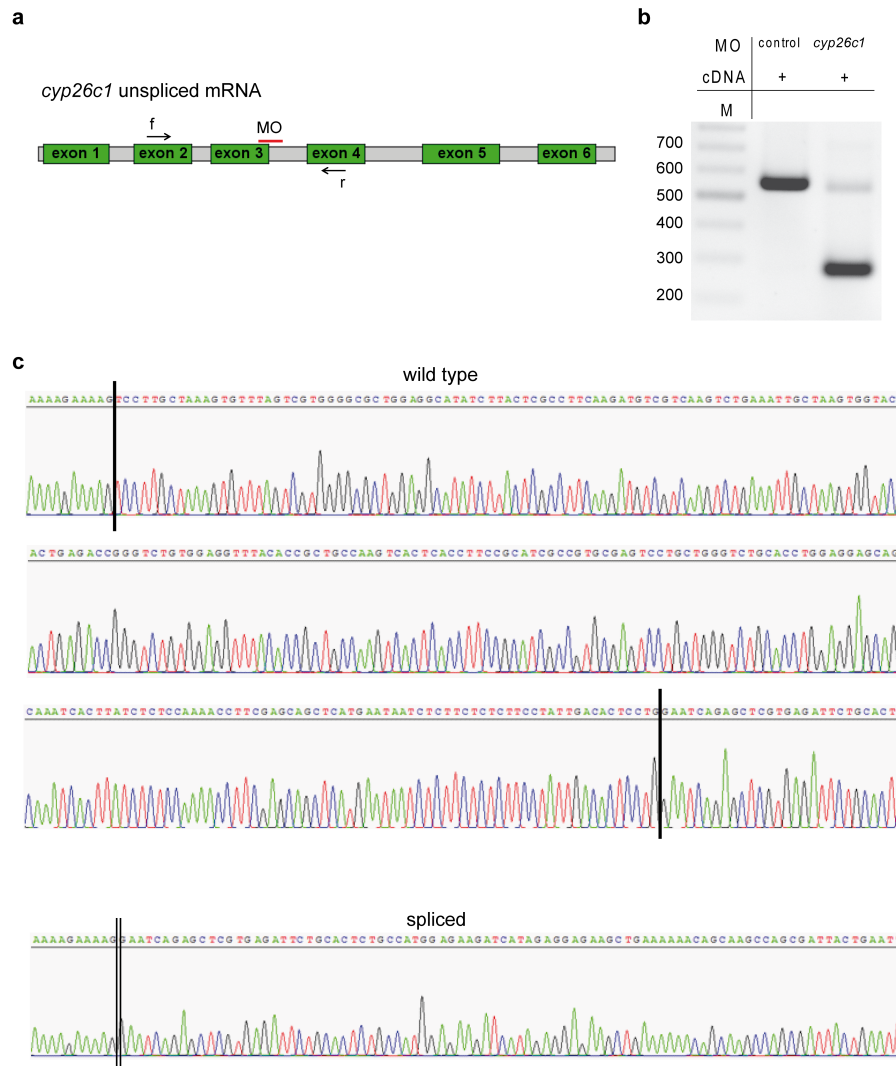


Figure 3.9: *cyp26c1* MO efficacy analysis. (a) Scheme of *cyp26c1* unspliced mRNA. Red bar, region targeted by *cyp26c1* MO; arrows, position of the primers to analyse MO efficacy; f, forward primer; r, reverse primer. (b) RT-PCR analysis of *cyp26c1* MO efficacy. The 530 bp band represents the expected wild type product. Water was used as negative control (-) for the PCR. Samples were obtained from 48hpf embryos. (c) RT-PCR products were cloned in pUC19 and sequenced. *cyp26c1* MO leads to the exclusion of exon 3. Black vertical segments enclose the out-spliced sequence.

3.4.2 *shox* MO knock-down phenotype

We first assessed the effect of *shox* knockdown. Upon *shox* MO injection, the zebrafish embryos showed an overall delayed growth and a strong impairment of pectoral fins development (**Figure 3.10a and b**). *shox* reduction with MO2 led to similar results (**Figure 3.11**). Similar results have been reported in another zebrafish *shox* knockdown model⁶⁵. Antisense probe staining of *sox9*, a known marker of chondrocytes, clearly shows the dramatic pectoral fins phenotype caused by *shox* knockdown (**Figure 3.10c**), although we did not observe any significant change in the expression. Staining of *col2a1*, another marker of chondrocytes, shows that its expression is missing specifically in the *shox* MO injected embryos (**Figure 3.10d**). Finally, pectoral fin areas were measured using ImageJ. We found a dramatic reduction of the pectoral fins suggesting that *shox* role in limb development is highly conserved among vertebrates (**Figure 3.10e**).

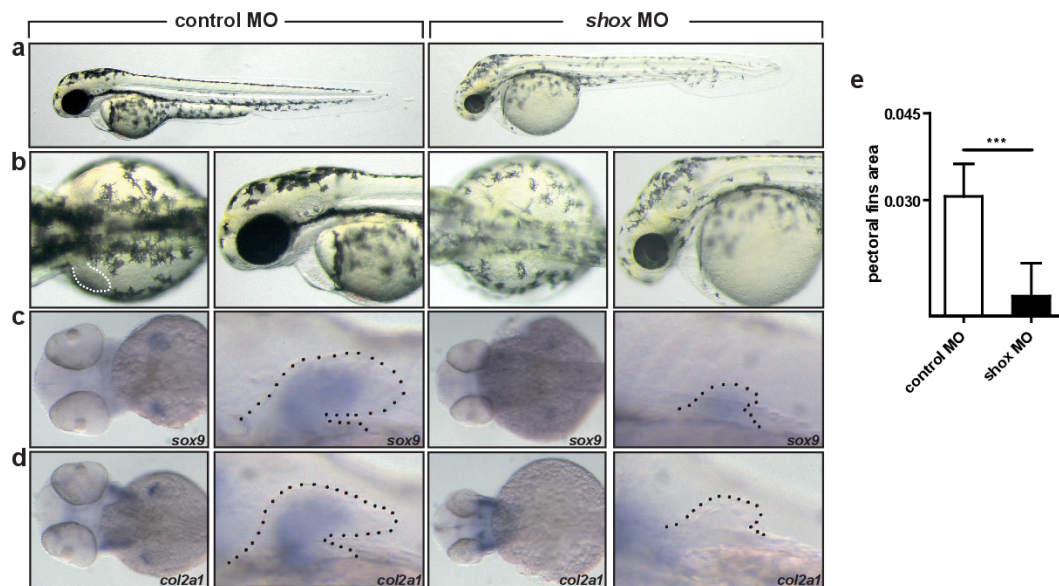


Figure 3.10: Pattern of defects in zebrafish embryos injected with anti-*shox* morpholino. Pattern of defects in zebrafish embryos injected with anti-*shox* morpholino. (a-c) Wild-type embryos injected with control MO or injected with 1-2 ng *shox* MO. (a) Lateral views of the embryos at 55 hpf (hours post fertilization). (b) Dorsal view and magnification on the lateral view of the embryos. White dots mark the pectoral fins. *shox* morphants show smaller fins compared to controls (n=30 embryos). (c and d) Expression at 55 hpf of *sox9* and *col2a1* was examined by *in situ* hybridization in wild-type embryos injected with control MO and with *shox* MO. Black dots mark the protruding pectoral fin. (e) Pectoral fins area was measured by imageJ (n=30 embryos). Data are shown as means \pm SD; *** p-value = 0.0001, two-tailed unpaired Student's t test.

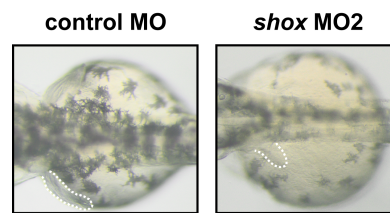


Figure 3.11: Validation of *shox* MO1 pattern of defects with *shox* MO2. Wild type embryos injected with control MO or with *shox* MO2 (n=30 embryos). Dorsal view of the embryos at 55 hpf. Dotted line, pectoral fins.

3.4.3 *cyp26c1* MO knock-down phenotype

We then analyzed the effect of *cyp26c1* knockdown in zebrafish embryos. Injection of *cyp26c1* MO resulted in a significant reduction of pectoral fins size (**Figure 3.12a and b**). Moreover, the embryos showed an abnormal development of the otic vesicles and pharyngeal arches, and a pericardial edema (**Figure 3.12a and b**). *In situ* hybridization of *sox9* revealed a stronger expression upon *cyp26c1* MO injection (**Figure 3.12c**). On the other hand, expression analysis of *shox* was decreased upon *cyp26c1* knockdown (**Figure 3.12e**) which was confirmed by quantitative PCR (**Figure 3.13c**). Expression of *col2a1* was overall reduced, and absent in the pectoral fins (**Figure 3.12d**).

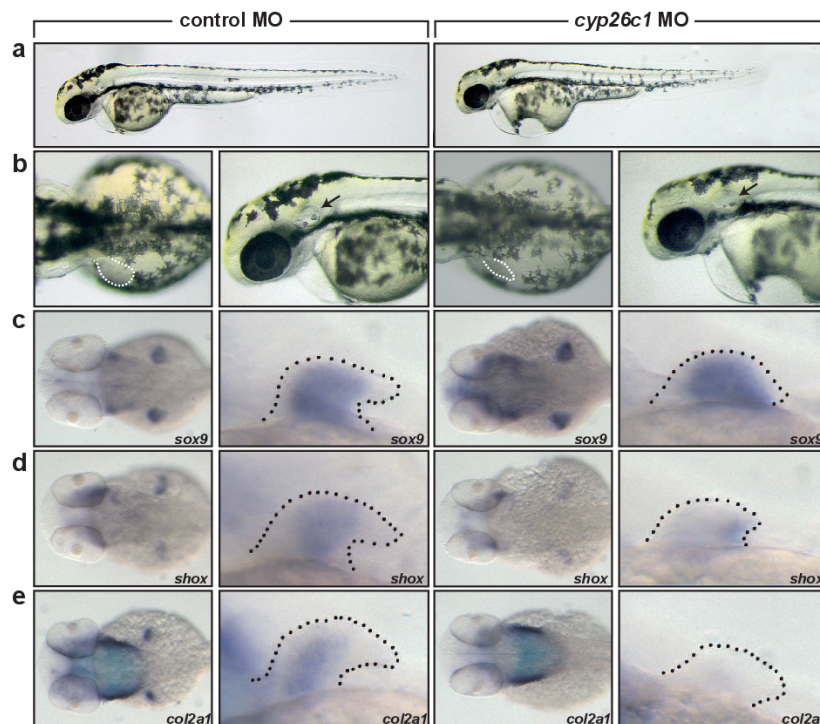


Figure 3.12: Pattern of defects in zebrafish embryos injected with anti-*cyp26c1* MO. (a-e) Wild-type embryos injected with control MO or injected with 1-2 ng of *cyp26c1* MO. (a) Lateral views of the embryos at 55 hours post fertilization (hpf). (b) Dorsal view and magnification on the lateral view of the embryos. White dots mark the pectoral fins. Arrows indicate the otic vesicles. *cyp26c1* morphants show smaller fins compared to controls (n=40). (c-e) Expression at 55 hpf of *sox9*, *col2a1* and *shox* were examined by *in situ* hybridization in embryos injected with control MO or with *cyp26c1* MO. (c) Dorsal view and magnification on the pectoral fins of *sox9* expression. (d) Dorsal view and magnification on the pectoral fins of *col2a1* expression. (e) Dorsal view and magnification on the pectoral fins of *shox* expression. Black dots mark the protruding pectoral fin.

Pectoral fins areas were measured using ImageJ. Knockdown of *cyp26c1* led to a significant reduction of the pectoral fins (**Figure 3.13a**). Moreover, we tested whether CYP26C1 regulates RA levels in zebrafish embryos by co-injecting control or *cyp26c1* MO together with the

Signal RARE-System assay. In accordance with a role of CYP26C1 in RA degradation, MO knockdown of this gene led to a significant increase of RA levels compared to control MO (Figure 3.13b). Finally, we tested whether RA downregulates *Shox* expression in zebrafish embryos as observed in human primary chondrocytes and chicken limb buds. Treatment of zebrafish embryos with 50 nM did not lead to a decrease of *shox* expression, whereas treatment with 100 nM significantly reduced *shox* transcripts. Altogether these data suggest that CYP26C1 plays a role in limb development by exerting its control over RA levels. Moreover, this model further corroborate the hypothesis that *CYP26C1* deficiency leads to an excess of RA which induces a downregulation of *SHOX* expression.

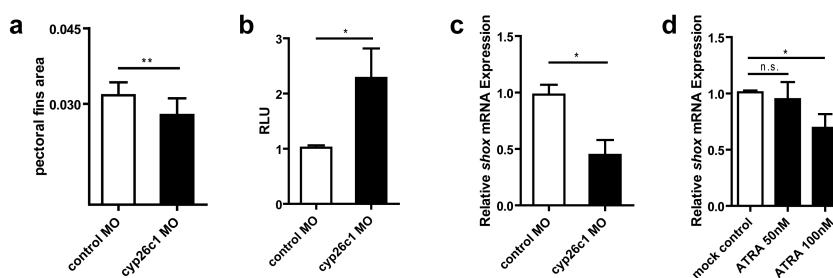


Figure 3.13: Pattern of defects in zebrafish embryos upon MO reduction of *cyp26c1* and RA treatment. (a) Pectoral fins area was measured by imageJ (n=30 embryos). Data are shown as means \pm S.D.; ** p-value = 0.0119, two-tailed unpaired Student's t test. (b) Signal-RARE system luciferase assay testing *cyp26c1* MO on RA acid levels in zebrafish embryos (n = 20-30 embryos, n = 4 replicates). Data are shown as means \pm SD; RLU, Relative Light Units; * p-value = 0.0286, two-tailed Mann-Whitney non-parametric t test. (c) Relative expression of *shox* mRNA normalized to those of housekeeping genes *efl1a* and β -*actin* zebrafish embryos injected with control MO or *cyp26c1* MO (n=20-30 embryos, n=3 replicates). Data are shown as means \pm SD; * p-value = 0.0286, two-tailed Mann-Whitney non-parametric t test.

3.4.4 Double *shox* and *cyp26c1* MO knock-down phenotype

To further test the hypothesis that *CYP26C1* is a modifier of *SHOX* deficiency, we co-injected *shox* and *cyp26c1* MOs. Injections were performed using concentrations of *shox* and *cyp26c1* MOs titrated down to the effect that single knockdown of *shox* or *cyp26c1* MO did not lead to a reduction of the pectoral fins. Upon double knockdown of *shox* and *cyp26c1*, a significant reduction of the pectoral fins was observed (Figure 3.14a). Staining of *sox9* clearly showed the pectoral fins impairment, although difference in the expression of this marker could not be observed (Figure 3.14b). Staining of *col2a1* displayed the pectoral fins reduction and decrease of its expression (Figure 3.14c).

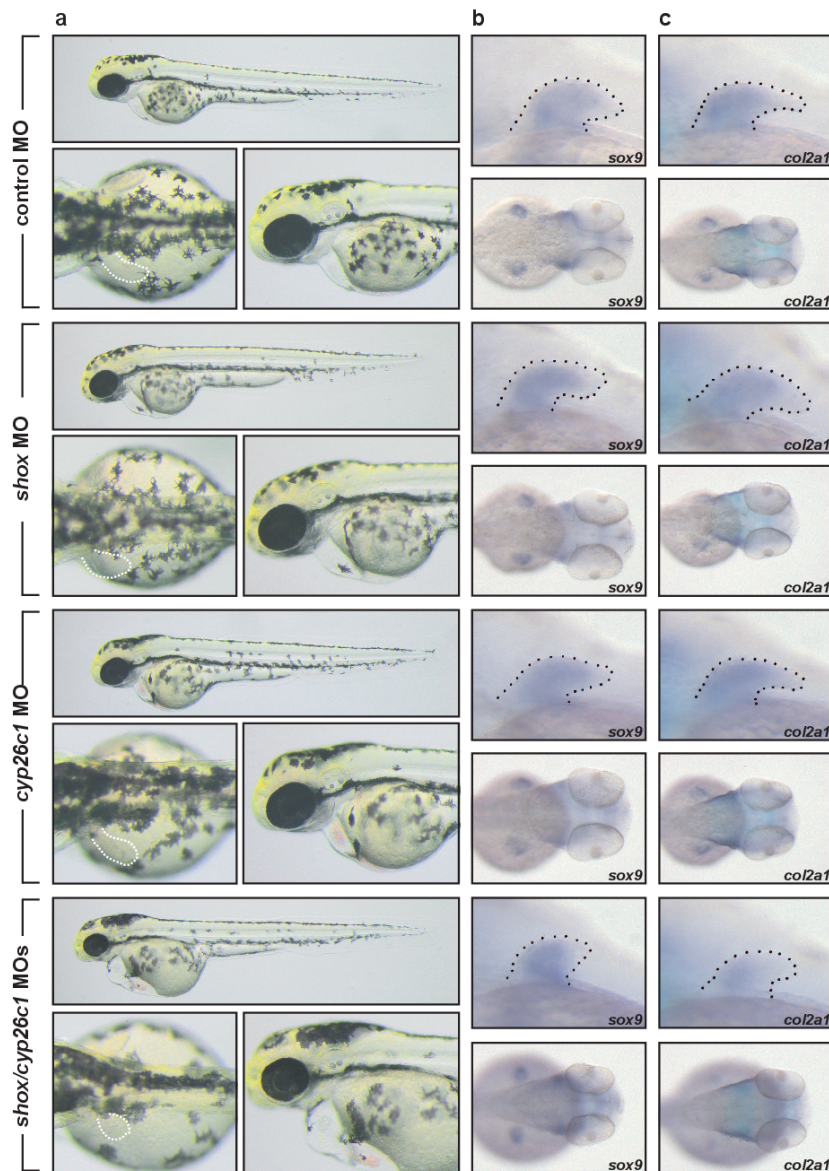


Figure 3.14: Pattern of defects in zebrafish embryos co-injected with anti-*shox* and anti-*cyp26c1* MOs. Wild-type embryos injected with control MO, subphenotypic doses of *shox* MO (100 pg), *cyp26c1* MO (800 pg) or a combination of *shox/cyp26c1* MOs. (a) Lateral view, dorsal view and magnification on the lateral view of the embryos at 55 hpf (hours post fertilization). White dots mark the pectoral fins. *shox/cyp26c1* double morphants show smaller fins compared to control and single MOs (n=20-30 embryos). (b and c) Expression at 55 hpf of *sox9* and *col2a1* was examined by *in situ* hybridization. Dorsal view and magnification on the pectoral fins of *sox9* and *col2a1* expression is shown. Black dots mark the protruding pectoral fin.

Pectoral fins areas were measured by ImageJ. Double knockdown resulted in a significant reduction of the fins (**Figure 3.15a**). Finally, *shox* expression was measured by quantitative PCR. Double knockdown led to a significant decrease of *shox* mRNA expression (**Figure 3.15b**). Altogether, these data corroborate the hypothesis that co-occurrence of *SHOX* and *CYP26C1* deficiency leads to severe short stature phenotypes.

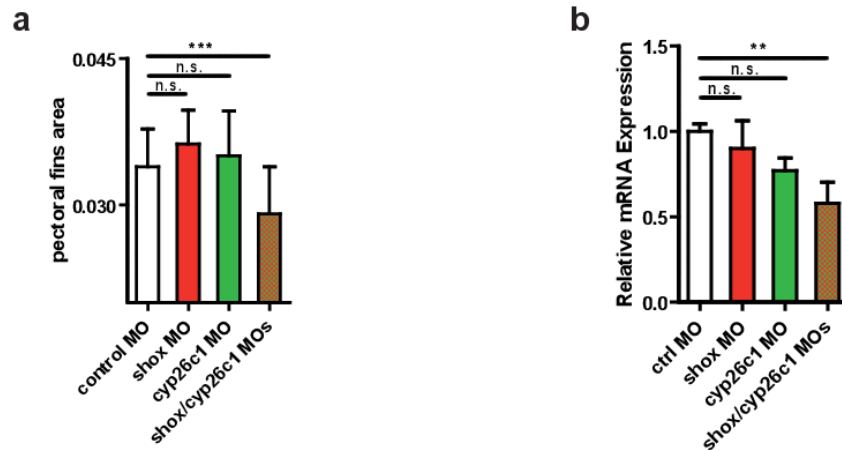


Figure 3.15: Double MO knockdown of *shox* and *cyp26c1* leads to reduced pectoral fins. (a) Pectoral fins area was measured by imageJ (n=20-30 embryos). Data are shown as means \pm SD; *** p-value = 0.0001, one-way ANOVA Bonferroni's multiple comparison test. (b) Relative expression of *shox* mRNA normalized to those of housekeeping genes *efl1 α* and *β -actin* zebrafish embryos injected with control MO, *shox* MO, *cyp26c1* MO, or *shox/cyp26c1* MOs (n=20-30 embryos, n=3 replicates). Data are shown as means \pm SD; ** p-value = 0.0048, Klustal-Wallis Dunn's multiple comparison test.

4 Discussion

Identification of *CYP26C1* as a genetic modifier for *SHOX* deficiency

Phenotype is the result of the relationship between genotype and environment. It has always been of interest to understand how this relationship leads to the phenotypic variability among individuals. Since a phenotype depends on the genotype inherited and since genotypes are easier to tackle than environmental factors, scientists have been mainly focusing on the inheritance of genes to explain specific traits. Many genotypes have been associated to specific phenotypes, however, several studies have reported that a certain genotype does not always lead to the same or related phenotype. For many Mendelian diseases, the identical mutation does not always lead to the same disease phenotype in all individuals who carry it. Some individuals may express a mild phenotype; others a very severe one. Some individuals will never develop the disease; others may be diagnosed at an early age. Based on these observations, already in 1926 Oskar Vogt introduced the terms "penetrance" and "expressivity" as measures of the percentage of individuals in which the genotype is expressed in phenotype and the degree of expression, respectively. Incomplete penetrance and variable expressivity can be explained by the interactions between the genotype correlated to the expected phenotype and genetic and/or environmental factors. The genetic factors, usually addressed as "genetic background", have been indicated as modifier genes: loci that can alter the phenotypic output of another gene⁶⁸. In the literature, only few cases of modifier genes of human phenotypes have been reported, although there are many examples in laboratory mice. Modification can occur at different levels, from a direct effect on the transcription of the target gene, through intermediate phenotypes at the molecular level such as protein-protein interactions, to phenotypes at the level of the whole organism.

Modifier genes may lead to more severe, less severe, novel or wild-type phenotypes by affecting penetrance, expressivity, dominance and pleiotropy⁶⁸. Taken a population of individuals carrying a particular genotype, penetrance indicates the frequency of individuals presenting with the associated phenotype. Unaffected individuals carrying the disease genotype give evidence of reduced penetrance. One example of modifier genes affecting penetrance in human is the case of non-syndromic deafness. Individuals carrying homozygous mutations in the gene *DFNB26* usually present with non-syndromic hearing loss. However, individuals with deficiency of *DFNB26* but normal hearing have been identified. A dominant not yet defined modifier on chromosome 7 protects these individuals from hearing loss, leading to reduced penetrance⁶⁸.

Expressivity describes the extent to which a certain genotype is expressed in the respective phenotype. A disease phenotype may be more severe, mild or even suppressed to seem almost normal. One example of a modifier gene that reduces expressivity is the case of familial hypercholesterolemia. Genetic studies have identified a region on chromosome 13q as bearing a modifier that reduces LDL levels protecting from hypercholesterolemia⁶⁸.

Dominance of a genotype depends on many variables such as allele, genetic background and environmental factors. A phenotype can be inherited in a dominant manner, but behave as recessive on a certain genetic background or *vice versa*. An example of a genetic modifier

affecting dominance is the case of the *PRP1* gene. Homozygous mutations in *PRP1* lead to retinitis pigmentosa indicating that this phenotype is inherited in a recessive manner. However, there are individuals who bear *PRP1* heterozygous mutations but also develop the disease. It has been shown that variants in an independent gene, *ROM1*, modify the retinitis pigmentosa phenotype from a recessive trait to a dominant one in *PRP1* heterozygous individuals⁶⁸.

Pleiotropy describes mutations in single genes which lead to diverse phenotypic effects. Individuals with the same genotype may present different combinations of disease phenotypes depending on the genetic background. Individuals carrying damaging mutations in both the alleles of the pyrin/marenostrin gene present with familial Mediterranean fever. Some individuals with this condition may also be affected by complications like renal amyloidosis. A variant in the gene serum amyloid A has been associated with amyloidosis in individuals with familial Mediterranean fever⁶⁸.

In this PhD project I describe *SHOX* deficiency, a Mendelian disorder with wide phenotypic variability which provides a unique opportunity to identify the genetic causes of such variability. The whole idea shaped when we studied a large family with LWD affected individuals (**Figure 3.1**). Screening *SHOX* gene in this family led to the identification of the variant p.Val161Ala in the five affected individuals. This variant showed a strong effect on *SHOX* transactivation activity (**Figure 3.2**), therefore we thought that the diagnosis was ready to be communicated to the family. Surprisingly, we identified three family members carrying the damaging variant but presenting with normal stature and no skeletal dysmorphisms. This finding prompted us to postulate genetic modifier effects as the possible reasons for such phenotypic variability. In order to identify potential genetic modifiers, we combined whole genome linkage and whole exome sequencing analysis in the family and found a variant in *CYP26C1* co-segregating with the clinical phenotype.

Screening of 68 further unrelated individuals with LWD and damaging variants in *SHOX*, led to the identification of two further unrelated cases presenting with mutations in both *SHOX* and *CYP26C1* (**Figure 3.8**). Family 2 was of paramount importance to corroborate our hypothesis. Individual I:1 (the father) was asymptomatic despite bearing a damaging mutation within the *SHOX* homeodomain, p.Leu132Val. The unaffected daughter (II:1) was described with short stature and carrying the missense *SHOX* variant, but dysmorphic signs were not reported. The daughter presenting the more severe phenotype in this family, carried also a *CYP26C1* variant, p.Arg38His. The mother (I:2) was also normal stature and most likely carried the *CYP26C1* damaging variant; DNA from this individual was not available to confirm inheritance. The third case was a girl carrying a deletion of *SHOX* and a damaging missense variant in *CYP26C1*. This patient presented with severe dysproportionate short stature and Madelung deformity. Her parents and the brother were reported with normal stature. The *SHOX* deletion was confirmed by MLPA analysis only in the daughter indicating that it is a *de novo* event. Therefore, it is possible that the deletion alone is sufficient to lead to the observed phenotype. Although the identified *CYP26C1* heterozygous variant cannot demonstrate specific co-segregation, it adds to overall evidence that damaging variants in *SHOX* and *CYP26C1* co-occur in individuals with severe LWD phenotypes.

Hence, in addition to family 1 we identified two out of 68 unrelated patients with *SHOX* deficiency and damaging mutations in *CYP26C1*. No damaging mutations in *CYP26C1* were found in 140 controls. No individuals from our cohort was found with deleterious variants in both genes. Moreover, we screened TGP for individuals carrying damaging mutations in

both *SHOX* and *CYP26C1*. TGP is an international research effort that has the most detailed catalogue of human genetic variation available to the public so far. TGP assigns a code to each genome. It is therefore possible to track every variant identified in each individual genome present in this database. Most of the *SHOX* variants described in TGP are associated with short stature, but it is not possible to retrieve the individual code. However, for some *SHOX* variants it is possible to retrieve the individual code. I selected those individuals carrying *SHOX* damaging variants and asked whether they bear damaging variants also in *CYP26C1*. No individual from the TGP database was found to carry damaging variants in both genes. Altogether, these data suggest that co-occurrence of *SHOX* deficiency and damaging mutations in *CYP26C1* in LWD patients is not coincidental.

***CYP26C1* exerts its modifier effects by regulating *SHOX* expression through the control of RA levels**

CYP26C1 is an enzyme belonging to the cytochrome P450 superfamily and is involved in the oxidation of RA to generate polar retinoid species which are readily excreted. Thus, *CYP26C1* is involved in the catabolism of RA⁶². Accordingly, we found that damaging mutations in *CYP26C1* reduce its RA catabolizing activity leading to a higher concentration of this retinoid in U2OS cells (**Figure 3.6d and 3.8c**).

RA exerts its function by regulating the transcriptional activity of nuclear retinoic acid receptors (RARs). RARs heterodimerize with retinoic X receptors (RXRs) to function as transcription factors. Binding of RA to these receptors triggers activation or repression of their target genes⁴. RA plays a key role in development, including formation of the body axis and skeleton⁶³. During skeletal development, RA coordinates the development of central body axis, limb axis and cranium. Moreover, it controls chondroblast differentiation and coordinates maturation and replacement of bone tissue during endochondral ossification⁴. RA also plays a role in the post-natal maintenance of bone⁶. An excess or a deficiency of RA dysregulate the expression of the respective target genes, which has a dramatic effect on development⁴. Excess or deficiency of RA have, for example, been shown to impair limb development in zebrafish and mice embryos⁶⁹⁻⁷³. Hence, a tight regulation of RA metabolism is essential.

We demonstrated for the first time that *CYP26C1* is expressed on RNA and protein level in human primary chondrocytes (**Figure 3.7a**), suggesting a role for *CYP26C1* in the fine regulation of RA in these cells. It would be interesting to test whether loss of function of this gene in primary chondrocytes, e.g. by genome editing with the CRISPR-Cas9 system, leads to a higher sensitivity to exposure to excess of RA. I tested several transfection reagents and nucleofection to introduce external DNA inside primary chondrocytes. Former lab members also tried similar approaches several years ago. Only lentiviral transduction proved to be successful, although low efficiency was observed (PD Dr. Antonio Marchini, personal communication).

Damaging variants in *CYP26C1* that affect its RA oxidation activity may lead to high levels of this retinoid. Previous experiments on chicken limbs have shown that treatment with excess RA strongly reduces *Shox* expression³⁴. Consistent with a role of RA in *SHOX* regulation, we have shown that treatment of human primary chondrocytes and zebrafish embryos with a concentration of 100 nM RA significantly reduced *Shox* mRNA expression

(**Figure 3.7b** and **3.16**). *Shox* transcription was not significantly affected by 10-50 nM RA, suggesting that a main function of CYP26C1 is to protect cells from the effect of excessive RA on its target genes expression. In support of this hypothesis, we found that knockdown of *cyp26c1* in zebrafish embryos increased RA levels, reduced *col2a1* and *shox* expression and upregulated *sox9* expression (**Figure 3.15** and **3.16**). Sox9 is a key transcription factor necessary for the differentiation of mesenchymal progenitors into chondrocytes. Sox9 is highly expressed in chondroblasts and proliferative chondrocytes and is downregulated during hypertrophy. Col2a1 is a major component of cartilage matrix during the early stages of endochondral differentiation. Shox is a transcription factor which is expressed in resting, proliferative and terminally differentiated hypertrophic chondrocytes. High expression of *SHOX* can be observed in the hypertrophic region. We showed that the increase in RA levels induced by *cyp26c1* knockdown in zebrafish embryos alters the expression of different genes. Upregulation of *sox9* and downregulation of *col2a1* and *shox*, among the genes which are dysregulated by high levels of RA, may lead to inhibition of hypertrophy and delayed or defective ossification. These cellular phenotypes eventually may manifest with shortened limbs and dysmorphic signs like Madelung deformity.

In order to test whether RA reduces *SHOX* expression directly or indirectly, I performed *in silico* analysis of *SHOX* locus. Several putative binding sites were identified both in the promoter regions and in introns. I decided to focus the analysis on the published P1 and P2 promoter. To test RA effect on these sequences, I cloned P1 and P2 in the pGL3basic vector together with the CNE3 enhancer and performed luciferase assays in U2OS cells. P1 did not show any effect on luciferase expression (data not shown). The P2 promoter, however, induced luciferase expression in U2OS cells as previously shown³³. Interestingly, treatment with ATRA led to a significant reduction of luciferase activity. These data suggest that P2 is regulated by RA. To verify whether this was a direct or indirect effect, I mutated the three putative RXR α binding site identified in P2. Luciferase downregulation upon RA treatment did not significantly change in this mutant suggesting that RA regulation of P2 does not depend on this DNA sequence but rather RA exerts an indirect effect. Further analysis is needed to clarify the molecular mechanisms by which RA exerts its control over *SHOX* expression regulation. It would be interesting, for example, to perform reverse chromatin immunoprecipitation assays coupled with mass spectrometry analyses to identify potential regulators of *SHOX* expression upon RA treatment.

Is there an interaction between RA and estrogen signalling over *SHOX* expression regulation?

Several studies have reported that mesomelia and Madelung deformity are more severe in adult females than in children or adult males. Madelung deformity is difficult to diagnose in prepubertal patients, although slight mesomelia and subtle dysmorphisms are usually observed in LWD individuals⁴⁶. The mother (II:4), an aunt (II:8) and the stepsister (III:1) of the index patient (III:2) in family 1 presented, for example, short stature but dysmorphic skeletal signs were not diagnosed. These individuals did not carry damaging variants neither in *SHOX* nor in *CYP26C1*, suggesting that different factors contribute to the short stature phenotype observed in these family members. Mesomelia and Madelung deformity phenotypes were present only in those individuals carrying damaging variants in *SHOX* and *CYP26C1* in the three families identified in this study.

We also reported male individuals in family 1 (III:5, III:6) and family 2 (I:1) with damaging *SHOX* variants but normal stature. Hence, gender bias could explain the reported severe phenotypes in the affected individuals in these two families independently of *CYP26C1*. However, in family 1 the father (II:3) of the index patient (III:2) presented with short stature, mesomelia and borderline Madelung deformity, and bore damaging variants in both *SHOX* and *CYP26C1*. The sister (III:4) of the index patient (III:2) presented with height within the normal range and no skeletal phenotype, and had only the *SHOX* damaging variant. In family 2, the sister (II:1) of the patient presented with short stature but neither mesomelia nor Madelung deformity were identified; she bore only the damaging variant in *SHOX*. Together, these data suggest that damaging missense variants in *CYP26C1* play an important role as modifiers of *SHOX* deficiency towards more severe dysmorphic phenotypes. Since in family 1 the father (II:3) of the index patient (III:2) presented with milder mesomelia and borderline Madelung deformity, it is obvious that gender exerts a modifier effect on *SHOX* deficiency even in presence of *CYP26C1* damaging variants. We cannot exclude that the non-affected daughters in family 1 and 2 bearing only the *SHOX* variants will develop dysmorphic phenotypes during puberty. Noteworthy, diagnoses of the affected daughters in family 1 and 2 bearing damaging variants both in *SHOX* and *CYP26C1* identified severe phenotypes already before puberty (**Table 3.1 and 3.2**).

It has been suggested that gonadal estrogens aggravate effects in patients with *SHOX* deficiency by enhancing premature epiphyseal fusion¹⁷. In support to this hypothesis, a combination of *SHOX* overdosage and gonadal estrogen deficiency has been associated to tall stature²⁵.

The males reported in this thesis presented with normal or milder *SHOX* deficiency phenotypes even in the presence of damaging variants in *CYP26C1*, in accordance with the aforementioned observation that LWD affects more females than males.

Estrogens exert their function through the regulation of the estrogen receptors (ERs) transcription factors ER α and ER β . Studies in breast cancer reported that RAR α and ER α interact to regulate gene expression. In particular, it has been shown that RAR α and ER α can bind overlapping DNA sequences and cooperate or antagonize to regulate gene expression^{74;75}. Such interactions may occur also to regulate *SHOX* expression. I performed *in silico* analysis on the *SHOX* locus to identify potential binding sites for ERs and identified different sequences in the *SHOX* promoter and intronic regions. Interestingly, some of these sites overlapped with RARs and RXRs binding sites. It would therefore be interesting to test whether estrogens regulate *SHOX* expression, whether there is interactions between estrogens and retinoids, and what the nature of such interactions is. Such data could help elucidating the molecular mechanisms underlying the clinical manifestations variability observed in *SHOX* deficiency male and female patients thereby broadening the understanding of the intricate network regulating *SHOX* expression during bone development.

***SHOX* dosage plays an important role on individual height**

Height depends mostly on the longitudinal growth of the limbs. Longitudinal growth of bones occurs at the epiphysial plates or growth plates. Each growth plate is characterized by three zones: the resting zone populated by round resting chondrocytes; the proliferating zone consisting of flattened proliferating chondrocytes which organize in columns in the direction of longitudinal growth; hypertrophic zone, composed of chondrocytes which undergo through terminal differentiation by withdrawing from the cell cycle and increasing their volumes. The

volume increase of hypertrophic chondrocytes contributes to long bone lengthening. These processes are tightly regulated and are orchestrated by a complex network of factors and genes; *SHOX* is a key player among them. Single nucleotide variants and deletions in *SHOX* gene and enhancers have been shown to lead to variable short stature phenotypes. Interestingly, gene dosage of *SHOX* has been shown to determine height: *SHOX* deficiency causes short stature, whereas *SHOX* overdosage has been associated to tall stature in Klinefelter individuals or 47,XXX females²⁵. *SHOX* has been suggested to repress growth plate fusion and skeletal maturation in the distal limbs. *SHOX* deficiency is characterized by premature epiphyseal plate fusion and relatively advanced skeletal maturation. In Klinefelter patients, for example, a *SHOX* overdosage leads to a delayed growth plate fusion and consequently to longer limbs²⁵. Thus, different dosages of the *SHOX* protein play an important role in determining the height of an individual. We have found that damaging mutations in *CYP26C1* increases RA levels, which reduces *SHOX* dosage and exacerbate *SHOX* deficiency phenotypes. To corroborate this hypothesis, we titrated the amount of each MOs down to a concentration not sufficient to trigger a phenotype. We have demonstrated that the co-injection of these subphenotypic dosages of *shox* and *cyp26c1* MOs strongly shortened pectoral fins (**Figure 3.17**).

***CYP26C1*, not only a modifier for *SHOX* deficiency**

In our zebrafish model of *cyp26c1* MO knockdown pectoral fins were affected. Embryos showed also abnormalities of otic vesicles and pharyngeal arches (**Figure 3.12**).

Homozygous/compound heterozygous damaging variants in *CYP26C1* have been previously associated with focal facial dysplasia type IV (FFDD4), a mild disorder of the skin characterized by bitemporal or preauricular vesicular skin lesions⁷⁶. In this study, only the skin lesions were described; other abnormalities were not reported and height and skeleton were not analysed. Interestingly, zebrafish otic vesicles and pharyngeal arches are structures that encompass the sites of the skin lesions observed in FFDD4 patients. Thus, the *cyp26c1* zebrafish MO knockdown may represent a model for the analysis of both LWD and FFDD4.

CYP26C1 heterozygous individuals were reported as not affected in the FFDD4 study. In *SHOX* deficiency patients with *CYP26C1* heterozygous damaging variants as reported in this thesis, skin lesions were not diagnosed. Moreover, we also report an individual (Family 3, the father) carrying a damaging variant in *CYP26C1* who did neither show an obvious skeletal nor FFDD4 phenotype. It is therefore possible that, in contrast to our zebrafish model, deficiency of *CYP26C1* alone does not lead to obvious short stature and/or dysmorphic phenotypes nor FFDD4.

As mentioned in the Introduction, *CYP26A1*, *B1* and *C1* are all members of the cytochrome P450 26s subfamily of enzymes. All three genes are able to catabolize RA⁸ and are present in human, mice, and zebrafish. Uehara et al. have shown that loss of *Cyp26a1* in mice leads to hindbrain defects. *Cyp26a1* knockout mice brain phenotypes are, however, milder when compared to RA treated animals. Loss of *Cyp26c1* does not affect embryonic development and mice are viable and fertile⁷², suggesting functional redundancy among *Cyp26s* genes. Interestingly, loss of both *Cyp26a1* and *Cyp26c1* leads to severe brain abnormalities during development when compared to single knockout and these phenotypes resemble those induced by RA treatment. These data suggest that *Cyp26a1* and *Cyp26c1* play redundant roles in the control of RA levels. Similar data have been shown in zebrafish embryos hindbrain devel-

opment⁷⁷ and likewise, Kinkel et al. reported functional redundancy among the three *cyp26s* genes in the regulation of the pancreatic field in zebrafish embryos⁷⁸. It is therefore possible that damaging mutations in *CYP26C1* are compensated by *CYP26A1* and/or *CYP26B1* to prevent the cells to be exposed to excessive RA levels, protecting from FFDD4 and skeletal phenotypes in the context of a *SHOX* wildtype genotype. However, *CYP26C1* heterozygous damaging variants can still lead to RA amounts high enough to downregulate *SHOX* expression and to up- or down-regulate other genes in the limbs, modifying towards more severe *SHOX* deficiency phenotypes.

To address the question whether *CYP26C1* damaging variants alone can play a role in short stature, we analyzed the coding sequence of this gene in 256 individuals with ISS and LWD where *SHOX* deficiency could be excluded. The present data do not provide support for a role of *CYP26C1* alone in the aetiology of short stature (**Figure 3.5**). On the other hand, this hypothesis cannot be excluded without a systematic analysis, as it may lead to less dramatic effects compared to *SHOX* deficiency. Screening of a larger cohort of short stature individuals with detailed clinical data could answer this question. Based on the present data, we postulate that certain *CYP26C1* variants do not have detectable effects in the absence of *SHOX* deficiency but are capable of modifying the phenotypic outcome of *SHOX* deficiency towards higher penetrance and stronger severity. Accordingly to this hypothesis, Grüneberg defined modifier genes as "capable of modifying the manifestation of a mutant gene without having an obvious effect on the normal condition"⁷⁹.

Conclusions

The aim of my thesis was to elucidate the genetic causes of clinical variability observed in patients with *SHOX* deficiency. Only a few genetic modifiers have been reported in the literature so far⁸⁰⁻⁸⁵, but recent technological advances are helping to broaden the understanding of the molecular basis of quantitative or discrete qualitative differences in phenotype. A primary reason to identify disease modifiers is to enable the accurate prediction of disease progression and improve therapeutic development. We uncovered one of the component of the RA pathway, *CYP26C1*, as biological modifier of the penetrance and expressivity of *SHOX* deficiency. Based on the reported data we propose the following model: In individuals with normal height, *SHOX* wild type regulates the transcription of its target genes to accomplish endochondral ossification. *CYP26C1* controls that the RA intracellular levels do not exceed a determined concentration leading to normal growth and development (**Figure 4.1a**). In individuals with heterozygous mutations or deletions of *SHOX* gene, the complex and delicate network of factors and genes is dramatically affected, leading to LWD. However, the penetrance of *SHOX* deficiency is not complete and some individuals present with stature within the normal range and no dysmorphic phenotype. Damaging variants in *CYP26C1* affect its catabolic activity leading to high levels of RA which alter the gene expression program regulating endochondral ossification. *SHOX* is among the genes which are disregulated by higher levels of RA. Hence, the combination of *SHOX* and *CYP26C1* deficiencies alter chondrocytes differentiation and hypertrophy at the growth plates of long bones resulting in shortened mesomelic limbs and Madelung deformity (**Figure 4.1b**). We propose that manipulating the RA signalling pathway in these patients may be therapeutically beneficial.

Finally, I would like to conclude by addressing an important point which needs to be clarified by further studies. Why do some individuals bearing *SHOX* damaging variants (Family

1, individuals III:3, III:5 and III:6; Family 2, individuals I:1 and II:1) not present with LWD? In family 1, individuals III:4 and the twins III:5 and III:6 do not share the same parents. Therefore, it is unlikely that they bear common genetic factors that protect them from SHOX deficiency. The *SHOX* variant identified in Family 2, p.L132V, has already been reported in another independent family suggesting that it can lead to LWD (although it would be interesting to analyze *CYP26C1* in this family). Moreover, functional analyses of the *SHOX* variants identified in family 1 and 2 show a strong damaging effect on protein activity, further corroborating causality. Not only missense mutations but also deletions of *SHOX* exome or its regulatory regions have been reported in normal stature individuals without dysmorphic signs^{19;47;48}. Hence, I hypothesize that the genetic background has a stronger effect than *SHOX* allelic variability in the clinical variability observed in *SHOX* deficiency individuals.

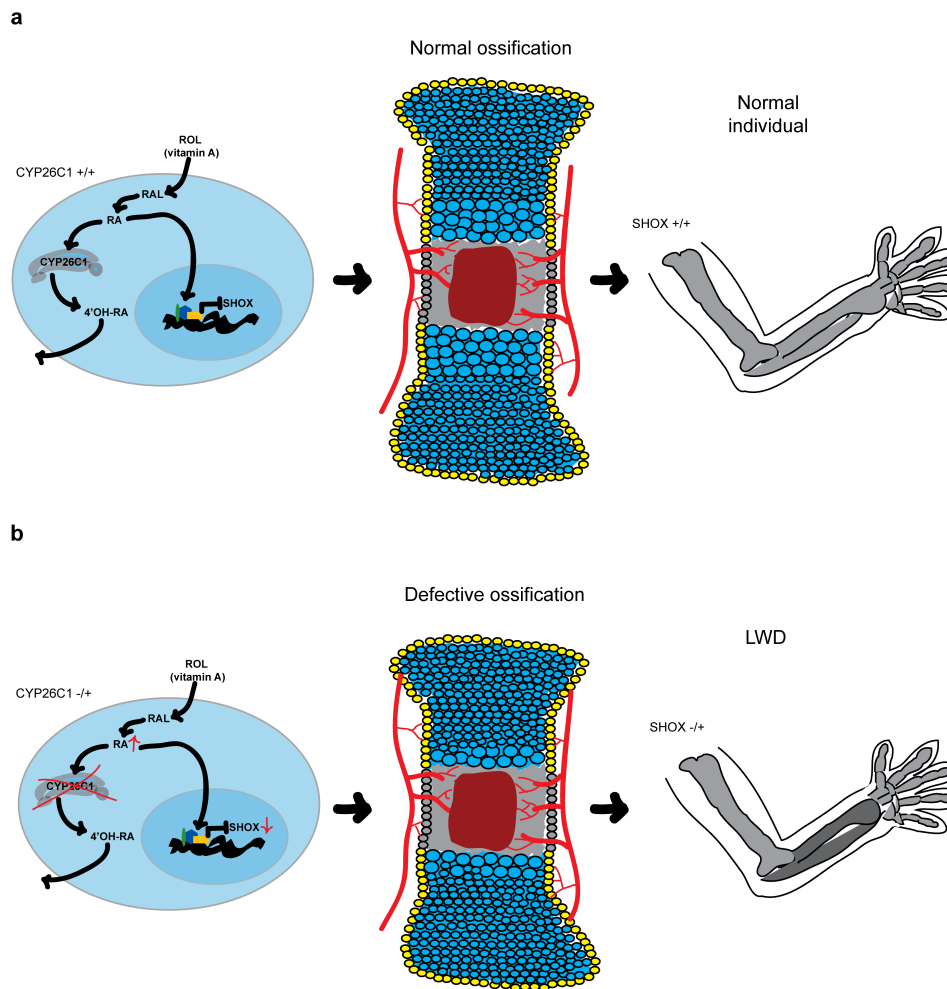


Figure 4.1: Schematic representation of *CYP26C1* modifier effect on *SHOX* deficiency. (a) Individuals with *SHOX* and *CYP26C1* wildtype. *CYP26C1* regulates RA levels within the physiologic concentration range. The complex network of factors and genes involved in endochondral ossification remains unaffected leading to a normal phenotype. Normal height can also be observed in some cases of *SHOX* deficiency since penetrance is not 100%. Individuals carrying *CYP26C1* damaging variants show normal height. (b) Individual carrying damaging mutations in *SHOX* and *CYP26C1*. Damaging mutations in *CYP26C1* affect its catabolic activity leading to higher intracellular levels of RA. Excess of RA dysregulates its target genes expression; *SHOX* is downregulated. In case of *SHOX* deficiency, further decrease of its protein affects the complex network regulating bone formation leading to delayed ossification. These cellular/molecular mechanisms exacerbate the penetrance and severity of LWD.

Bibliography

- [1] Judge TA and Cable DM.(2004). The effect of physical height on workplace success and income: preliminary test of a theoretical model. *J Appl Psychol.* 89, 428-441.
- [2] Cooper KL, Oh S, Sung Y, Dasari R, Kirschner MW, Tabin CJ. (2013). Multiple phases of chondrocyte enlargement underlie differences in skeletal proportions. *Nature.* 495, 375-378.
- [3] Tsang KY, Chan D, Cheah KS. (2014). The chondrocytes journey in endochondral bone growth and skeletal dysplasia. *Dev Growth Differ.* 57, 179-192.
- [4] Weston AD, Hoffman LM, Underhill TM. (2003). Revisiting the role of retinoid signaling in skeletal development. *Birth Defects Res C Embryo Today.* 69, 156-173.
- [5] Solomon LA, Berube NG, Beier F. (2008). Transcriptional regulators of chondrocyte hypertrophy. *Birth Defects Res C Embryo Today.* 84, 123-130.
- [6] Green AC, Martin TJ, Purton LE. (2016). The role of vitamin A and retinoic acid receptor signalling in post-natal maintenance of bone. *J Steroid Biochem Mol Biol.* 155, 135-146.
- [7] Ranke MB. (1994). The KIGS aetiology classification system. Ranke MB and Gunnarson R (editors), In Progress in growth hormone therapy-5 years of KIGS. Mannheim: J&J Verlag GmbH. pp. 51-61.
- [8] Pennimpede T, Cameron DA, MacLean GA, Li H, Abu-Abed S, Petkovich M. (2010). The role of CYP26 enzymes in defining appropriate retinoic acid exposure during embryogenesis. *Birth Defects Res A Clin Mol Teratol.* 88, 883-894.
- [9] Durand C and Rappold GA. (2013). Height matters-from monogenic disorders to normal variation. *Nat Rev Endocrinol.* 9, 171-177.
- [10] Baron J, Säwendahl L, De Luca F, Dauber A, Philip M, Wit JM, Nilsson O. (2015). Short and tall stature: a new paradigm emerges. *Nat Rev Endocrinol.* 11, 735-746.
- [11] Horton WA, Machado MA, Ellard J, Campbell D, Bartlev J, Ramirez F, Vitale E, Lee B. (1992). Characterization of a type II collagen gene (COL2A1) mutation identified in cultured chondrocytes from human hypochondrogenesis. *Proc Natl Acad Sci USA.* 89, 4583-4587.
- [12] Prinos P, COsta T, SOMmer A, Kilpatrick MW, Tsipouras P. (1995). A common FGFR3 gene mutation in hypochondroplasia. *Hum Mol Genet.* 4, 2097-2101.
- [13] Rao E, Weiss B, Fukami M, Rump A, Niesler B, Mertz A, Muroya K, Binder G, Kirsch S, Winkelmann M, Nordsiek G, Heinrich U, Breuning MH, Ranke MB, Rosenthal A, Ogata T, Rappold GA. (1997). Pseudoautosomal deletions encompassing a novel homeobox gene cause growth failure in idiopathic short stature and Turner syndrome. *Nat Genet.* 16, 54-63.
- [14] Belin V, Cusin V, Viot G, Girlich D, Toutain A, Moncla A, Le Merrer M, Munnich A, Cornier-Daire V. (1998). SHOX mutations in dyschondrosteosis (Leri-Weill syndrome). *Nat Genet.* 19, 67-69.

Bibliography

- [15] Shears DJ, Vassal HJ, Goodman FR, Palmer RW, Reardon W, Superti-Furga A, Scambler PJ, Winter RM. (1998). Mutation and deletion of the pseudoautosomal gene SHOX cause Leri-Weill dyschondrosteosis. *Nat Genet.* 19, 70-73.
- [16] Marchini A, Ogata T, Rappold GA. (2016). A track record on SHOX: from basic research to complex models and therapy. *Endocr Rev.* er20161036.
- [17] Seki A, Jinno T, Suzuki E, Takayama S, Ogata T, Fukami M. (2014). Skeletal deformity associated with SHOX deficiency. *Clin Pediatr Endocrinol.* 23, 65-72.
- [18] Benito-Sanz S, Thomas NS, Huber C, Gorbenko del Blanco D, Aza-Carmona M, Crolla JA, Maloney V, Rappold G, Argente J, Campos-Barros A, Cormier-Daire V, Heath KE. (2005). A novel class of Pseudoautosomal region 1 deletions downstream of SHOX is associated with Leri-Weill dyschondrosteosis. *Am J Hum Genet.* 77, 533-544.
- [19] Benito-Sanz S, Royo JL, Barroso E, Paumard-Hernandez B, Barreda-Bonis AC, Liu P, Gracia R, Lupski JR, Campos-Barros A, Gómoez-Skarmeta JL, Heath JE. (2012). Identification of the first recurrent PAR1 deletion in Léri-Weill dyschondrosteosis and idiopathic short stature reveals the presence of a novel SHOX enhancer. *J Med Genet.* 49, 442-450.
- [20] Ogata T, Onigata K, Htsubo T, Matsuo N, Rappold G. (2001). Growth hormone and gonadotropin-releasing hormone analog therapy in haploinsufficiency of SHOX. *Endocr J.* 48, 317-322.
- [21] Zinn AR. (1997). Growing interest in Turner syndrome. *Nat Genet.* 16, 3-4.
- [22] Sybert VP and McCauley E.(2004). Turner's syndrome. *N Engl J Med.* 351, 1227-1238.
- [23] Clement-Jones M, Schiller S, Rao E, Blaschke RJ, Zuniga A, Zeller R, Robson SC, Binder G, Glass I, Strachan T, Lindsay S, Rappold G. (2000). The short stature homeobox gene SHOX is involved in skeletal abnormalities in Turner syndrome. *Hum Mol Genet.* 9, 695-702.
- [24] Seo GH, Kang E, Cho JH, Lee BH, Choi JH, Kim GH, Seo EJ, Yoo HW. (2015). Turner syndrome presented with tall stature due to overdosage of the SHOX gene. *Ann Pediatr Endocrinol Metab.* 20, 110-113.
- [25] Ogata T, Matsuo N, Nishimura G. (2001). SHOX haploinsufficiency and overdosage: impact of gonadal function status. *J Med Genet.* 38, 1-6.
- [26] Durand C, Roeth R, Dweep H, Vlatkovic, Decker E, Schneider KU, Rappold G. (2011). Alternative splicing and nonsense-mediated RNA decay contribute to the regulation of SHOX expression. *PLoS One.* 6, e18115. doi:10.1371/journal.pone.0018115.
- [27] Munns CF, Glass IA, LaBrom R, Hayes M, Flanagan S, Bery M, Hyland VJ, Batch JA, Philips GE, Vickers D. (2001). Histopathological analysis of Leri-Weill dyschondrosteosis: disordered growth plate. *Hand Surg.* 6, 13-23.
- [28] Marchini A, Marttila T, Winter A, Caldeira S, Malanchi I, Blaschke RJ, Häcker B, Rao E, Karperien M, Wit JM, Richter W, Tommasino M, Rappold GA. (2004). The short stature homeodomain protein SHOX induces cellular growth arrest and apoptosis and is expressed in human growth plate chondrocytes. *J Biol Chem.* 279, 37103-37114.
- [29] Blaschke RJ, Töpfer C, Marchini A, Steinbeisser H, Janssen JW, Rappold GA. (2003). Transcriptional and translational regulation of the Ler-Weill and Turner syndrome homeobox gene SHOX. *J Biol Chem.* 278, 47820-47826.

Bibliography

- [30] Sabherwal N, Bangs F, Röth R, Weiss B, Jantz K, Tiecke E, Hinkel GK, Spaich C, Hauffa BP, van der Kamp H, Kapeller J, Tickle C, Rappold G. (2007). Long-range conserved non-coding SHOX sequences regulate expression in developing chicken limb and are associated with short stature phenotypes in human patients. *Hum Mol Genet.* 16, 210-222.
- [31] Durand C, Bangs F, Signolet J, Decker E, Tickle C, Rappold G. (2010). Enhancer elements upstream of the SHOX gene are active in the developing limb. *Eur J Hum Genet.* 18, 527-532.
- [32] Kenyon EJ, McEwen GK, Callaway H, Elgar G. (2011). Functional analysis of conserved non-coding regions around the short stature hox gene (shox) in whole zebrafish embryos. *PLoS One.* 6, e21498. doi:10.1371/journal.pone.0021498.
- [33] Verdin H, Fernández-Miñán A, Benito-Sanz S, Janssens S, Callewaert B, De Waele K, De Schepper J, François I, Menten B, Heath KE, Gómez-Skarmeta JL, De Baere E. (2015). Profiling of conserved non-coding elements upstream of SHOX and functional characterization of the SHOX cis-regulatory landscape. *Sci Rep.* 5, 17667. doi: 10.1038/srep17667.
- [34] Tiecke E, Bangs F, Blaschke R, Farrell ER, Rappold G, Tickle C. (2006). Expression of the short stature homeobox gene Shox is restricted by proximal and distal signals in chick limb buds and affects the length of skeletal elements. *Dev Biol.* 298, 585-596.
- [35] Rao E, Blaschke RJ, Marchini A, Niesler B, Burnett M, Rappold GA. (2001). The Leri-Weill and Turner syndrome homeobox gene SHOX encodes a cell-type specific transcriptional activator. *Hum Mol Genet.* 10, 3083-3091.
- [36] Marchini A, Häcker B, Marttila T, Hesse V, Emons J, Weiss B, Karperien M, Rappold G. (2007). BNP is a transcriptional target of the short stature homeobox gene SHOX. *Hum Mol Genet.* 16, 3081-3087.
- [37] Aza-Carmona M, Shears DJ, Yuste-Checa P, Barca-Tierno V, Hisado-Oliva A, Belinchón A, Benito-Sanz S, Rodríguez JI, Argente J, Campos-Barros A, Scambler PJ, Heath KE. (2011). SHOX interacts with the chondrogenic transcription factors SOX5 and SOX6 to activate the aggrecan enhancer. *Hum Mol Genet.* 20, 1547-1559.
- [38] Decker E, Durand C, Bender S, Rödelsperger C, Glaser A, Hecht J, Schneider KU, Rappold G. (2011). FGFR3 is a target of the homeobox transcription factor SHOX in limb development. *Hum Mol Genet.* 20, 1524-1535.
- [39] Beiser KU, Glaser A, Kleinschmidt K, Scholl I, Röth R, Li L, Gretz N, Mechttersheimer G, Karperien M, Marchini A, Richter W, Rappold GA. (2014). Identification of novel SHOX target genes in the developing limb using a transgenic mouse model. *PLoS One.* 29, e98543. doi: 10.1371/journal.pone.0098543.
- [40] Sabherwal N, Blaschke RJ, Marchini A, Heine-Suner D, Rosell J, Ferragut J, Blum WF, Rappold G. (2004). A novel point mutation A170P in the SHOX gene defines impaired nuclear translocation as a molecular cause for Léri-Weill dyschondrosteosis and Langer dysplasia. *J Med Genet.* 41, e83.
- [41] Sabherwal N, Schneider KU, Blaschke RJ, Marchini A, Rappold G. (2004). Impairment of SHOX nuclear localization as a cause for Léri-Weill syndrome. *J Cell Sci.* 117, 3041-3048.
- [42] Schneider KU, Marchini A, Sabherwal N, Röth R, Niesler B, Marttila T, Blaschke RJ, Lawson M, Dumic M, Rappold G. (2005). Alteration of DNA binding, dimerization, and nuclear translocation of SHOX homeodomain mutations identified in idiopathic short stature and Leri-Weill dyschondrosteosis. *Hum Mutat.* 26, 44-52.

Bibliography

- [43] Marchini A, Daeffler L, Marttila T, Schneider KU, Blaschke RJ, Schnölzer M, Rommelaere J, Rappold G. (2006). Phosphorylation on Ser106 modulates the cellular functions of the SHOX homeodomain protein. *J Mol Biol.* 355, 590-603.
- [44] Hristov G, Marttila T, Durand C, Niesler B, Rappold GA, Marchini A. (2014). SHOX triggers the lysosomal pathway of apoptosis via oxidative stress. *Hum Mol Genet.* 23, 1619-1630. doi: 10.1093/hmg/ddt552.
- [45] Schiller S, Spranger S, Schechinger B, Fukami M, Merker S, Drop SL, Tröger J, Knoblauch H, Kunze J, Seidel J, Rappold GA. (2000). Phenotypic variation and genetic heterogeneity in Léri-Weill syndrome. *Eur J Hum Genet.* 8, 54-62.
- [46] Binder G. (2011). Short stature due to SHOX deficiency: genotype, phenotype, and therapy. *Horm Res Paediatr.* 75, 81-89. doi: 10.1159/000324105.
- [47] Huber C, Rosilio M, Munnich A, Cormier-Daire V; French SHOX GeNeSIS Module. (2006). High incidence of SHOX anomalies in individuals with short stature. *J Med Genet.* 43, 735-739.
- [48] Bunyan DJ, Baker KR, Harvey JF, Thomas NS. (2013). Diagnostic screening identifies a wide range of mutations involving the SHOX gene, including a common 48 kb deletion 160 kb downstream with a variable phenotypic effect. *Am J Med Genet A.* 161A, 1329-1338.
- [49] Untergasser A, Cutcutache I, Koressaar T, Ye J, Faircloth BC, Remm M, Rozen SG. (2012). Primer3—new capabilities and interfaces. *Nucleic Acids Res.* 40, e115.
- [50] Zhang Y, Werling U, Edelmann W. (2012). SLiCE: a novel bacterial cell extract-based DNA cloning method. *Nucleic Acids Res.* 40, e55. doi: 10.1093/nar/gkr1288.
- [51] Jowett T and Lettice L. (1994). Whole-mount in situ hybridizations on zebrafish embryos using a mixture of digoxigenin- and fluorescein-labelled probes. *Trends Genet.* 10, 73-74.
- [52] Schindelin J, Arganda-Carreras I, Frise E, Kaynig V, Longair M, Pietzsch T, Preibisch S, Rueden C, Saalfeld S, Schmid B, Tinevez JY, White DJ, Hartenstein V, Eliceiri K, Tomancak F, Cardona A. (2012). Fiji: an open-source platform for biological-image analysis. *Nat Methods.* 9, 676-682.
- [53] Messeguer X, Escudero R, Farre D, Nunez O, Martinez J, Alba MM. (2002). PROMO: detection of known transcription regulatory elements using species-tailored searches. *Bioinformatics.* 18, 333-334.
- [54] Farre D, Roset R, Huerta M, Adsuara JE, Rosello L, Albà MM, Messeguer X. (2003). Identification of patterns in biological sequences at the ALGGEN server: PROMO and MALGEN. *Nucleic Acids Res.* 31, 3651-3653.
- [55] Liu W, Xie Y, Ma J, Luo X, Nie P, Zuo Z, Lahrmann U, Zhao Q, Zheng Y, Zhao, Y, Xue Y, Ren J. (2015). IBS: an illustrator for the presentation and visualization of biological sequences. *Bioinformatics.* 31, 3359-3361.
- [56] Haack TB, Hogarth F, Kruer MC, Gregory A, Wieland T, Schwarzmayr T, Graf E, Sanford L, Meyer E, Kara E, Cuno SM, Harik SI, Dandu VH, Nardocci N, Zorzi G, Dunaway T, Tarnopolsky M, Skinner S, Frucht S, Hanspal E, Schrandt-Stumpel C, Héron D, Mignot C, Garavaglia B, Bhatia K, Hardy J, Strom TM, Boddaert N, Houlden HH, Kurian MA, Meitinger T, Prokisch H, Hayflick SJ. (2012). Exome sequencing reveals de novo WDR45 mutations causing a phenotypically distinct, X-linked dominant form of NBIA. *Am J Hum Genet.* 91, 1144-1149.
- [57] Schwarz JM, Roedelsperger C, Schuelke M, Seelow D. (2010). MatationTaster evaluates disease-causing potential of sequence alterations. *Nat Methods.* 7, 575-576.

Bibliography

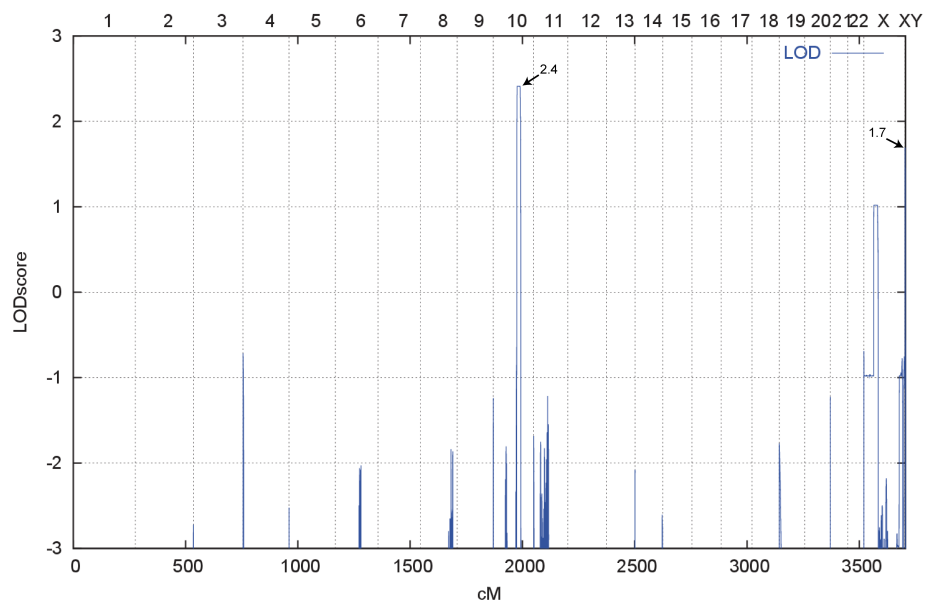
- [58] Adzhubei I, Jordan DM, Sunyaev SR. (2013). Predicting functional effect of human missense mutations using PolyPhen-2. *Curr Protoc Hum Genet* 10.1002/0471142905.hg0720s76.
- [59] Vaser R, Adusumalli S, Leng SN, Sikic M, Ng PC. (2016). SIFT missense predictions for genomes. *Nat Protoc.* 11, 1-9.
- [60] Choi Y and Chan, AP. (2015). PROVEAN web server: a tool to predict the functional effect of amino acid substitutions and indels. *Bioinformatics.* 31, 2745-2747.
- [61] Panda S, Sato TK, Castrucci AM, Rollag MD, DeGrip WJ, Hogenesch JB, Provencio I, Kay SA. (2002). Melanopsin (Opn4) requirement for normal light-induced circadian phase shifting. *Science.* 298, 2213-2216.
- [62] Taimi M, Helvig C, Wisniewski J, Ramshaw H, White J, Amad M, Korcyak B, Petkovich M (2004). A novel human cytochrome P450, CYP26C1, involved in metabolism of 9-cis and all-trans isomers of retinoic acid. *J Biol Chem.* 279, 77-85.
- [63] Cunningham TJ and Duyster G. (2015). Mechanisms of retinoic acid signaling and its roles in organ and limb development. *Nat Rev Mol Cell Biol.* 16, 110-123.
- [64] Laue K, Pogoda HM, Daniel PB, van Haeringen A, Alanay Y, von Ameln S, Rachwalski M, Morgan T, Gray MJ, Breuning MH, Sawyer GM, Sutherland-Smith AJ, Nikkes PG, Kubisch C, Bloch W, Wollnik B, Hammerschmidt M, Robertson SP. (2011). Craniosynostosis and multiple skeletal anomalies in humans and zebrafish result from a defect in the localized degradation of retinoic acid. *Am J Hum Genet.* 89, 595-606.
- [65] Sawada R, Kamei H, Hakuno F, Takahashi S, Shimizu T. (2015). In vivo loss of function study reveals the short stature homeobox-containing (shox) gene plays indispensable roles in early embryonic growth and bone formation in zebrafish. *Dev Dyn.* 244, 146-156. doi: 10.1002/dvdy.24239.
- [66] Gu X, Xu F, Wang X, Gao X, Zhao Q. (2005). Molecular cloning and expression of a novel CYP26 gene (cyp26d1) during zebrafish early development. *Gene Expr Patterns.* 5, 733-739.
- [67] Liang D, Jia W, Li J, Li K, Zhao Q. (2012). Retinoic acid signaling plays a restrictive role in zebrafish primitive myelopoiesis. *PLoS One.* 7, e30865. doi: 10.1371/journal.pone.0030865.
- [68] Nadeau JH. (2001). Modifier gene in mice and humans. *Nat Rev Genet.* 2, 165-174.
- [69] Akimenko MA and Ekker M. (1995). Anterior duplication of the Sonic hedgehog expression pattern in the pectoral fin buds of zebrafish treated with retinoic acid. *Dev Biol.* 170, 243-247.
- [70] Begemann G, Schilling TF, Rauch GJ, Geisler R, Ingham PW. (2001). The zebrafish neckless mutation reveals a requirement for raldh2 in mesodermal signals that pattern the hindbrain. *Development.* 128, 3081-3094.
- [71] Emoto Y, Wada H, Okamoto H, Kudo A, Imai Y. (2005). Retinoic acid-metabolizing enzyme Cyp26a1 is essential for determining territories of hindbrain and spinal cord in zebrafish. *Dev Biol.* 278, 415-427.
- [72] Uehara M, Yashiro K, Mamiya S, Nishino J, Chambon P, Dolle P, Sakai Y. (2007). CYP26A1 and CYP26C1 cooperatively regulate anterior-posterior patterning of the developing brain and the production of migratory cranial neural crest cells in the mouse. *Dev Biol.* 302, 399-411.
- [73] Cunningham TJ, Zhao X, Sandell LL, Evans SM, Trainor PA, Duyster G. (2013). Antagonism between retinoic acid and fibroblast growth factor signaling during limb development. *Cell Rep.* 30, 1503-1511.

Bibliography

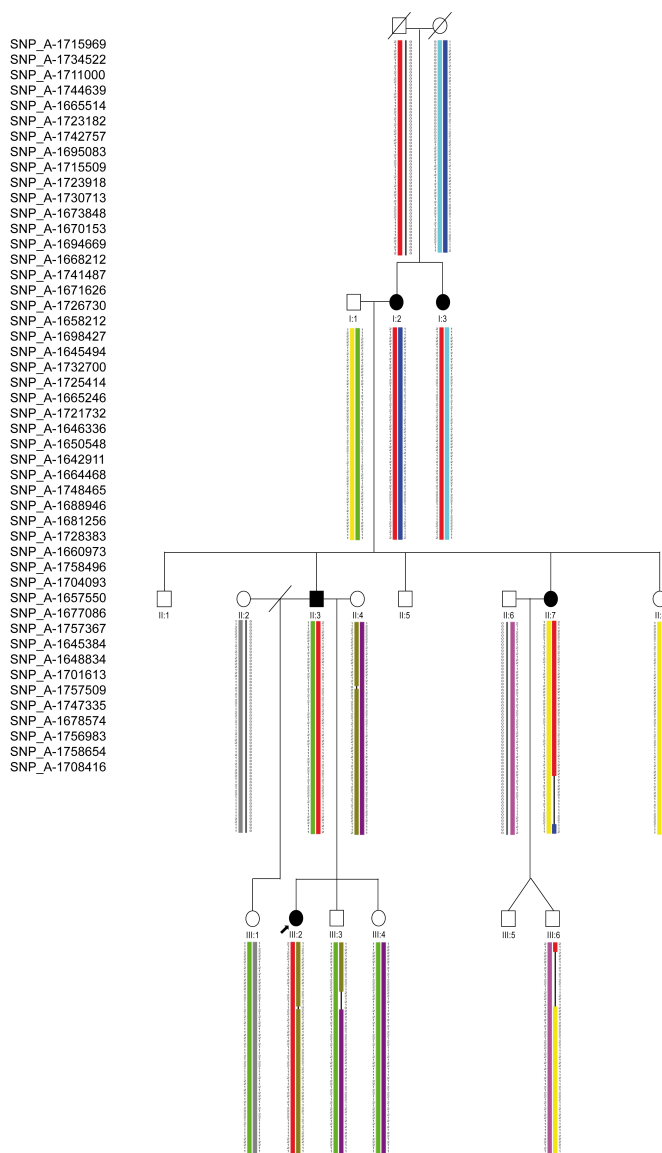
- [74] Hua S, Kittler R, White KP. (2009). Genomic antagonism between retinoic acid and estrogen signaling in breast cancer. *Cell*. 137, 1259-1271.
- [75] Ross-Innes CS, Stark R, Holmes KA, Schmidt D, Spyrou C, Russell R, Massie CE, Vowler SL, Eldridge M, Carroll JS. (2010). Cooperative interaction between retinoic acid receptor- α and estrogen receptor in breast cancer. *Genes Dev*. 24, 171-182.
- [76] Slavotinek AM, Mehrotra P, Nazarenko I, Tang PL, Lao R, Cameron D, Li B, Chu C, Chou C, Marqueling AL, Yahyavi M, Cordoro K, Frieden I, Glaser T, Prescott T, Morren MA, Devriendt K, Kwok PY, Petkovich M, Desnick RJ. (2013). Focal facial dermal dysplasia, type IV, is caused by mutations in *CYP26C1*. *Hum Mol Genet*. 22, 696-703.
- [77] Hernandez RE, Putzke AP, Myers JP, Margaretha L, Moens CB. (2007). Cyp26 enzymes generate the retinoic acid response pattern necessary for hindbrain development. *Development*. 134, 177-187.
- [78] Kinkel MD, Sefton EM, Kikuchi Y, Mizoguchi T, Ward AB, Prince VE. (2009). Cyp26 enzymes function in endoderm to regulate pancreatic field size. *Proc Natl Acad Sci USA*. 106, 7864-7869.
- [79] Grüneberg H. (1963). *The Pathology of Development; a Study of Inherited Skeletal Disorders in Animals*. Wiley, New York, USA. pp 309.
- [80] Oprea GE, Kröber S, McWhorter ML, Rossoll W, Müller S, Krawczak M, Bassell GJ, Beattie CE, Wirth B. (2008). Plastin 3 is a protective modifier of autosomal recessive spinal muscular atrophy. *Science*. 320, 524-527.
- [81] Ebermann I, Phillips JB, Liebau MC, Koenekoop RK, Schermer B, Lopez I, Schäfer E, Roux AF, Dafinger C, Bernd A, Zrenner E, Claustres M, Blanco B, Nürnberg G, Nürnberg P, Ruland R, Westerfield M, Benzing T, Bolz HJ. (2010). PDZD7 is a modifier of retinal disease and a contributor to digenic Usher syndrome. *J Clin Invest*. 120, 1812-1823.
- [82] Becanovic K, Norremolle A, Neal SJ, Kay C, Collins JA, Arenillas D, Lilja T, Gaudenzi G, Manoharan S, Doty CN, Beck J, Lahiri N, Portales-Casamar E, Warby SC, Connolly C, De Souza RA; REGISTRY Investigators of the European Huntington's Disease Network, Tabrizi SJ, Hermanson O4, Langbehn DR, Hayden MR, Wasserman WW, Leavitt BR. (2015). A SNP in the HTT promoter alters NF-KB binding and is a bidirectional genetic modifier of Huntington disease. *Nat Neurosci*. 18, 807-816.
- [83] Corvol H, Blackman SM, Boëlle PY, Gallins PJ, Pace RG, Stonebraker JR, Accurso FJ, Clement A, Collaco JM, Dang H, Dang AT, Franca A, Gong J, Guillot L, Keenan K, Li W, Lin F, Patrone MV, Raraigh KS, Sun L, Zhou YH, O'Neal WK, Sontag MK, Levy H, Durie PR, Rommens JM, Drumm ML, Wright FA, Strug LJ, Cutting GR, Knowles MR. (2015). Genome-wide association meta-analysis identifies five modifier loci of lung disease severity in cystic fibrosis. *Nat Commun*. 6, 8382. doi: 10.1038/ncomms9382.
- [84] Guo T, Chung JH, Wang T, McDonald-McGinn DM, Kates WR, Hawula W, Coleman K, Zackai E, Emanuel BS, Morrow BE. (2015). Histone Modifier Genes Alter Conotruncal Heart Phenotypes in 22q11.2 Deletion Syndrome. *Am J Hum Genet*. 97, 869-877.
- [85] Genetic Modifiers of Huntington's Disease (GeM-HD) Consortium. (2015). Identification of Genetic Factors that Modify Clinical Onset of Huntington's Disease. *Cell*. 162, 516-526.

Appendix

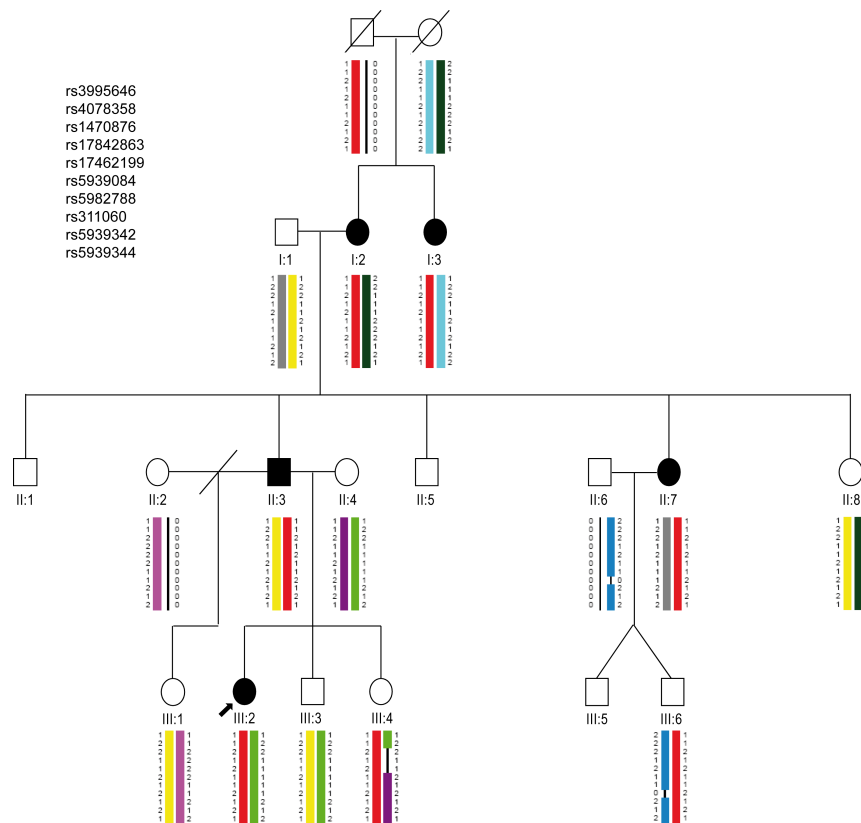
Appendix contains Appendix Figures 1-3 and Appendix Tables 1-4.



Appendix Figure 1: Schematic representation of genome-wide LOD score calculations. LOD scores calculated with ALLEGRO are given along the y-axis relative to genomic position cM (centi Morgan) on the x-axis. Note the highest peak (LOD score 2.4) in the region on chromosome 10 and a second lower peak in the XY PAR1 (LOD score 1.7). This analysis was performed by Dr. Gudrun Nuernberg.



Appendix Figure 2: Chromosome 10 region identified by whole-genome linkage analysis. Pedigree of the family with associated SNPs co-segregating with the disease phenotype on chromosome 10 is represented. A total LOD score of 2.4 was identified between the flanking markers rs10509480 and rs10509758 and covering a 19.2 Mb region (chr10: 85477515-104681710; hg19). Filled symbol, LWD affected individual; symbol with a slash, deceased individual; slash, divorced; arrow, index patient. Colored chromosomal regions show traceable inheritance; red color regions, common haplotype co-segregating with LWD; black lines, regions affected by a crossing over of unknown location. This analysis was performed by Dr. Gudrun Nuernberg.



Appendix Figure 3: Chromosome X, PAR1 region identified by whole-genome linkage analysis. Pedigree of the family with associated SNPs in the pseudo-autosomal region 1 (PAR1) of chromosome X is represented. A total LOD score of 1.7 was identified between the flanking markers rs3995646 and rs5939344 and covering a 2.02 Mb sequence (chrX: 706800-2735491; hg19). Filled symbol, LWD affected individual; symbol with a slash, deceased individual; slash, divorced; arrow, index patient. Colored chromosomal regions show traceable inheritance: red color regions, common haplotype co-segregating with LWD; black lines, regions affected by a crossing over of unknown location. This analysis was performed by Dr. Gudrun Nuernberg.

Appendix Table 1: Variants identified by whole exome sequencing of individuals II:3 and III:2 in Family 1. *, variants analysed by Sanger sequencing.

Gene symbol	Position (hg19)	Annotation	Reference allele	Altered allele	Protein change
MYOM3	chr1:24411024-24411024	missense	C	T	Gly>Ser
MACF1*	chr1:39853900-39853900	missense	G	A	Arg>Gln
DMAP1	chr1:44680270-44680270	missense	A	G	His>Arg
IGSF3*	chr1:117120054-117120054	missense	G	C	Ser>Arg
PRRC2C	chr1:171501788-171501788	missense	C	T	Leu>Phe
LAX1	chr1:203740509-203740509	missense	C	T	Leu>Phe
CR1L	chr1:207871016-207871016	missense	G	C	Arg>Thr
EXO1*	chr1:242023901-242023901	missense	A	G	Asn>Ser
PLB1*	chr2:28843766-28843766	missense	C	G	Pro>Ala
SFXN5	chr2:73198732-73198732	missense	G	T	Asn>Lys
IFIH1	chr2:163137930-163137930	missense	C	T	Val>Met
UNC80	chr2:210680059-210680059	missense	C	T	Arg>Cys
TRNT1	chr3:3170866-3170866	missense	C	A	Leu>Met
CX3CR1	chr3:39307125-39307125	missense	G	C	Ile>Met
ZNF501	chr3:44776352-44776352	missense	A	G	Ile>Val
KIF15	chr3:44842943-44842943	missense	C	A	Asp>Glu
KIF15	chr3:44842940-44842940	missense	A	G	Asn>Asp
DALRD3	chr3:49053308-49053308	missense	A	G	Leu>Pro
USP19*	chr3:49150049-49150049	missense	C	T	Arg>His
KIAA1407	chr3:113755502-113755502	missense	T	C	Lys>Glu
LRRC31	chr3:169558026-169558026	missense	T	C	Ala>Val
LSG1	chr3:194362876-194362876	missense	G	A	Ala>Val
FAM53A	chr4:1643268-1643268	missense	G	A	Val>Leu
HTT	chr4:3138013-3138013	missense	C	G	Asp>Asn
RCHY1	chr4:76434139-76434139	missense	G	T	Gln>Lys
HNRNPD	chr4:83277824-83277824	missense	T	C	Asn>Ser
LARP7*	chr4:113574284-113574284	missense	G	A	Asp>Asn
C4orf43	chr4:164436515-164436515	missense	G	A	Ser>Asn
NKD2	chr5:1038357-1038359	indel	GAG	delGAG	delGlu
AGXT2	chr5:35026520-35026520	missense	T	C	Ile>Val
SPEF2	chr5:35654784-35654784	missense	C	T	Arg>Trp
IQGAP2	chr5:75886262-75886262	missense	G	A	Ala>Thr
ECSCR	chr5:138837381-138837381	missense	C	T	Gly>Ser
FAT2*	chr5:150885332-150885332	missense	G	A	Arg>Trp
ADAM19*	chr5:156915281-156915281	missense	C	T	Val>Ile
TRIM7	chr5:180622230-180622230	missense	T	C	Gln>Arg

Appendix

PKHD1	chr6:51915066-51915066	missense	C	A	Arg>Leu
LRRC1	chr6:53767447-53767447	missense	A	G	Ile>Val
CHCHD2	chr7:56172142-56172142	missense	G	T	Pro>His
HIP1	chr7:75184840-75184840	missense	G	A	Leu>Phe
PCLO*	chr7:82764707-82764707	missense	G	A	Ala>Val
OR2A12	chr7:143792647-143792647	missense	A	G	Ile>Met
BLK	chr8:11418747-11418747	missense	G	T	Gln>His
FDFT1	chr8:11683560-11683560	missense	G	A	Gly>Arg
PIP5K1B*	chr9:71509400-71509400	missense	G	C	Gly>Ala
NDOR1	chr9:140110737-140110737	missense	A	G	Met>Val
ZNF33B*	chr10:43088356-43088356	missense	A	G	Ile>Thr
SUPV3L1*	chr10:70968696-70968696	missense	A	G	Met>Val
OPN4*	chr10:88419701-88419701	nonsense	C	T	Gln>Stop
CYP26C1*	chr10:94828408-94828408	missense	T	G	Phe>Cys
SUFU*	chr10:10463959-10463959	missense	C	T	Ala>Val
NRAP*	chr10:115401182-115401182	missense	C	T	Gly>Glu
DOCK1*	chr10:1292311563-1292311563	missense	A	T	Asp>Val
OR51G1	chr11:4944650-4944650	missense	T	C	Lys>Arg
PDE3B	chr11:14853242-14853242	missense	A	G	Ile>Met
DCDC1	chr11:31159274-31159274	missense	T	C	Met>Val
TNKS1BP1*	chr11:57087776-57087776	missense	C	T	Glu>Lys
ZDHHC5	chr11:57456934-57456934	missense	T	C	Val>Ala
OR1S2*	chr11:57971241-57971241	missense	G	A	Ala>Val
VWCE	chr11:61026257-61026257	missense	C	T	Val>Met
SLC22A25	chr11:62932035-62932035	missense	T	C	Thr>Ala
USP28*	chr11:113683078-113683078	missense	C	A	Arg>Ile
GPD1*	chr12:50500117-50500117	missense	T	C	Ile>Thr
RIMBP2*	chr12:130926846-130926846	missense	C	T	Val>Ile
PCDH8*	chr13:53421007-53421007	missense	C	T	Arg>His
SLC10A2*	chr13:103701773-103701773	missense	G	A	Thr>Met
LIG4*	chr13:108861778-108861778	missense	T	G	Lys>Asn
NRXN3	chr14:79181204-79181204	missense	G	A	Arg>His
TJP1	chr15:30010841-30010841	missense	C	A	Gly>Cys
OAZ2	chr15:64980961-64980961	missense	C	T	Arg>Gln
ACAN*	chr15:89395216-89395216	missense	A	T	Thr>Ser
FLYWCH1*	chr16:2983445-2983445	missense	A	T	Ser>Cys
ABAT	chr16:8868826-8868826	missense	G	A	Gly>Asp
TXNDC11*	chr16:11791994-11791994	missense	G	A	Pro>Leu
ZNF267*	chr16:31927549-31927549	missense	A	G	Tyr>Cys
CHD3	chr17:7814208-7814208	missense	C	T	Ala>Val
PIK3R6*	chr17:8796223-8796223	missense	G	A	Ala>Val

Appendix

AOC2*	chr17:40997824-40997824	missense	G	A	Arg>Gln
ANKRD40	chr17:48784984-48784984	missense	T	A	Gln>Leu
CLTC*	chr17:57760484-57760484	missense	C	T	Thr>Ile
TMC6	chr17:76120993-76120993	missense	G	A	Arg>Trp
TMC8	chr17:76135150-76135150	missense	G	A	Arg>His
LAMA1*	chr18:6950948-6950948	missense	G	A	Arg>Cys
DOHH	chr19:3492394-3492394	missense	G	A	Pro>Leu
ZNF266	chr19:9524511-9524511	missense	T	A	Asn>Tyr
ANKRD27	chr19:33110404-33110404	missense	G	A	Ser>Phe
FTL	chr19:49469240-49469240	missense	A	G	Arg>Gly
NAT14	chr19:55998176-55998176	missense	G	T	Met>Ile
CST5	chr20:23860141-23860141	missense	A	C	Val>Gly
SYNDIG1*	chr20:24646111-24646111	missense	G	A	Ala>Thr
TUBB1	chr20:57598870-57598870	missense	C	G	Leu>Val
BIRC7*	chr20:61867717-61867717	missense	G	A	Arg>His
IFNAR2	chr21:34621124-34621124	missense	G	A	Val>Ile
AP1B1	chr22:29750745-29750745	missense	C	T	Gly>Ser
SLC5A1	chr22:32479136-32479136	missense	G	T	Gly>Val
TRMU	chr22:46752825-46752825	missense	C	G	Pro>Ala
DMD	chrX:31284928-31284928	missense	C	T	Gly>Ser
KIF4A*	chrX:69510287-69510287	missense	AG	AC	-

Appendix Table 2: Variants identified in Family 1 and by screening the coding regions of *CYP26C1* in 68 individuals with *LWD* and *SHOX* deficiency.

Transcript	c.356A>C	c.639C>T	c.705+4C>T	c.734G>A	c.1191+69_1191+75delCTGCCGC	c.1191+52C>T
Protein	p.Gln119Pro	p.Thr213=	p.-	p.Arg245Gln	p.-	p.-
Annotation	missense	synonymous	splice region	missense	intron	intron
rsID	rs201284617	rs55843714	rs58993699	rs11187265	rs76924069	-
Mutation taster	disease causing	polymorphism	polymorphism	polymorphism	polymorphism	polymorphism
Polyphen2	probably damaging	unknown	unknown	benign	unknown	unknown
Provean	deleterious	neutral	neutral	neutral	unknown	unknown
SIFT	tolerated	tolerated	tolerated	tolerated	unknown	unknown
CADD	23.5	-	-	-	-	-
Allele frequency our cohort	0.0072 (1/138) Family 3	0.2898 (40/138)	0.0144 (2/138)	0.0869 (12/138)	0.1449 (20/138)	0.0144 (2/138)
Allele frequency ExAC	0.000206 (1/14556)	0.4687 (53306/113722)	0.01679 (1790/106604)	0.09819 (11798/120154)	not found	0.0001859 (1/5380)
Allele frequency TGP	0.0012 (6/5002)	0.2823 (1414/3594)	0.033 (165/4843)	0.074 (370/4638)	not found	not found
Allele frequency EVS	not found	0.4401 (5673/7217)	0.0289 (352/11796)	0.085 (106/11900)	not found	not found
SHOX mutation	deletion	not shown	not shown	not shown	not shown	not shown
SHOX mutation frequency	not found in ExAC, TGP and EVS					

Transcript	c.1133G>A	c.1401C>G	c.1523T>G
Protein	p.Arg378His	p.Ala467=	p.Phe508Cys
Annotation	missense	synonymous	missense
rsID	rs200442762	rs61729502	-
Mutation taster	disease causing	disease causing	disease causing
Polyphen2	probably damaging	unknown	probably damaging
Provean	deleterious	neutral	deleterious
SIFT	damaging	tolerated	damaging
CADD	35	-	24
Allele frequency our cohort	0.0072 (1/138) Family 2	0.0072 (1/138)	- - Family 1
Allele frequency ExAC	not found	0.003851 (270/70118)	not found
Allele frequency TGP	0.0002 (1/5007)	0.0006 (3/5005)	not found
Allele frequency EVS	not found	0.0022 (28/12412)	not found
SHOX mutation	p.Leu132Val	not shown	p.Val161Ala
SHOX mutation frequency	not found in ExAC, TGP, and EVS		not found in ExAC, TGP, and EVS

Appendix Table 3: Variants identified by screening of CYP26C1 in 140 healthy control individuals.

Transcript	c.639C>T	c.705+4C>T	c.734G>A	c.1191+69_1191 + 75delCTGCCGC
Protein	p.Thr213=	p.-	p.Arg245Gln	p.-
Annotation	synonymous	splice region	missense	intron
rsID	rs55843714	rs58993699	rs11187265	rs76924069
Mutation taster	polymorphism	polymorphism	polymorphism	polymorphism
Polyphen2	unknown	unknown	benign	unknown
Provean	neutral	neutral	neutral	unknown
SIFT	tolerated	tolerated	tolerated	unknown
Allele frequency our cohort	0.4857 (136/280)	0.0035 (1/280)	0.1178 (33/280)	0.2464 (69/280)
Allele frequency ExAC	0.4687 (53306/113722)	0.01679 (1790/106604)	0.09819 (11798/120154)	not found
Allele frequency TGP	0.2823 (1414/3594)	0.033 (165/4843)	0.074 (370/4638)	not found ()
Allele frequency EVS	0.4401 (5673/7217)	0.0289 (352/11796)	0.085 (106/11900)	not found

Appendix Table 4: Variants identified in Family 1 and by screening the coding regions of *CYP26C1* in 68 individuals with *LWD* and *SHOX* deficiency.

Transcript	c.148C>T	c.356A>C	c.639C>T	c.705+4C>T	c.564C>T	c.734C>A	c.861+131G>T	c.885C>T	c.861-3C>T
Protein	p.Pro50Ser	p.Gln119Pro	p.Thr213=	p.-	p.Leu188=	p.Arg245Gln	p.-	p.Phe295=	p.-
Annotation	missense	missense	synonymous	splice region	synonymous	missense	intron	synonymous	intron
rsID	rs200946223	rs201284617	rs55843714	rs58993699	-	rs11187265	rs117507138	rs147253174	-
Mutation taster	disease causing	disease causing	polymorphism	polymorphism	disease causing	polymorphism	polymorphism causing	disease causing	disease causing
Polyphen2	probably damaging	probably damaging	unknown	benign	unknown	benign	unknown	unknown	unknown
Provean	deleterious	deleterious	neutral	neutral	neutral	neutral	unknown	neutral	unknown
SIFT	damaging	tolerated	tolerated	tolerated	tolerated	tolerated	unknown	tolerated	unknown
CADD	29.9	23.5	-	-	-	-	-	-	-
Allele frequency our cohort	0.0019 (1/512) Family 4	0.0019 (1/512)	0.188 (91/484)	0.0082 (4/484)	0.002 (1/484)	0.0488 (25/512)	0.0097 (5/512) Family 5	0.0021 (1/474)	0.0021 (1/474)
Allele frequency ExAC	0.00004946 (1/20220)	0.000206 (1/14556)	0.4687 (53306/113722)	0.01679 (1790/106604)	not found	0.09819 (11798/120154)	not found	0.002449 (187/76356)	not found
Allele frequency TGP	0.0002 (1/5007)	0.0012 (6/5002)	0.2823 (1414/3594)	0.033 (165/4843)	not found	0.074 (370/4638)	0.0032 (16/4992)	0.0006 (3/5005)	not found
Allele frequency EVS	not found	not found	0.4401 (5673/7217)	0.0289 (352/11796)	not found	0.085 (1106/11900)	not found	0.0006 (9/12883)	not found

Transcript	c.1491C>T	c.1401C>G	c.*114A>G
Protein	p.Ile497=	p.Ala467=	p-
Annotation	synonymous	synonymous	3'UTR
rsID	rs140502479	rs61729502	rs563178362
Mutation taster	disease causing	disease causing	unknown
Polyphen2	unknown	unknown	unknown
Provean	neutral	neutral	unknown
SIFT	tolerated	tolerated	unknown
CADD	-	-	-
Allele frequency our cohort	0.0019 (1/502)	0.0019 (1/502)	0.0039 (2/512)
Allele frequency ExAC	0.001431 (98/68478)	0.003851 (270/70118)	not found
Allele frequency TGP	0.0004 (2/5006)	0.0006 (3/5005)	0.0004 (2/5006)
Allele frequency EVS	0.0004 (6/12558)	0.0022 (28/12412)	not found